

ENGINEERING PATTERNS TO STUDY VASCULAR BIOLOGY

Jan D. Baranski

A DISSERTATION

in

Bioengineering

Presented to the Faculties of the University of Pennsylvania

in

Partial Fulfillment of the Requirements for the

Degree of Doctor of Philosophy

2012

Supervisor of Dissertation:

Christopher S. Chen, Professor, Bioengineering

Graduate Group Chairperson:

Beth A. Winkelstein, Professor, Bioengineering

Dissertation Committee:

Peter F. Davies, Professor, Pathology and Laboratory Medicine

Sandra W. Ryeom, Assistant Professor, Cancer Biology

Daeyeon Lee, Assistant Professor, Chemical and Biomolecular Engineering

ACKNOWLEDGMENTS

I owe a wealth of gratitude to the many people who have supported me during this long endeavor. I would like to first thank my advisor, Chris Chen for his mentorship and support. His enthusiasm and passion for science have provided constant inspiration, and his lab provided a rich and stimulating environment that allowed me to freely pursue my ideas. I owe thanks to my committee for taking time to evaluate my work and for pushing me to always strive for a higher standard.

Next, I would like to express my gratitude to past and present lab members who have provided much insightful feedback, support, and camaraderie. Ravi, Sami, Colette, Wes, Colin, Jeroen, Jordan, Esteban, and Michele helped guide me through the daily toils of graduate school. I owe immense gratitude to my collaborators, especially Ritu, Mike, Dana, Kelly, and Sri, who have directly contributed to the work presented in this dissertation.

Lastly, I would like to thank my family and friends for their unwavering support and motivation. A special thank you to my Mom, Dad, and family overseas, jestem bardzo wdzięczny za waszą miłość, wsparcie, i wiarę w moich możliwościach. To my wife, Vanesa, I am forever grateful for your enduring love and support. You provide me with daily inspiration and a reminder of what our journey through life is all about. I eagerly look forward to the joy, opportunities, and challenges that the future will bring.

ABSTRACT

ENGINEERING PATTERNS TO STUDY VASCULAR BIOLOGY

Jan D. Baranski

Christopher S. Chen

Proper growth of blood vessels is critical for development, wound healing and homeostasis. This process is regulated by a variety of microenvironmental cues including growth factor signaling, cell-cell contacts and mechanical and biochemical signals from the extracellular matrix. The work presented in this dissertation encompasses the application of engineering principles to the study of angiogenesis and vascular biology within the contexts of tissue engineering and vascular disease.

In Chapter 2, we present a novel strategy for generating a spatially patterned vascular network *in vivo*. Future development of clinically viable engineered tissues hinges on the ability to generate functional vasculature capable of delivering blood to parenchymal cells deep within the tissue. The vascularization strategy described here utilizes tissue constructs that contain patterned ‘cords’ of endothelial cells. Implantation of these constructs into mice leads to the formation of stable capillaries in a spatially controlled geometry. The capillaries become perfused with host blood as early as 3 days post implantation, remain stable for at least 28 days *in vivo*, are largely comprised of implanted endothelial cells, and are invested by α -SMA positive pericytes. We further demonstrate that spatial patterning of vascular architecture improves the function of engineered hepatic tissues. Specifically, co-implantation of patterned endothelial cell

cords with primary hepatocyte aggregates suggested that organized vascular architecture significantly improved albumin promoter activity within the tissues.

In Chapter 3, we describe the development of an organotypic vascular wall model and show that pulmonary arterial smooth muscle cells (PASMCs) isolated from patients with idiopathic pulmonary arterial hypertension (IPAH) exhibit a hyperproliferative phenotype in culture. While normal control PASMCs display Rac1-mediated growth control, the higher proliferation in IPAH PASMCs is dependent on increased RhoA activity. We observed that focal adhesion assembly and focal adhesion kinase signaling are abnormally increased in IPAH PASMCs and show that antagonizing adhesion signaling by direct inhibition of FAK abrogates IPAH PASMC hyperproliferation *in vitro*.

In summary, our strategy for rapidly inducing the formation of spatially controlled capillaries comprises a novel technique for spatial control of vessel growth *in vivo*. Functional studies with engineered hepatic tissues also demonstrate the potential of this technique to be used in vascularizing engineered solid organs. Findings from our investigation into aberrant IPAH SMC proliferation suggest that a mechanosensitive proliferative control mechanism underlies IPAH etiology.

TABLE OF CONTENTS

ACKNOWLEDGMENTS	ii
ABSTRACT.....	iii
LIST OF FIGURES	ix
CHAPTER 1: BACKGROUND AND SIGNIFICANCE	1
1.1 Scope of dissertation.....	1
1.2 Introduction to tissue engineering.....	1
1.2.1 General strategies in tissue engineering.....	2
1.2.2 Current challenges in engineering solid tissues.....	4
1.2.3 Organotypic models of vascular smooth muscle	4
1.3 Angiogenesis in physiology and disease.....	6
1.3.1 Steps of angiogenesis.....	6
1.3.2 Regulation of angiogenesis by growth factors.....	8
1.3.3 Regulation of angiogenesis by the extracellular matrix.....	11
1.3.4 Regulation of angiogenesis by cell-cell contacts.....	13
1.3.5 Therapeutic angiogenesis and its role in the clinic	15
1.4 Tissue engineering approaches to promote angiogenesis	17
1.4.1 Biofunctional materials for inducing angiogenesis.....	18
1.4.2 Cell-based strategies for generating microvasculature	19
1.5 The vasculature in a disease context: pulmonary arterial hypertension	22
1.5.1 Pathology and current treatments.....	23
1.5.2 The role of vascular smooth muscle cells in pulmonary hypertension.....	26

1.5.3 Regulation of smooth muscle cell proliferation by the microenvironment	28
1.6 Summary	30
CHAPTER 2: Patterned vascular networks improve function of engineered tissues <i>in vivo</i>	31
2.1 Introduction.....	31
2.2 Generation of patterned endothelial cell ‘cords’ <i>in vitro</i>	32
2.2.1 Design, fabrication and optimization of a second-generation device for generating patterned cell cords	32
2.2.2 Screening cell types and coculture ratios for use in cords.....	41
2.2.3 <i>In vitro</i> characterization of endothelial cell cords.....	46
2.3 Vascularizing engineered tissues <i>in vivo</i> via implantation of endothelial cell cords	54
2.3.1 Development of <i>in vivo</i> implantation model.....	54
2.2.2 Implantation of endothelial cell cords drives formation of mature capillaries <i>in vivo</i>	62
2.2.3 Implantation of patterned endothelial cell constructs yields a perfused <i>in vivo</i> vasculature with conserved geometry.....	71
2.2.4 Patterned vasculature within engineered hepatic tissues maintains hepatocyte function	74
2.4 Materials and Methods.....	79
2.5 Conclusions.....	86
CHAPTER 3: Proliferative regulation by adhesion and RhoGTPases in smooth muscle cells is altered in idiopathic pulmonary arterial hypertension	88
3.1 Introduction.....	88

3.2 Development of an organotypic arterial wall model.....	92
3.3 Contractility measurements of IPAH PASMCs.....	98
3.4 Further characterization of IPAH PASMCs	103
3.5 Proliferative regulation by adhesion and Rho GTPases is altered in IPAH PASMCs	109
3.5.1 Proliferation in IPAH SMCs is Rho-dependent.....	109
3.5.2 Adhesion signaling is altered in IPAH PASMCs	111
3.5.3 High proliferation in IPAH PASMCs is mediated by altered adhesion signaling	114
3.6 Materials and Methods.....	115
3.7 Conclusions.....	120
CHAPTER 4: Discussion and Future Directions.....	122
4.1 Discussion of patterned endothelial cell cords for vascularizing engineered tissues	122
4.1.1. <i>In vitro</i> generation of endothelial cell cords	122
4.1.2 The vascularization response to implanted endothelial cell cords.....	124
4.1.3 Role of cell type in the vascularization response upon implantation of endothelial cell cords	126
4.1.4 Role of growth factor signaling in the vascularization response upon implantation of endothelial cell cords.....	128
4.1.5 Role of the extracellular matrix in the vascularization response upon implantation of endothelial cell cords.....	130

4.1.6 Role of cell-cell contacts in the vascularization response upon implantation of endothelial cell cords	132
4.1.7 Anastomosis with the host vasculature	134
4.1.8 Patterning of vasculature via implantation of endothelial cell cords	136
4.1.9 Remaining challenges for vascularization of engineered tissues via implantation of endothelial cell cords	138
4.2 Discussion of studies on proliferative regulation in IPAH SMCs	140
4.2.1 Generation of an <i>in vitro</i> arterial wall model	140
4.2.2 Mechanisms underlying abnormal proliferation in IPAH smooth muscle cells	143
4.2.2 Assessing the phenotype of IPAH smooth muscle cells	145
4.2.3 Clinical translation of findings	146
4.3 Future directions	147
4.3.1 Applications of vascularization via patterned EC cords	147
4.3.2 Future understanding of proliferative regulation in IPAH	149
BIBLIOGRAPHY	151

LIST OF FIGURES

Figure 2.1 Early technique for generating patterned cell cords	34
Figure 2.2 Removal of cords from PDMS template	35
Figure 2.3 First- and second-generation devices for generating cords.	37
Figure 2.4 Removal of EC cords into fibrin.....	40
Figure 2.5 Schematic of process used to generate EC cords using second-generation PDMS devices.....	41
Figure 2.6 Networking behavior of e.End2 cells in collagen gels	43
Figure 2.7 Networking behavior of HUVECs in collagen gels	44
Figure 2.8 Networking behavior of HUVECs + C3H10T1/2 cells collagen gels.....	46
Figure 2.9 Relative distribution of HUVECs, 10T1/2s within collagen in EC cords	47
Figure 2.10 Cytoskeletal tension is required for cord contraction.....	49
Figure 2.11 Contribution of C3H10T1/2 cells to cord contractility	51
Figure 2.12 Generation of EC cords with varying diameters and geometries	53
Figure 2.13 Gross anatomy of tissue constructs resected 5 days post-implantation.....	55
Figure 2.14 Early evidence of blood in implanted tissue constructs containing EC cords	56
Figure 2.15 Development and implantation of a backing structure implantable tissue constructs	58
Figure 2.16 Preservation of geometry and presence of blood in EC cords resected 7 days post-implantation	60
Figure 2.17 Frozen sectioning of tissue constructs	61
Figure 2.18 Implanted EC cords drive formation of mature capillaries	63
Figure 2.19 Quantification of the vascularization response.....	65

Figure 2.20 Composition of vessels at graft periphery.....	67
Figure 2.21 Cells are required for vascularization.....	68
Figure 2.22 Effect of varying 10T1/2 to HUVEC ratios on <i>in vivo</i> capillary formation .	70
Figure 2.23 Effects of cord diameter on vascularization <i>in vivo</i>	71
Figure 2.24 Perfusion with host blood and patterning of <i>in vivo</i> vasculature.....	73
Figure 2.25 Capillary sprouting between adjacent cords.....	74
Figure 2.26 EC cords within engineered rat hepatic tissues improve function.....	76
Figure 2.27 EC cords within engineered human hepatic tissues improve function.....	78
Figure 3.1 Ascorbic acid treatment of bPASCs.....	93
Figure 3.2 Culture of bPAECs atop a layer of bPASCs (medium density).....	95
Figure 3.3 Culture of bPAECs atop a layer of bPASCs (high density).....	96
Figure 3.4 ‘Reverse’ arterial wall model.	97
Figure 3.5 ppMLC expression levels in IPAH PASCs.....	99
Figure 3.6 IPAH SMC contractility in collagen gels.	100
Figure 3.7 Measurements of traction forces generated by IPAH PASCs.....	102
Figure 3.8 Adhesion of control and IPAH PASCs to fibronectin-coated substrates..	104
Figure 3.9 Effects of cell density and N-cadherin expression on IPAH PASC proliferation.....	106
Figure 3.10 SMC marker expression levels of control versus IPAH PASCs.....	108
Figure 3.11 Perlecan deposition patterns in IPAH PASC cultures	109
Figure 3.12 Proliferation rates of control and IPAH SMCs in culture	111
Figure 3.13 Focal adhesion size, structure, and FAK phosphorylation status in IPAH PASCs	113
Figure 3.14 Adhesion-mediated proliferative control in IPAH PASCs	115

CHAPTER 1: BACKGROUND AND SIGNIFICANCE

1.1 Scope of dissertation

Two studies are presented in this dissertation. In Chapter 2, we describe the development and application of a novel strategy for vascularizing engineered tissues *in vivo*. In Chapter 3, while we begin with a description of work aimed at developing an organotypic arterial wall model, our main focus shifts to a study into proliferative control mechanisms that might underlie smooth muscle cells in pulmonary arterial hypertension. A common introduction to these two studies is presented here in Chapter 1 and is organized as follows: 1) brief definition and overview of tissue engineering, 2) introduction to angiogenesis and vascular biology, 3) overview of strategies for promoting angiogenesis via tissue engineering approaches, and 4) introduction to the pathology of vascular disease and pulmonary arterial hypertension. Topics including remaining challenges and future directions are discussed in Chapter 4.

1.2 Introduction to tissue engineering

As medical technology improves and life expectancy throughout the world increases, the demand for organs grows. Currently, approximately 500,000 patients benefit from organ transplants in the US each year, and millions of additional surgical procedures are performed to help replace or reconstruct damaged tissue (Langer & Vacanti, 1993; Network & Recipients, 2011). The number of organs available for transplant, however,

continues to severely outpace demand by an ever-greater margin. Indeed, the median waiting period for a kidney in the US in 2005 was 1,269 days (Network & Recipients, 2011). Apart from whole organ transplants, therapies utilizing tissue regeneration or replacement hold much promise for treating a variety of conditions. Considering diabetes alone, the potential is enormous – 17.5 million patients were affected in the US in 2007, and the disease represents a \$116 billion annual burden in excess medical expenditures (American Diabetes Association, 2007).

Since first being described in the late 1980s, the field of tissue engineering is slowly beginning to meet some of the demands for organs and organ replacement therapies. Its goal is to develop biological substitutes that maintain, improve or restore normal tissue function (Heineken & Skalak, 1991; Langer & Vacanti, 1993; Vacanti, 2012). Tissue engineering embodies efforts to create new therapies that rely on a fundamental understanding and control of the structure-function relationship in native tissues. It is an inherently multidisciplinary field that marries the application of engineering principles with a fundamental understanding of the underlying biological processes (Orlando, Wood, et al., 2011b). Though clinical trials with tissue-engineered therapies have only recently begun, preliminary results from these and other *in vitro* and preclinical animal studies strongly suggest that many novel therapies will emerge over the next several decades.

1.2.1 General strategies in tissue engineering

Tissue engineering originally emerged from the biomaterials field in the 1980s – as the biophysical properties of natural and synthetic materials were becoming better

understood, a growing number of studies utilizing these materials and their interactions with cells as a means of repairing or replacing injured tissues quickly coalesced into its own field (Vacanti, 2012). Today, tissue engineering strategies can be divided into two general categories: 1) ones that rely solely on growth-inducing substances and scaffolds and 2) ones that rely on cells placed on or within synthetic scaffolds or natural matrices (Langer & Vacanti, 1993). Accordingly with the field's origins, a substantial amount of research has focused on efforts to generate materials with bioactive properties (R. R. Chen & Mooney, 2003; Lutolf & Hubbell, 2005). Indeed, within the context of vascular tissue engineering, much work has focused on using biomaterials to help drive the body's natural angiogenic processes (Cleary et al., 2012; Lovett, Lee, Edwards, & Kaplan, 2009; Phelps & García, 2010). Significant contributions in this area include the controlled release of growth factors for inducing vessel growth (Peters, Polverini, & Mooney, 2002), insights into of the role of matrix mechanics on capillary morphogenesis (Ghajar, Chen, Harris, Suresh, et al., 2008a), and the development of a variety of synthetic materials with broad applications in tissue engineering (Lin & Anseth, 2008; X. Liu, Holzwarth, & Ma, 2012).

To date, tissues with cells of virtually every type have been created in the laboratory (Orlando, Baptista, et al., 2011a; Orlando, Wood, et al., 2011b). A critical issue, however, has been a limitation in the number of autologous cells that are available for use in patients (C. J. Koh & Atala, 2004; Rustad, Sorkin, Levi, Longaker, & Gurtner, 2010). The discovery of inducible pluripotent stem cells in 2006 has provided a potential solution to the problem of cell source and cell-based therapies are seeing much renewed

interest (Rustad et al., 2010). While significant challenges remain, advances in the study of materials and cell biology are continuing to drive the development of novel and increasingly effective tissue-engineered therapies.

1.2.2 Current challenges in engineering solid tissues

Therapies for replacing organs such as engineered skin, bladder, airways, urethra and large blood vessels have recently showed promise in early stage clinical trials and have already become available to small numbers of patients (Hibino et al., 2011; Macchiarini et al., 2008; Orlando, Wood, et al., 2011b; H. Yanaga, Imai, Fujimoto, & Yanaga, 2009). The ability to engineer large solid organs with high metabolic demands such as kidney, liver and pancreas, however, remains elusive. These cell dense and highly vascularized tissues are complex and remain difficult to construct in the laboratory (Vacanti, 2012). A key obstacle to their design is the limitation of diffusion of nutrients and waste products to and from cells within the tissue. Since cells must be located within 100 - 200 μm of blood vessels to ensure survival, our ability to create a functional vasculature remains paramount to overcoming the challenge of creating large organs for use in humans (Rouwkema, Rivron, & van Blitterswijk, 2008). The development of a strategy to effectively vascularize engineered tissue is a major goal of the work described in Chapter 2 of this dissertation.

1.2.3 Organotypic models of vascular smooth muscle

An ancillary goal within the field of tissue engineering is to generate physiologically relevant models of normal and diseased tissues (Garlick, 2007; Inamdar & Borenstein,

2011; Paquet et al., 2010). Such models allow a much wider variety of manipulations and are used for the *in vitro* study of phenomena that might otherwise be prohibitively expensive, time consuming, or invasive for *in vivo* experimentation. In the context of vascular biology, current organotypic models include microfluidic devices and similar systems that mimic one or more physiological processes within angiogenesis, vascular injury, inflammation, and tumor extravasation (Chrobak, Potter, & Tien, 2006; Kamat et al., 2011; Zervantonakis et al., 2012; Zheng et al., 2012). While the adoption of endothelial-only angiogenic models has been growing significantly, the development of more complete arterial wall models has been largely unexplored. Indeed, the few reported uses of an *in vitro* EC-SMC bilayer focus on the direct interactions between ECs and SMCs, and we found no reports of its use to study disease (Fillinger, Sampson, Cronenwett, Powell, & Wagner, 1997; Niwa, Sakai, Watanabe, Ohyama, & Karino, 2007; Ziegler, Alexander, & Nerem, 1995). In a study presented in Chapter 3 of this dissertation, we sought to create an organotypic model of vascular smooth muscle for use in the study of pulmonary arterial hypertension.

Given that smooth muscle cells often differentiate into a synthetic phenotype when cultured in traditional tissue culture models (Thyberg, Hedin, Sjölund, Palmberg, & Bottger, 1990), we predicted that an organotypic model such as the one described here might allow for additional study of IPAH pathobiology in a more physiologically relevant context.

1.3 Angiogenesis in physiology and disease

Angiogenesis, or the sprouting of capillaries from preexisting blood vessels, is a complex process that relies on a number of spatiotemporally regulated biochemical and mechanical cues . When tissues within multicellular organisms grow to sizes beyond the diffusion limit, they rely on angiogenesis to recruit new vessels and gain access to the blood supply (Carmeliet & Jain, 2000). Furthermore, formation of a functional vasculature is critical for tissues' ability to receive nutrients and remove metabolic waste, and angiogenesis plays a central role in development, wound healing and a number of disease states with each step regulated by a balance between pro- and anti-angiogenic cues .

1.3.1 Steps of angiogenesis

Angiogenesis requires the cooperative signaling of a variety of growth factor-mediated biochemical and matrix-mediated adhesive and mechanical cues. The process begins with the stimulation of quiescent endothelial cells within existing vessels by proangiogenic cues (D'Amore & Thompson, 1987). Growth factors such as vascular endothelial growth factor (VEGF) first stimulate the normally quiescent endothelial cells to begin degrading the surrounding extracellular matrix (Ferrara, Gerber, & LeCouter, 2003). During these first steps of angiogenesis, the now active endothelial cells begin secreting matrix metalloproteinases (especially MMP1, MMP2 and MT1-MMP) to degrade the basal lamina and the surrounding adventitial matrix (Adams & Alitalo, 2007; Carmeliet, 2003). Concurrently, the cells begin proliferating and migrating away from the original vessel and towards the source of guidance cues such as gradients of VEGF or gradients of

neural guidance cues such as semaphorins and plexins (Torres-Vázquez et al., 2004). The intricate sprouting process is further regulated notch and delta-like-4 (Dll4) interactions in the emerging sprout (Phng & Gerhardt, 2009). While individual endothelial cells first initiate the sprouting process, the emerging sprout consists of numerous stalk cells following the guidance of a leader, or tip cell. The sprouting cells actively compete for the tip cell position in a process that involves the up- and down-regulation of VEGF receptors and is mediated by Notch and Dll4 signaling (Jakobsson et al., 2010). As sprouting continues, additional gradients of molecules including platelet-derived growth factor B (PDGFB) and angiopoietin help recruit supporting pericytes to the nascent endothelial sprouts (Hellberg, Ostman, & Heldin, 2010; Jain, 2003). At this stage of angiogenesis, the newly formed vessels begin to form lumens capable of carrying blood via a process of vacuole fusion (Kamei et al., 2006; Strilic et al., 2009). The maturing vessels are further stabilized by the presence of blood flow, establishment of tight junctions via cell-cell interactions between claudins and occludins, and adherens junctions via VE-cadherin interactions (Dejana & Giampietro, 2012; Dejana, Tournier-Lasserre, & Weinstein, 2009; Jain, 2003). Ultimately, all of these tightly coordinated steps lead to the development of functional, blood-carrying vessels that may be further pruned in order to generate an optimal network of vessels capable of effectively delivering blood to growing or injured tissues (Hlushchuk et al., 2011). Lastly, the dysregulation of vessel growth contributes to the pathogenesis of many disorders including pulmonary hypertension (Adams & Alitalo, 2007; Carmeliet, 2003; Carmeliet & Jain, 2011).

1.3.2 Regulation of angiogenesis by growth factors

The process of angiogenesis is regulated by a diversity of cues from growth factors, the ECM, and cell-cell interactions. Of the soluble factors that regulate angiogenesis, the VEGF signaling pathway has been the most widely studied. The VEGF gene family consists of VEGF-A, VEGF-B, VEGF-C, VEGF-D and placental growth factor (PlGF) (Ferrara et al., 2003). By far, the most studied isoform is VEGF-A, which signals primarily through VEGFR2 (Adams & Alitalo, 2007). It is essential for embryonic angiogenesis and deletion of a single allele results in embryonic lethality (Carmeliet et al., 1996). In general, VEGF-A has been found to be critical for all tissues and developmental stages in which vessel growth is essential. The VEGF isoforms are capable of binding to a set of receptor tyrosine kinases, mainly VEGFR-1, VEGFR-2 and VEGFR-3 (Adams & Alitalo, 2007; Ferrara et al., 2003). VEGFR-2 seems to play a primary role in modulating the growth and permeability actions of VEGF, and studies have shown that its knockout in mice leads to a lethal defect in which the vasculature fails to properly form (Shalaby et al., 1995). In contrast, studies have suggested that VEGFR-1 may play an inhibitory role by suppressing signaling through VEGFR-2. In mice, knockout of VEGFR-1 leads to an excess of endothelial cells that assemble into non-functional disorganized tubules (Fong, Rossant, Gertsenstein, & Breitman, 1995). While the role of VEGFR-3 is still not entirely clear in angiogenesis, it has been shown to be important in sprouting and tip cell regulation, lymphatic vessel development, and most recently, in tumor progression (J.-L. Su et al., 2006; Taipale et al., 1999).

Platelet-derived growth factor (PDGF) is critical to the later stages of the angiogenic process (Jain, 2003). Once sprouting is underway, endothelial cells release PDGF-B to recruit pericytes, which express PDGF receptor-beta (Gaengel, Genové, Armulik, & Betsholtz, 2009; Hellberg et al., 2010). *In vivo* studies have shown that knockout of PDGF-B leads to pericyte deficiencies, which result in fragile and leaky vessels (Quaegbeur, Segura, & Carmeliet, 2010). PlGF, first thought to be a proangiogenic factor critical during development, is dispensable during development and is relevant only in disease (Carmeliet et al., 2001). Similar to VEGF, basic fibroblast growth factor was one of the first angiogenic factors to be discovered (Carmeliet & Jain, 2011). bFGF and the related family of FGFs bind to FGF receptors (FGFRs) on endothelial cells or can stimulate angiogenesis indirectly by inducing the release of angiogenic factors from other cell types (Beenken & Mohammadi, 2009). Most notably, the inhibition of FGFR signaling in quiescent endothelial cells was shown to cause vessel disintegration, suggesting that basal levels of FGF are required for the maintenance of vascular integrity (Murakami et al., 2008).

Recently, a number of studies have focused on the role of the Ang/Tie signaling system in angiogenesis (Carmeliet & Jain, 2011). This signaling pathway consists of two receptors, Tie-1 and Tie-2, and three ligands, Ang-1, Ang-2 and Ang-4. Overall, the Ang/Tie receptor/ligand system provides a switch between maintaining vessel quiescence and allowing existing vessels to respond to angiogenic stimuli. Ang-1 functions as a Tie2 agonist and is released by mural cells, while Ang-2 is a competitive Ang-1 antagonist and is released by endothelial tip cells (Augustin, Koh, Thurston, & Alitalo, 2009; Gaengel et

al., 2009). In quiescent endothelial cell layers such as those present in mature vessels, Ang-1 helps further stimulate quiescence by causing Tie2 clustering at cell-cell junctions, recruiting additional mural cells, and stimulating basement membrane deposition (Saharinen et al., 2008). In an angiogenic context, however, endothelial tip cells release Ang-2, which antagonizes Ang-1/Tie2 signaling and causes increased angiogenic activity through enhanced mural cell detachment, increased vascular permeability through loosening of cell-cell junctions, and eventually increased endothelial cell sprouting (Augustin et al., 2009).

The most recently implicated signaling system in angiogenesis is the Notch signaling pathway. During sprouting, activation of VEGFR-2 in tip cells upregulates the expression of Dll4, a soluble ligand for the Notch receptor (Hellström et al., 2007; Phng & Gerhardt, 2009). In turn, the Notch activation in neighboring endothelial cells downregulates VEGFR-2 and upregulates VEGFR-1, making the stalk cells less responsive to the sprouting activity of VEGF. This interplay between VEGFR-1 and VEGFR-2 expression in neighboring cells coordinates the cells' migration toward the tip cell position within growing sprouts (Gaengel et al., 2009; Jakobsson et al., 2010).

The angiogenic process is tightly regulated by a complex milieu of growth factors, which are only briefly discussed here. Many additional intricacies in the regulation of angiogenesis by soluble factors such as Dll4/Notch-mediated competition between tip and stalk cells, crosstalk between different VEGF isoforms and its receptors, and the guidance of sprouts via hypoxic and neurovascular guidance cues are also recent

topics of investigation (Arima et al., 2011; Greenberg et al., 2008; Jakobsson et al., 2010).

1.3.3 Regulation of angiogenesis by the extracellular matrix

The ECM provides cells with a physical anchorage to their surrounding environment and is often a dynamic component of the cellular microenvironment. Vascular cells adhere to the surrounding ECM through integrins and actively degrade and secrete new matrix during periods of angiogenic activity (Carmeliet, 2003; D'Amore & Thompson, 1987). Due to the heterodimeric nature of integrins and their ability to signal bidirectionally, integrin signaling during angiogenesis is both more complex and less well understood than growth factor signaling. While not all integrins are expressed in quiescent endothelium, integrins $\alpha 1\beta 1$, $\alpha 2\beta 1$, $\alpha 4\beta 1$, $\alpha 5\beta 1$, $\alpha 6\beta 1$, $\alpha 9\beta 1$, $\alpha 6\beta 4$, $\alpha \nu\beta 3$ and $\alpha \nu\beta 5$ have all been implicated in angiogenesis (Avraamides, Garmy-Susini, & Varner, 2008; Desgrosellier & Cheresh, 2010; HodiVala-Dilke, 2008). Animal and *in vitro* studies and have shown that blocking integrin $\alpha \nu\beta 3$, $\alpha \nu\beta 5$, $\alpha 5\beta 1$, $\alpha 1\beta 1$, or $\alpha 2\beta 1$ inhibits angiogenesis *in vivo* or in *ex vivo* angiogenic models (Brooks, Silletti, Schalscha, Friedlander, & Cheresh, 1998; Friedlander et al., 1995; Kim, Bell, Mousa, & Varner, 2000; Senger et al., 1997). Integrins $\alpha \nu\beta 3$ and $\alpha \nu\beta 5$ are particularly well studied and appear to be upregulated in response to proangiogenic factors in both healthy tissues and in tumors (Avraamides et al., 2008; R. Silva, D'Amico, HodiVala-Dilke, & Reynolds, 2008). Further complexity, however, is suggested by integrin knockout studies, which suggest that integrins $\alpha \nu$, $\beta 3$, $\beta 5$ and $\alpha 2$ are not always required for angiogenesis (Bader, Rayburn, Crowley, & Hynes, 1998; X. Huang, Griffiths, Wu, Farese, & Sheppard, 2000; Zhang et al., 2008).

Given integrins' ability to transmit signals bidirectionally across the cell membrane and to interact with a variety of extracellular molecules, they are said to function as hubs that coordinate endothelial cell behavior during angiogenesis (Contois, Akalu, & Brooks, 2009). Specifically, integrins possess the ability to bind to growth factors such as VEGF, bFGF, and Ang-1 as well as receptors including VEGFR-2 and FGFR (Avraamides et al., 2008). These interactions have been shown to stimulate vessel growth by upregulating and activating proteases secreted by invading tip cells and promoting vessel maturation by enhancing the adhesion of endothelial cells and pericytes to their shared basement membrane (Desgrosellier & Cheresh, 2010; HodiVala-Dilke, 2008).

Finally, it is important to note the role of the ECM components in regulating angiogenesis. Endothelial cells and the surrounding pericytes share a basement membrane that is primarily composed of laminin and type IV collagen (Carmeliet, 2003; Simon-Assmann, Orend, Mammadova-Bach, Spenlé, & Lefebvre, 2011). During sprouting, the basement membrane and surrounding ECM components must be degraded in order to allow for the migration of emerging sprouts. Upon induction of angiogenic sprouting, proteases such as MT1-MMP proteolytically degrade the basement membrane and expose cryptic chemotactic motifs in the ECM (Carmeliet, 2003; Chun et al., 2004). The degradation of the surrounding matrix allows for the deposition of provisional matrix proteins such as fibronectin and denatured collagen, which again signal through integrins (Arroyo & Iruela-Arispe, 2010). In addition, the newly exposed cryptic binding sites provide additional proangiogenic signaling cues that were not present in the quiescent

state (Ghajar, George, & Putnam, 2008b). A specific example includes the cleavage of type IV collagen, which exposes cryptic binding sites that bind upregulated $\alpha\beta3$ integrins during angiogenesis (J. Xu et al., 2001). During quiescence, the presence of the surrounding ECM components helps maintain endothelial cells in an antiproliferative state (Carmeliet & Jain, 2011). Lastly, MMPs help regulate the angiogenic process by liberating matrix-bound growth factors such as VEGF and FGF (Bergers et al., 2000). While matrix bound isoforms of VEGF have been shown to support vessel branching, soluble VEGF that has been cleaved by MMPs has been shown to enlarge vessels (Iruela-Arispe & Davis, 2009). An additional layer of complexity is introduced into the regulation of angiogenesis by proteases due to their ability to release anti-angiogenic signals such as angiostatin (Folkman, 2007).

1.3.4 Regulation of angiogenesis by cell-cell contacts

Due to the multicellular nature of blood vessels, cell-cell junctions play a fundamental role in all steps of angiogenesis (Nguyen & D'Amore, 2001). Notably, a major form of endothelial cell-cell signaling occurs through gap junctions via the connexin family of proteins (Söhl & Willecke, 2004). These proteins have traditionally been studied most thoroughly in quiescent vessels, where endothelial cells use this signaling mechanism for long distance communication. In this context, studies have shown that signaling via gap junctions regulates growth and differentiation of cells within the vessels (Gärtner et al., 2012). The role of connexins in angiogenesis, however, is less well understood. 21 different connexins have been identified in humans and they exhibit tissue-specific expression patterns (Söhl & Willecke, 2004). Additional complexity is introduced by the

involvement of different connexins in endothelial-endothelial, smooth muscle-smooth muscle and endothelial-smooth muscle gap junctions. Nevertheless, studies have shown that endothelial specific knockout of Cx40 and Cx37 in mice results in severe vascular abnormalities (Simon & McWhorter, 2002). In conjunction with cell culture models, these studies have suggested the importance connexins in the angiogenic process (Bazzoni & Dejana, 2004; Hill, Rummery, Hickey, & Sandow, 2002). The underlying mechanisms, however, remain an area of ongoing research.

In addition to gap junctions, quiescent endothelial cells normally maintain cell-cell junctions via tight junctions (claudins, occludins) and adherens junctions (cadherins) (Jain, 2003). During angiogenesis, however, the junctions between endothelial cells are temporarily dissociated, thus limiting the role of cell-cell junctional proteins in sprouting endothelial cells to steps in which the cells are acting as a synchronized unit (Wallez & Huber, 2008). Within this context, studies have shown that VE-cadherin is required for proper lumen formation and localization of CD34 (Strilic et al., 2009). During the latter stages of angiogenesis, N-cadherin stabilizes contacts between endothelial cells and pericytes, which in turn enhance the production of basement membrane proteins including laminins and collagen IV (Stratman, Malotte, Mahan, Davis, & Davis, 2009). Ultimately, it is a complex interplay of pro- and antiangiogenic growth factors, extracellular signals from the ECM, and cell-cell signals that drive the coordinated process of vessel formation. Given the complexity of this system, it ensures that an optimal vascular network is formed during development and wound healing. It is this

complexity, however, that also makes angiogenic pathways susceptible to a variety of misregulated signals during disease (Ferrara & Kerbel, 2005).

1.3.5 Therapeutic angiogenesis and its role in the clinic

Blood vessels nourish virtually every organ in the body and are critical for development, wound healing and maintenance of homeostasis. In disease, however, insufficient vessel growth can lead to stroke, myocardial infarction, ulcerative disorders and neurodegeneration (Carmeliet & Jain, 2000). Abnormal vessel growth helps drive cancer, inflammatory disorders and pulmonary hypertension among other diseases (Carmeliet, 2003; Folkman, 2007). While anti-angiogenic therapies are by far more widely studied, therapeutic vascularization of ischemic tissues remains a central goal in the study of angiogenesis. Treatment of ischemic heart disease via angiogenic therapies, for example, is receiving significant interest after several clinical studies have demonstrated preliminary success in providing additional blood flow to poorly vascularized areas in patients with myocardial ischemia (Laham et al., 1999; Rosengart et al., 1999; Schumacher, Pecher, Specht, & Stegmann, 1998). In such physiologic contexts where revascularization of injured tissues is delayed or pathological due to insufficient vessel growth, VEGF-related therapies remain the most widely studied (Carmeliet, 2003). Other angiogenic therapies, however, that attempt to introduce angiogenic cues from sources such as platelets and monocytes are also being considered (Bottomley et al., 1999; Griga, Werner, Köller, Tromm, & May, 1999).

Given the inherent complexities that underlie the formation of a stable and functional vasculature, effective angiogenic therapy remains a difficult goal. Indeed,

attempts at promoting new vessel growth that hinge upon the delivery of single growth factors such as VEGF or bFGF have led to the formation of leaky vessels and failed in clinical trials (Henry et al., 2001; Stewart et al., 2009). As additional angiogenic pathways are being elucidated, new clinical targets are continually emerging. For example, angiopoietin has now been shown to help repair or prevent damaged and leaky vessels in diabetic retinopathy, acute macular degeneration, and ischemia/reperfusion injury (Thurston et al., 2000; 1999). Overall, molecules from the VEGF family, Angiopoietin-1, β -Estradiol, the FGF family, IL-8, Leptin, MCP-1, MMPs, NOS, PDGF-BB, TNF- α , Angiogenin, TGF have all been studied in various animal models with promising preclinical results (Pandya, Dhalla, & Santani, 2006).

A variety of novel approaches to deliver proangiogenic agents have also recently been developed. These range from gene therapy approaches utilizing viral delivery of recombinant growth factors to biomaterials with controlled release properties (Ferrara & Kerbel, 2005; Folkman, 2007; Pandya et al., 2006). Despite advances, the clinical viability of these therapies remains to be tested in a controlled setting. Notably, initial trials in which patients with myocardial or limb ischemia were treated with VEGF-A, VEGF-C, FGF-1, FGF-2 and FGF-4 showed promising results, but larger placebo-controlled trials that utilized recombinant proteins or gene therapy later yielded only marginal results (Henry et al., 2003; Lederman et al., 2002; Simons, 2005). Most recently, attempts at cell-based strategies for revascularization using bone-marrow derived endothelial progenitor cells have demonstrated additional promise (Rafii & Lyden, 2003). Transplantation of bone marrow mononuclear cells into ischemic muscle

of patients suffering from peripheral arterial disease resulted in restored limb function (Tateishi-Yuyama et al., 2002; Tomita et al., 1999). Larger placebo-controlled studies, however, will again be required to validate these findings and assess long-term benefits.

The failures of growth factor therapies and emergence of cell-based strategies highlights the need for a more integrated approach to angiogenic therapies (Yoshida et al., 2010). In an attempt to help restore the appropriate microenvironmental cues necessary for proper vascularization of tissue, many tissue-engineered vascularization strategies are quickly emerging as potentially viable methods for properly revascularizing injured tissues (Thwaites, Reebye, Mintz, Levicar, & Habib, 2012).

1.4 Tissue engineering approaches to promote angiogenesis

Shortly after the inception of tissue engineering as a field, vascularization quickly emerged as a central topic of research (Kaully, Kaufman-Francis, Lesman, & Levenberg, 2009; Lovett et al., 2009). The need to vascularize engineered tissues combined with unmet clinical needs for therapeutic angiogenesis have sparked significant research efforts. Novel integrated approaches that utilize growth factors, synthetic matrices and cells often in combination hold great promise. It should be noted, however, that this area of research is in a much more nascent state than the angiogenic therapies discussed in the previous section, and none of the approaches discussed here have yet been thoroughly tested in human clinical trials. As these efforts begin to enter human trials over the coming years, a number of viable approaches are likely to emerge (Orlando, Wood, et al., 2011b). The current strategies for vascularization and promoting angiogenesis can be

categorized into two major categories: 1) approaches that utilize biofunctional materials and 2) approaches that utilize cells to induce vascularization (Lovett et al., 2009).

1.4.1 Biofunctional materials for inducing angiogenesis

Given our understanding of the role of cell-matrix and cell-cell adhesive and mechanical cues in the angiogenic process, it is clear that proper signals from the ECM are necessary for effective vessel growth. A variety of both natural and synthetic materials have been studied for their ability to provide these cues (Lutolf & Hubbell, 2005; Moon et al., 2011; Tian & George, 2011). Two synthetic material backbones have been primarily used for inducing vascularization: poly(lactic-co-glycolic acid) (PLGA) and polyethylene glycol (PEG) hydrogels. PLGA, a biodegradable and biocompatible polymer, has been used extensively in medicine as a temporary mechanical support in implantable medical devices (Athanasίου, Niederauer, & Agrawal, 1996). The use of synthetic polymers for inducing angiogenesis allows full control over a number of material properties and avoids the risks associated with using potentially immunogenic natural materials (Lutolf & Hubbell, 2005; Orlando, Wood, et al., 2011b). Most notably, Mooney and colleagues have developed implantable PLGA scaffolds that sequentially release VEGF and PDGF and induce vessel ingrowth when implanted into mice (R. R. Chen, Silva, Yuen, & Mooney, 2006). While promising, it is not yet clear whether this approach is capable of generating mature vessels that remain stable over long periods of time (Peters et al., 2002). Most recently, studies utilizing this approach have also demonstrated that combinations of bFGF, VEGF and S1P are also capable of inducing vascularization *in*

vivo (Tengood, Kovach, Vescovi, Russell, & Little, 2010; Tengood, Ridenour, Brodsky, Russell, & Little, 2011).

Recently, PEG hydrogels have emerged as an alternative synthetic scaffold for inducing angiogenesis (Zisch et al., 2003). Since natural ECMs are hydrogels, the structure of PEG provides a close synthetic mimic for host ECM (Moon et al., 2011). PEG hydrogels also possess highly tunable mechanical properties and can be functionalized with various proteins or peptides to render the material adhesive and degradable (Lutolf & Hubbell, 2003). Angiogenic studies with PEG hydrogels have demonstrated enhanced angiogenesis using the materials in *in vitro*, *ex vivo* and *in vivo* models of angiogenesis (Leslie-Barbick, Moon, & West, 2009; Moon, Lee, & West, 2007).

While promising, the application of synthetic or natural matrices alone has yet to demonstrate the ability to rapidly vascularize tissues. These approaches, however, are helping to provide insights into the design of more complicated strategies involving the use of exogenous cells. For example, Putnam and colleagues have focused on the interplay between ECM mechanics and vascularization potential (Ghajar, Chen, Harris, Suresh, et al., 2008a; Kniazeva & Putnam, 2009). This work is paving the road for understanding critical design parameters in developing the next generation of vascularization strategies.

1.4.2 Cell-based strategies for generating microvasculature

A critical drawback of vascularization strategies that rely on the use of acellular synthetic or natural matrices is the inability to rapidly vascularize an engineered or damaged host

tissue (X. Chen et al., 2010; Jain, Au, Tam, Duda, & Fukumura, 2005). Specifically, large engineered tissues must become quickly vascularized (1-2 days) upon implantation in order to prevent parenchymal cell death (Orlando, Baptista, et al., 2011a). In a disease setting, ischemic tissues need to be revascularized as quickly as possible to minimize necrosis and tissue damage. Accordingly, attempts to more rapidly vascularize tissues have attempted to leverage the use of cells embedded within natural or synthetic scaffolds to help speed up the vascularization process (Kaully et al., 2009; Lovett et al., 2009).

The driving principle behind cell-based vascularization strategies is to implant a rudimentary vascular network or a population of vascular cells capable of rapidly connecting with the host vasculature (X. Chen et al., 2009). Most current studies in this area remain limited to natural matrices. Though synthetic polymer chemistry is advancing rapidly, natural matrices inherently possess the proper adhesive, mechanical and degradable properties known to be necessary for proper vascularization (Kaully et al., 2009). It is likely that a switch to synthetic materials will occur over time as they become better understood and more tunable to these applications.

A seminal study in the area of cell-based vascularization approaches was first performed by Jain and colleagues in which they combined endothelial cells and embryonic mesenchymal cells in a type I collagen gel (Koike et al., 2004). Implantation of this construct into mice resulted in the formation of vessels that remained stable for four months. Furthermore, portions of the vessel walls contained the originally implanted cells, demonstrating for the first time that exogenous cells directly contribute to the formation of vessels. Subsequent studies have since focused on varying cell-type, ECM

material or *in vitro* culture conditions in an attempt to find a set of optimal conditions for generating functional vasculature *in vivo* (Lovett et al., 2009). In another study Jain and colleagues used endothelial progenitor cells to demonstrate the ability of their engineered vessels to remain stable up to one year *in vivo* upon implantation (Au, Tam, Fukumura, & Jain, 2008b). Most recently, work by George and colleagues has focused on rapidly vascularizing the engineered tissues once implanted. Using endothelial cells and a variety of supporting cell types embedded in a fibrin matrix, they demonstrated the formation of perfused vessels within one day of implantation (X. Chen et al., 2009; 2010). Additional biological insights have shown that the type of cell used within these engineered constructs can come from an autologous source (Melero-Martin et al., 2008), and that the presence of myeloid cells, an immune component, is necessary for proper vessel formation (Fantin et al., 2010). Evidence also suggests that implanted vascular cell networks anastomose with the host vasculature via a novel “wrapping-and-tapping” mechanism (Cheng et al., 2011).

While work is underway to gain a better understanding of the vascularization mechanisms within these engineered constructs – likely a combination of vascular network assembly, angiogenesis and anastomosis – basic insights have already begun to drive their application towards generating functional engineered tissues (Orlando, Baptista, et al., 2011a; Vacanti, 2012). One particular area of focus is that of vessel organization. To date, all cell-based vascularization techniques have used randomly seeded cells within a scaffold that provide no specific patterning cues to the growing vasculature (Zheng et al., 2011). Interestingly, George and colleagues have demonstrated

that by preculturing cells within fibrin constructs, which allows them to organize into rudimentary networks, a more rapid formation of perfused vasculature can be achieved *in vivo* upon implantation (X. Chen et al., 2009). More recent work has shown that organized vessel networks improve the function of skeletal muscle grafts upon implantation (Koffler et al., 2011). Together these studies suggest that patterning of engineered vasculature is an area worthy of further investigation. Indeed, vasculature generated via developmental processes is guided by a number of patterning cues and, through a sequence of regulated spatiotemporal signals, reaches a geometry that is optimal for the perfusion of the surrounding tissue (LaRue et al., 2003; Melani & Weinstein, 2010; Rivron et al., 2012; Ruhrberg et al., 2002). In the engineered context, an ability to pattern the vasculature *de novo* would usher in the possibility of studying optimal vessel patterns and subsequently using them to develop larger functional engineered tissues for use in the clinic (Orlando, Baptista, et al., 2011a; Rustad et al., 2010).

1.5 The vasculature in a disease context: pulmonary arterial hypertension

Proper vessel function is critical for maintaining homeostasis in healthy organisms. Malformations or aberrant vessel function contribute to the pathogenesis of many diseases, and cardiovascular disease remains the biggest cause of deaths worldwide (Carmeliet, 2003; Carmeliet & Jain, 2000; Lloyd-Jones et al., 2010). One specific example includes pulmonary arterial hypertension (PAH), a condition characterized by

elevated pulmonary arterial pressure (Lourenço, Fontoura, Henriques-Coelho, & Leite-Moreira, 2011). In patients with PAH, the increased vascular resistance in the pulmonary circulation places a greater workload on the heart and ultimately leads to right ventricular failure and premature death. PAH can be hereditary, associated with other conditions (including congenital heart disease, HIV and others) or idiopathic. Idiopathic pulmonary arterial hypertension (IPAH), which occurs in the absence of identifiable risks, is particularly difficult to diagnose (Gaine & Rubin, 1998; Rubin, 1997). Patients present with general symptoms and diagnosis is only made after the exclusion of other heart and lung diseases known to cause elevations in pulmonary arterial pressure (Chin & Rubin, 2008). In patients with IPAH, the estimated survival rates for patients receiving treatment at 1, 2, and 3 years are 83, 67, and 58%, respectively (Humbert et al., 2010). Despite advances in hypertension research, no cure currently exists for PAH (Agarwal & Gomberg-Maitland, 2011).

1.5.1 Pathology and current treatments

Pulmonary arterial hypertension is typified by hyperproliferation and remodeling within the small pulmonary arteries, which results in increased blood pressure within the lung vasculature. Characteristic abnormalities in the pulmonary arteries of PAH patients include thickening of the intimal, medial and adventitial compartments (Chin & Rubin, 2008; Gaine & Rubin, 1998; Rubin, 1997). Detailed histological examination of pulmonary arterioles in patients with IPAH shows neointimal thickening, pulmonary arteriolar occlusion, and plexiform lesions, suggesting that IPAH is a primarily vasoproliferative disease with accompanying vasoconstriction as well as catabolism and

de novo synthesis of components of the extracellular matrix (ECM) (Chin & Rubin, 2008; Farber & Loscalzo, 2004; Humbert et al., 2004; Jones & Rabinovitch, 1996; Jones, Cowan, & Rabinovitch, 1997; Pietra et al., 1989).

Three classes of drugs are currently used to treat PAH: prostacyclin analogs, endothelin receptor antagonists and phosphodiesterase type 5 inhibitors (Agarwal & Gomberg-Maitland, 2011). The vasoconstriction and progressive vascular cell proliferation seen in PAH patients may stem from low levels of endogenous prostacyclin (Rubin et al., 1982). Thus, prostacyclin analogs were introduced to target the prostaglandin I receptor, which is capable of inducing potent vasodilation through the activation of cyclic adenosine monophosphate (Agarwal & Gomberg-Maitland, 2011). The most notable drug in this category and the current first-line preferred drug for PAH treatment is epoprostenol. Its long-term benefits have been reported by two large centers and it remains as the only therapy for advanced PAH that has proven to enhance survival (Barst et al., 1996). While demonstrating very favorable outcomes and improving patients' quality of life significantly, its administration remains complicated due to the compounds' 3-5 min plasma half-life (Fuentes, Coralic, & Dawson, 2012). Because of this limitation, patients undergoing treatment with epoprostenol must use a continuous infusion IV pump, which requires daily care and maintenance (Agarwal & Gomberg-Maitland, 2011). More recently, two newer prostacyclin analogs have been introduced with longer half-lives, which allow for subcutaneous or inhalable routes of administration (Laliberte, Arneson, Jeffs, Hunt, & Wade, 2004; McLaughlin et al., 2010).

Endothelin-A and endothelin-B are targets of the second class of drugs used in the treatment of PAH . Endothelin-1 is a potent vasoconstrictor and has been shown to increase smooth muscle cell proliferation (Boniface & Reynaud-Gaubert, 2011). Endothelin-1 levels in the circulating plasma of PAH patients are increased, further suggesting that its receptors may be a good target for treating PAH (Rubens et al., 2001). Bosentan and ambrisentan are two endothelin receptor antagonists currently in use today. While administration of these two drugs must be closely monitored due to potential liver toxicity issues, they remain widely prescribed to PAH patients (Rubin et al., 2002; Vatter et al., 2002).

Phosphodiesterase inhibitors act by inhibiting phosphodiesterase 5 in the nitric oxide-cGMP pathway. Briefly, nitric oxide elicits vasodilatory and antiproliferative effects via the release of cyclic guanosine monophosphate (cGMP). cGMP, however, is typically rapidly broken down by phosphodiesterase 5 (Agarwal & Gomberg-Maitland, 2011). Thus, this category of PAH drugs aims to induce pulmonary vasorelaxation by preventing this rapid degradation of cGMP (Agarwal & Gomberg-Maitland, 2011). Sildenafil and tadalafil comprise this category of drugs and are both administered orally (Galie et al., 2009; Ghofrani et al., 2002).

Despite the continuous development of drugs in each category, none of these effectively treat the underlying pathophysiology of PAH. Exercise capacity and, more importantly, pulmonary arterial pressures are never returned to normal levels upon administration of these compounds. Over time, even despite the introduction of combination therapies, quality of life in patients remains relatively low and no further

treatments outside the realm of lung transplantation currently exist (Agarwal & Gomberg-Maitland, 2011; Lourenço et al., 2011). Lastly, it should be noted that most of the currently administered drugs have been approved based on short-term studies. Few long-term well-controlled studies have been done to assess clinical outcomes (Barst et al., 2009). In summary, while significant advances in the treatment of PAH have been made over the past two decades, no cure currently exists and little is understood about the underlying etiology of the disease.

1.5.2 The role of vascular smooth muscle cells in pulmonary hypertension

The majority of drugs first used in treating PAH were chosen for their vasodilatory effects. However, several have now demonstrated anti-proliferative effects *in vitro* and in animal models (Jiang, Zhou, & Liu, 2012; Wolf, Sauter, Risler, & Brehm, 2005).

Abnormal SMC proliferation within pulmonary arteries of PAH patients is one of the hallmark characteristics of the disease (Humbert et al., 2004; Lourenço et al., 2011).

Hyperproliferating SMCs are found in the plexiform lesions that are found occluding the intraluminal space in patients with severe PAH (Pietra et al., 1989).

It was shown more than thirty years ago that injured SMCs undergo a shift from a contractile phenotype to one that is synthetic and characterized by increases in proliferation, migration and ECM synthesis (Chamley, Campbell, McConnell, & Gröschel-Stewart, 1977). Subsequently, work over the past several decades has begun to focus on identifying drugs that are effective at inhibiting this proliferative response in PAH. Several studies demonstrated the ability of statins to inhibit SMC proliferation and migration and slow intimal hyperplasia (Corpataux, Naik, Porter, & London, 2005;

Corsini et al., 1999; Porter et al., 2002)). It has been reported that a possible mechanism of action in this context is through Rho GTPase prenylation (Laufs, Marra, Node, & Liao, 1999). More recent studies have specifically implicated aberrant PDGF signaling in SMC hyperproliferation (Humbert et al., 2004). Ito and colleagues showed that PDGF stimulation of SMCs isolated from lungs of PAH patients resulted in higher proliferation rates than those in control SMCs (Ogawa et al., 2005). In a follow-up study, they further demonstrated that simvastatin inhibits this PDGF-induced hyperproliferation through an upregulation of the cell cycle inhibitor p27 (Ikeda et al., 2010). Interestingly, they found that simvastatin treatment correlated with the disorganization of actin fibers and the inhibition of Rho translocation from the cytoplasm to the membrane, again suggesting that Rho GTPase signaling may play an important role. Their basic findings are also supported by studies that demonstrate the reversal of experimentally induced PAH in rodent models via the administration of PDGF inhibitors (Schermyly et al., 2005).

In addition to PDGF, studies have also begun to implicate serotonin in PAH SMC hyperplasia (Lourenço et al., 2011). Eddahibi and colleagues have found that increased serotonin activity through upregulation of the 5-HTT serotonin transporter in isolated PAH SMCs or animal models of PAH contribute to SMC hyperproliferation (Guignabert et al., 2006; Marcos et al., 2004). Inhibition of 5-HTT in a rodent PAH model also suggested that it is a novel target worthy of consideration in the search for additional therapies. Finally, two studies have implicated aberrant endothelial-SMC interactions (Eddahibi et al., 2006) and glycogen synthase kinase 3beta (Sklepiewicz et al., 2011) as

having direct involvement in the progression of PAH. Combined, these studies give hints at the types of molecular targets that might be at the focus of future PAH therapies.

1.5.3 Regulation of smooth muscle cell proliferation by the microenvironment

Fully differentiated smooth muscle cells in the healthy adult typically exhibit very low rates of proliferation (S. Schwartz, Campbell, & Campbell, 1986). During times of injury or vascular disease, however, these cells undergo a phenotypic switch and begin proliferating rapidly (A. W. Clowes, Reidy, & Clowes, 1983). While SMC proliferation is largely controlled by the same mechanisms as in other cell types, there are several microenvironmental cues that are of additional relevance when considering smooth muscle cell biology in the disease context. First, growth factors and other compounds that are involved in angiogenesis and vascular disease such as nitric oxide, EGF and PDGF have been shown to regulate SMC proliferation *in vivo* (Ferns et al., 1991; Lindner & Reidy, 1991; Nabel et al., 1993).

PDGF is a potent activator of SMC proliferation that is thought to primarily upregulate SMC proliferation via activation of ERK (Zhan et al., 2003). As discussed in the previous section, PDGF-induced hyperproliferation in PAH is now being directly targeted by several drugs. The effects of inhibiting downstream effectors such as ERK in PAH models, however, remain to be investigated. Although the antiproliferative effects of nitric oxide, a widely used and studied vasodilator, have been known for some time, its mechanisms of action are very broad and are still being studied today (Tsihlis et al., 2011). In general, however, it is known that NO relies on the upregulation of cGMP and subsequent downregulation of the EGF-MAP kinase cascade (Yu, Hung, & Lin, 1997).

Overall, essentially all potent SMC mitogens tend to activate receptors with intrinsic tyrosine kinase activity (Cadena & Gill, 1992). In turn, these receptors activate corresponding intracellular pathways including MAP kinase, protein kinase B and protein kinase C (Berra et al., 1993; Coffey, Jin, & Woodgett, 1998; Seger & Krebs, 1995). Ultimately, these growth factors share activation of the cyclin-dependent kinases in the cell cycle pathway as a final common signaling pathway (Newby & Zaltsman, 2000).

In addition to growth factors, vascular SMC proliferation is regulated by other extracellular cues derived from the surrounding ECM (Assoian & Marcantonio, 1997). Most notably, heparan sulfate proteoglycans inhibit proliferation directly by inhibiting signaling by growth factors via the protein kinase C pathway (Y. Wang & Kovanen, 1999). Other components of the basement membrane have also been shown to help maintain a non-proliferative phenotype in normal SMCs. Specifically, Ross and colleagues showed that fibrillar collagen (versus monomeric) inhibits SMC proliferation via Cdk2 (Koyama, Raines, Bornfeldt, Roberts, & Ross, 1996). Lastly, mechanical stimuli such as stretch and ECM stiffness have begun to emerge as additional effectors of SMC proliferation (Gambillara, Thacher, Silacci, & Stergiopoulos, 2008; C. Li & Xu, 2000; Shaw & Xu, 2003; Shyu, Chao, Wang, & Kuan, 2005). While regulation of proliferation via mechanical stimuli has been shown in other cell types, we now know that stretching of the ECM substratum can induce SMC proliferation in the absence of cell-cell contacts (W. F. Liu, Nelson, Tan, & Chen, 2007). Overall, recent insights into the pathophysiology of PAH suggest that regulation of SMC proliferation via ECM

signals and mechanics may play a role in the disease progression. This area of research, however, remains largely unexplored in the context of PAH.

1.6 Summary

Over the last several decades, our knowledge of vascular disease and the underlying biology have increased tremendously. Studies described in the preceding sections have served as the inspiration for the work presented in the subsequent chapters. First, a study on the topic of engineered vasculature is presented in Chapter 2. This research draws on existing insights into the fundamental processes that underlie angiogenesis and attempts to extend current microvascular engineering approaches by introducing the ability to geometrically pattern vessels *in vivo*. Second, our study of PAH presented in Chapter 3 provides new insights into the proliferative regulation of IPAH SMCs. In a broader context, these two studies comprise part of an ongoing paradigm shift in the fields of bioengineering. Drawing upon decades of ongoing research into fundamental biological processes, tissue engineering strategies and therapeutic approaches for treating vascular disease are increasingly being designed based less on anecdotal findings and more on a fundamental understanding of the underlying biological processes.

CHAPTER 2: Patterned vascular networks improve function of engineered tissues *in vivo*

2.1 Introduction

Engineered organ tissues are emerging as a new class of therapies to combat the scarce supply of heterologous donor organs available for transplant (Vacanti & Langer, 1999). While highly promising, a critical limitation in the field is the successful vascularization of large tissue constructs (Orlando, Baptista, et al., 2011a; Rustad et al., 2010). The future utility of engineered tissues relies on the development of vascular architectures that effectively deliver blood to these large and geometrically complex tissues (Kaully et al., 2009).

In vivo, native tissue is comprised of specialized cells and vasculature embedded within tissue specific ECM in a highly organized manner. The liver, in particular, has a precisely-defined microarchitecture involving a complex interplay between hepatocyte cords, bile canaliculi, and microvessel networks that is thought to impact metabolic mass transport and tissue function (Reid, Fiorino, Sigal, Brill, & Holst, 1992). Indeed, it is the loss of this architecture due to replacement by fibrotic tissue and regenerative nodules that defines chronic cirrhosis (Ishibashi, Nakamura, Komori, Migita, & Shimoda, 2009). Successful therapeutic tissue engineering strategies will rely in part on the ability to recapitulate proper tissue organization by integrating defined vascular networks with tissue specific cellular structures. However, current strategies to study the combined effects of vascular organization and parenchymal juxtaposition have been limited to

random vascular self-assembly and tubulogenesis within natural and engineered ECMs as described above in section 1.3.2. While promising, such strategies are currently unable to provide the spatial and geometric control of vessel architecture that is necessary for parenchymal cell survival within solid tissues (Vacanti, 2012).

In this chapter, we describe the development and application of a novel approach for creating functional, spatially organized vascular architectures within engineered tissues. The underlying hypothesis of our work is that patterned constructs of endothelial cells can be used to induce vascularization *in vivo*. Our approach utilizes micropatterning techniques to organize endothelial cells into geometrically defined ‘cords’ that drive the formation of fully functional, patterned capillaries upon implantation into mice. We also demonstrate the ability of our vascularization strategy to maintain the viability and proper function of engineered hepatic tissue.

2.2 Generation of patterned endothelial cell ‘cords’ *in vitro*

2.2.1 Design, fabrication and optimization of a second-generation device for generating patterned cell cords

Previous efforts in our laboratory have focused on the development of a technique for spatially patterning cells within micromolded collagen gels (Fig. 2.1A) (Raghavan, Nelson, Baranski, Lim, & Chen, 2010a). Using this technique, it was demonstrated that patterning endothelial cells embedded within collagen could be used to generate ‘cords’ that contain cell-cell junctions characteristic of physiologic endothelium (Fig 2.1B).

To enable their implantation and use in animal studies, we demonstrated that these cords could be removed from their underlying polydimethylsiloxane (PDMS) templates (Fig. 2.2). This removal was accomplished by embedding the fully formed cords within a collagen gel, allowing the entire collagen/cord construct to be mechanically separated from the PDMS device. Use of PBS during the removal process helped to reduce damage to the construct and aid in its removal .

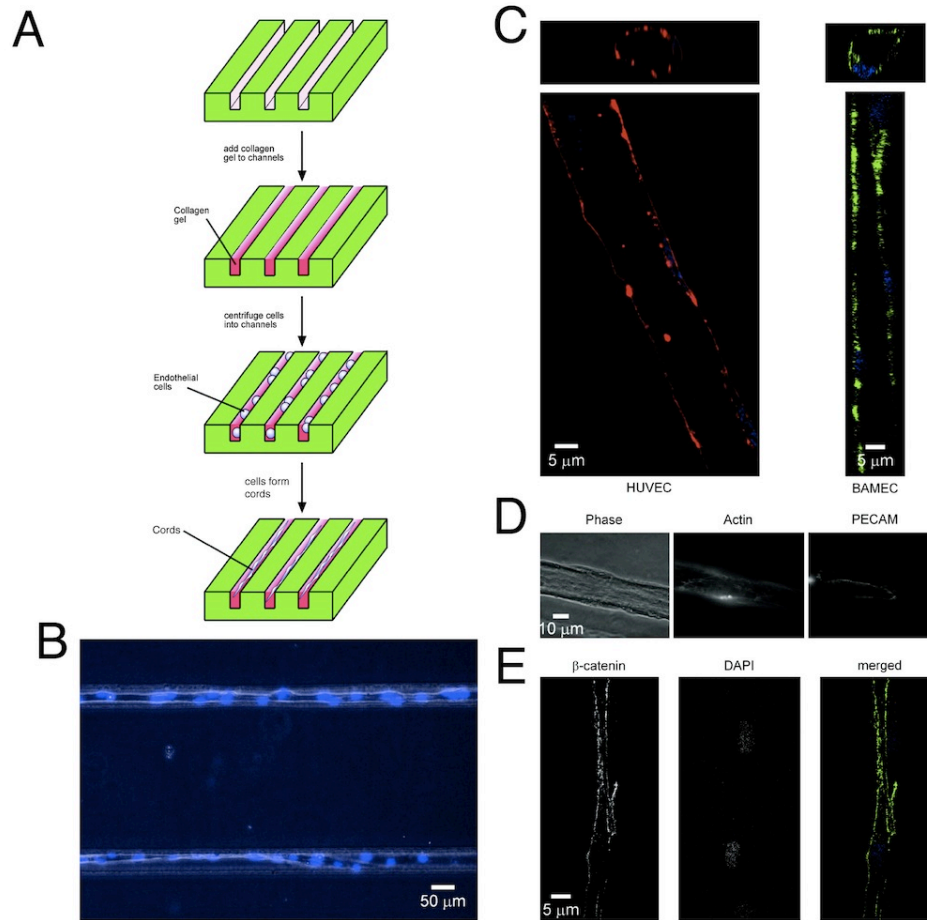


Figure 2.1 Early technique for generating patterned cell cords (A) Schematic of method for generating cords by organizing cells and collagen within microfabricated PDMS channels. (B) Phase contrast images of cords formed within 50 μm wide and 50 μm tall channels after 24 h in culture. (C) Fluorescence images of endothelial cell cords (red and green, actin; blue, nuclei) consisting of HUVECs and BAMECs cultured for 48 and 24 h, respectively. (D) PECAM (CD31) and β -catenin (E) are found at cell-cell junctions in EC cords. BAMECs, bovine adrenal microvascular endothelial cells. Data reprinted with permission (Raghavan, Shen, Desai, Sniadecki, Nelson, & Chen, 2010b).

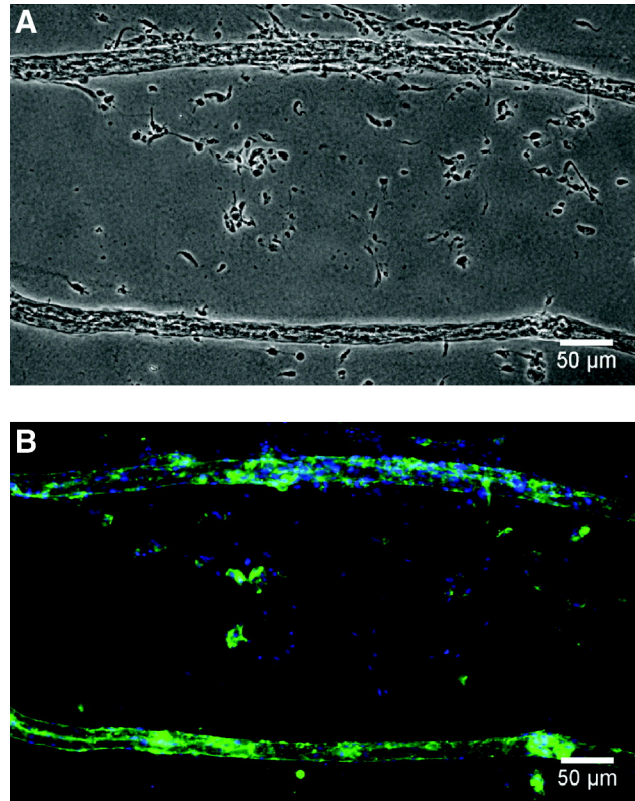


Figure 2.2. Removal of cords from PDMS template. Phase contrast (A) and fluorescence (B) images of HUVEC cords removed after 24 h in culture into 2.4 mg/ml collagen gel. Cells are labeled for actin (green) and nuclei (blue). Data reprinted with permission (Raghavan, Nelson, Baranski, Lim, & Chen, 2010a).

Given the ability to remove cords from the PDMS templates, we hypothesized that they could be used to generate geometrically defined vascular networks *in vivo*. Others have previously shown that improved organization of endothelial cell networks and transplanted capillary beds leads to improved vascularization (X. Chen et al., 2009;

Laschke et al., 2010). We predicted that the established cell-cell contacts within cords comprised of endothelial cells would help enhance their angiogenic potential and that patterned cord geometry would be preserved upon implantation and subsequent vessel formation *in vivo*. More broadly, we hypothesized that the implantation of patterned EC cords could be used to control the architecture of engineered vasculature *in vivo*.

While effective in demonstrating a proof of concept, use of the first-generation device for creating EC cords in extensive studies of vascularization was prohibitively time consuming, required large numbers of cells (> 6 million per device), and yielded cords that were limited in length (< 1 cm). To overcome these limitations, we designed, fabricated and optimized a second-generation system for producing and removing EC cords (Fig. 2.3). Fabrication of the new devices utilized a double-casting technique to generate microchannels with surrounding flat regions within a PDMS well rather than relying on a separate gasket (Fig. 2.3A, B). The second generation device was designed to enable generation of larger numbers of cords using fewer cells (2 million per device). The new device configuration allowed for cords to be easily removed from the underlying PDMS template and embedded within other ECM materials to generate implantable tissue constructs. The larger areas of cords could later be cut or ‘punched out’ with a biopsy punch in preparation for implantation. Overall, the redesign resulted in a twelve-fold reduction in the number of cells required to generate an implantable tissue construct.

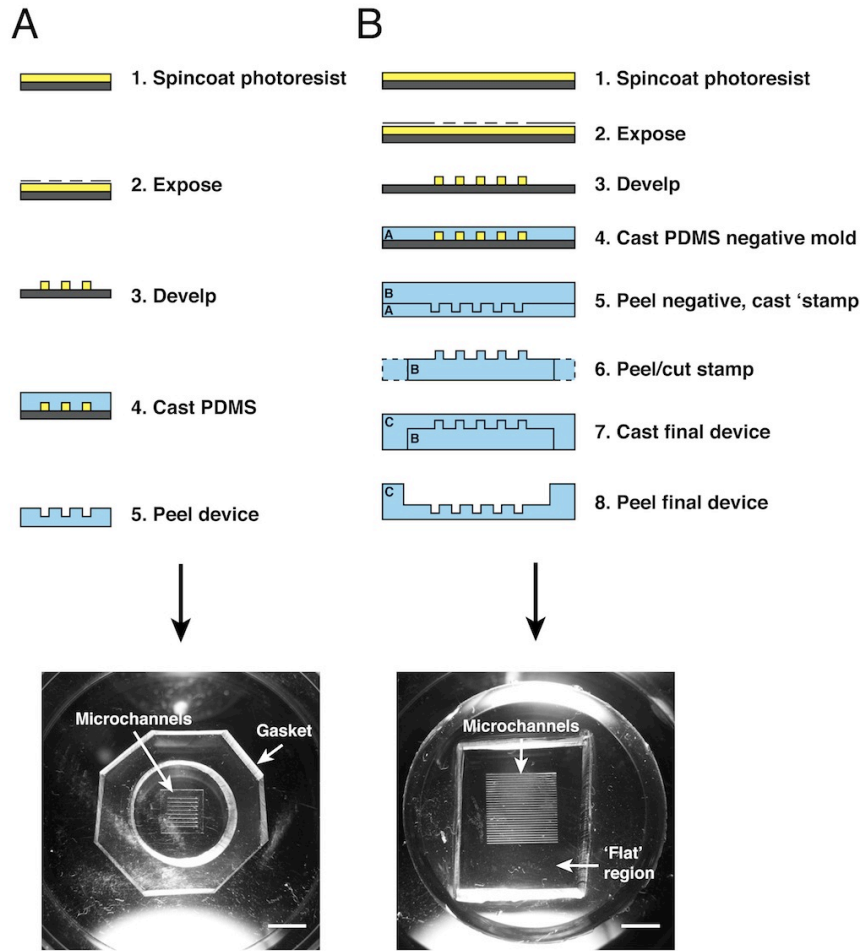


Figure 2.3. First- and second-generation PDMS devices for generating cords. (A) Process flow describing technique for fabricating first-generation device for generating cords. (B) Process flow describing technique for fabricating second-generation devices for generating cords. Macroscopic images of final devices are shown in bottom panels. (bars: 10 mm)

The complete redesign of the device required several optimizations to techniques for generating cords. First, treatment of the PDMS with Pluronic F-127 required modification. Pluronic, a nonionic, surfactant polyol, is used to render the surface of

PDMS hydrophilic, making it largely non-adhesive to proteins and cells (M.-H. Wu, 2009). Here, a Pluronic treatment that is too mild will prevent proper cord formation by allowing cells to adhere and migrate on the PDMS surfaces. Conversely, a Pluronic treatment that is too harsh will render the PDMS surfaces almost entirely non-adhesive causing the cords to float out of the microchannels upon addition of growth medium. Through empirical tests, we determined that proper Pluronic treatment that achieves the correct balance of adhesive cues is obtained by exposing the PDMS templates to a 0.02% (w/v) Pluronic F-127 solution for 10 minutes. While we found that decreasing the concentration to below 2×10^{-5} % was required to observe any effects of decreased concentration, the length of Pluronic treatment had a significant impact on its effect. Additionally, it should be noted that the negative PDMS masters from which the final devices are cast could be reused no more than three times. After three casts, we observed that the resulting devices were more adhesive to collagen and cells despite treatment with Pluronic. Due to the double casting process, devices cast more than three times also began to exhibit defects in the walls of the microchannels.

Given the larger volume of collagen within the microchannels in the second-generation device, application of the collagen and polymerization times also required optimization. To prevent possibly confounding results and limit the scope of our studies, we chose to fix the collagen concentration at 2.5 mg/ml. The design of the second-generation device, which included flat regions that surrounded the microchannels, allowed for simple dewetting of the collagen by tilting the device and aspirating excess collagen mixture. Proper Pluronic treatment was found to be critical for this dewetting

step. In addition, the time required for the polymerization of the collagen required a balance between ensuring that the gel has fully formed and preventing too much drying of the sample, which led to cell death. Through a series of optimizations, we found that inverting the sample for 5 minutes over a bath of water during polymerization achieved the correct balance of gelation time and humidity and resulted in viable cords. Additional complexity is introduced by the technique used when adding growth medium to the polymerized cords immediately prior to culture. Upon methodically employing a variety of techniques, we determined that allowing large drops of medium to fall onto the microchannels yielded the best results. Briefly, five drops of growth medium are first dispensed into the center and four corners of the microchannels from a height of several millimeters. Subsequent drops are dispensed in a similar manner into the regions between those already placed onto the substrate. As the second set of drops is introduced, the growth medium accumulates into a larger pool that covers the entire area of microchannels containing cords. The final volume of medium is brought up to 750 μ l by dispensing slowly into one of the corners of the device. Importantly, extreme care must be taken during this process not to dislodge the cords from the microchannels during these final steps.

Lastly, additional development of the technique was required to remove the cords into a PDMS-free ECM. While collagen was used in the first-generation device, we used fibrin for *in vivo* studies in order to take advantage of its proangiogenic effects (Hall, Baechi, & Hubbell, 2001; Lesman et al., 2011). After experimentation with a variety of methods, we found that cutting away of the surrounding PDMS well and inversion of the

microchannels containing cords onto a pool of pre-polymerized fibrin yielded the best results. Use of a PDMS gasket helps to ensure that constructs with a controlled thickness are generated. After 15 minutes of polymerization, the sample can then be flooded with PBS, which allows the positive buoyancy of the PDMS to help lift it off of the underlying fibrin matrix. Several layers of cords can be stacked on top of each other to generate more complex geometries. In the final step, an additional layer of fibrin is added to encapsulate the exposed surface of the cords. The large area of the microchannels allows for 6 mm discs to be generated, which are suitable for implantation into mice (Fig. 2.4). A schematic of the process for generating cords using the second-generation of devices is shown in Figure 2.5.

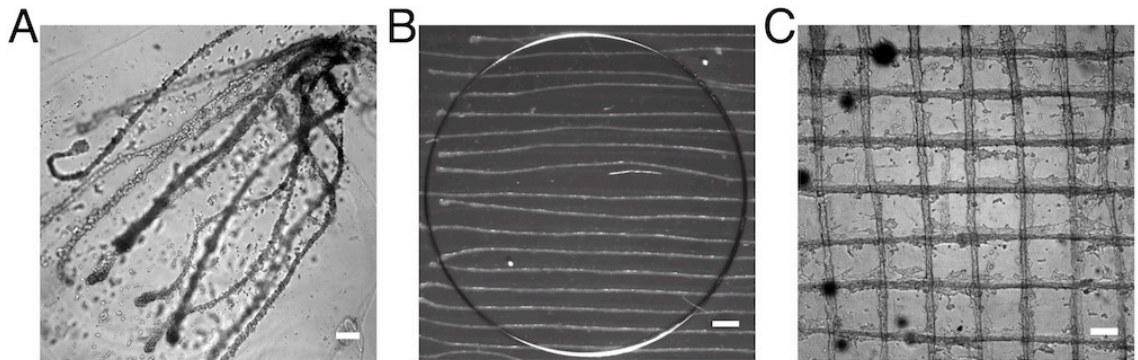


Figure 2.4 Removal of EC cords into fibrin (A) Previous methods of cord removal resulted in cords with disrupted morphology. (bar: 250 μm) (B) Inversion of microchannels onto gaskets containing fibrin results in a preserved cord geometry. Gels can be cut into 6 mm modular constructs suitable for implantation into mice. (bar: 500 μm) (C) Controlled method for removal of cords allows for stacking several devices to generate more complex geometries. (bar: 200 μm)

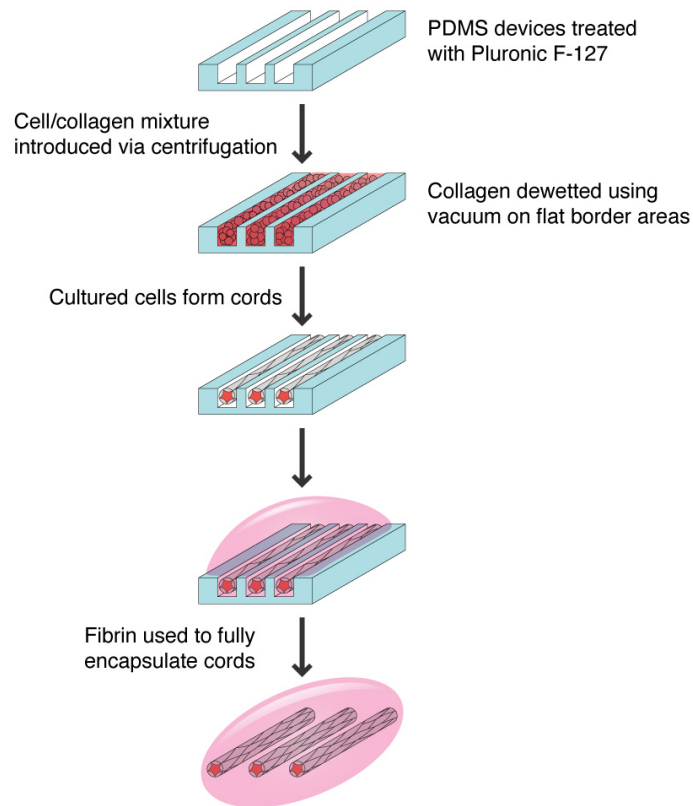


Figure 2.5 Schematic of process used to generate EC cords using second-generation PDMS devices. Design modifications including increased microchannel area and incorporation of flat border regions allow for the removal and generation of larger cords, which are amenable to implantation into mice.

2.2.2 Screening cell types and coculture ratios for use in cords

A variety of endothelial cell types have been used in tissue engineered vascularization strategies (Au, Daheron, Duda, Cohen, Tyrrell, et al., 2008a; Koike et al., 2004; Melero-

Martin et al., 2008; Traktuev et al., 2009). Here, we screened the ability of HUVECs and eEnd.2 cells to organize into networks when cultured within collagen gels *in vitro*. Given our hypothesis that established cell-cell contacts might help enhance the angiogenic effect of implanted cords, we attempted to choose a cell mixture capable of extensive cell-cell interactions and networking behavior. We first tested the eEnd.2 murine embryonic endothelial cell line by culturing the cells in a 2.5 mg/ml collagen gel for 4 days (Williams, Courtneidge, & Wagner, 1988). While these cells exhibited localized networking behavior, significant clumping was observed and large increases in cell number indicated high rates of proliferation (Fig. 2.6). This high rate of proliferation in 3D led us to conclude that the eEnd.2 cell type was a poor candidate for use in a vascularization strategy whose goal it is to generate stable vessels *in vivo*. Next, we tested human umbilical vein endothelial cells (HUVECs), a primary endothelial cell type commonly used in angiogenesis and tissue engineering studies, for their ability to form networks and extensive cell-cell contacts. After 4 days in culture within collagen gels, these cells exhibited limited networking behavior (Fig. 2.7). Proliferation, however, seemed significantly lower than in the eEnd.2 cells.

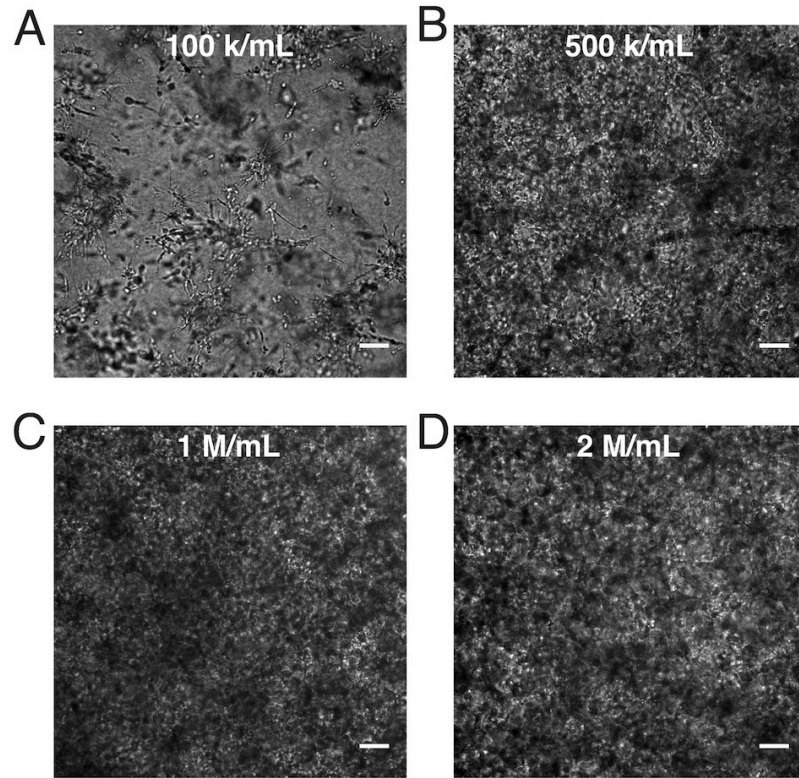


Figure 2.6 Networking behavior of e.End2 cells in collagen gels. Brightfield imaging of e.End2 cells cultured in 2.5 mg/ml collagen for 4 days at concentrations of 1×10^5 cells/ml (A), 5×10^5 cells/ml (B), 1×10^6 cells/ml (C) and 2×10^6 cells/ml (D) shows localized networking (clumping) and suggests extensive proliferation. (bars: 100 μ m)

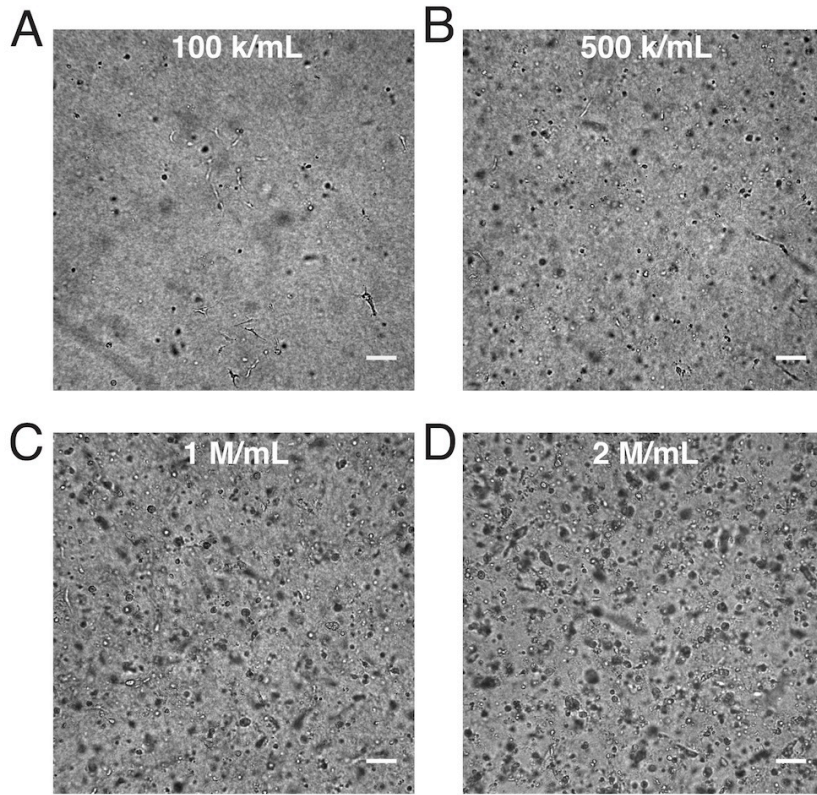


Figure 2.7 Networking behavior of HUVECs in collagen gels. Brightfield imaging of HUVECs cultured in 2.5 mg/ml collagen for 4 days at concentrations of 1×10^5 cells/ml (A), 5×10^5 cells/ml (B), 1×10^6 cells/ml (C) and 2×10^6 cells/ml (D) shows limited networking or cell-cell interactions. (bars: 100 μ m)

C3H10T1/2 is a murine cell line of mesenchymal origin with demonstrated potential to differentiate into pericytes and promote vessel maturation (Hirschi, Rohovsky, & D'Amore, 1998; Koike et al., 2004). We screened the behavior of HUVECs in the presence of varying ratios of 10T1/2s when cultured within collagen gels *in vitro*. Previous results indicated that a density of 1×10^6 HUVECs/ml yielded a cell dense environment that did not lead to clumping. Thus, we included 10T1/2s in culture with

HUVECs at ratios of 1:50, 1:30 and 1:10 (10T1/2s to HUVECs) while maintaining the total cell number at 1×10^6 cells. We assessed the behavior of this cell mixture after 4 days in culture in a 2.5 mg/ml collagen gel (Fig. 2.8). Evidence of networking and increased cell-cell contacts was increased when 10T1/2s were added to the HUVEC/collagen mixture. Increased 10T1/2 ratios seemingly led to increased networking behavior. At higher concentrations of 10T1/2s, some clumping was evident. Based on these preliminary screens and existing studies, a ratio of 1:50 10T1/2s to HUVECs was ultimately chosen for generating EC cords. Unless otherwise noted, this mixture of cells was used throughout the remaining studies described in this dissertation.

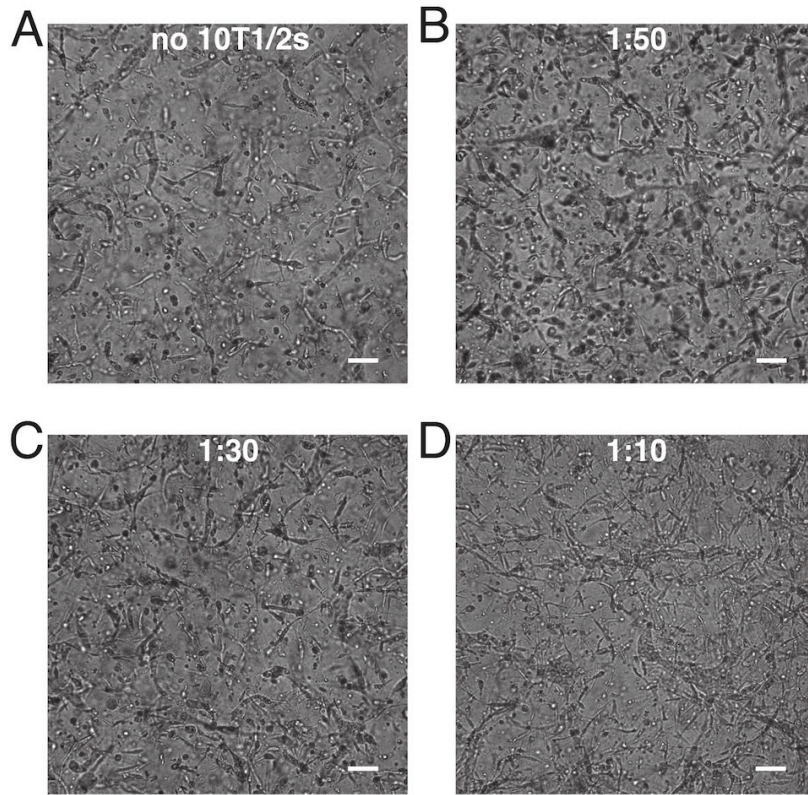


Figure 2.8 Networking behavior of HUVECs + C3H10T1/2 cells collagen gels. Brightfield imaging of 1×10^6 HUVECs cultured in 2.5 mg/ml collagen for 4 days at with no 10T1/2s (A), 1:50 (B), 1:30 (C) or 1:10 (D) ratios of 10T1/2s to HUVECs. (bars: 100 μm)

2.2.3 *In vitro* characterization of endothelial cell cords

Having created a robust platform for generating cords, we performed several characterizations to better understand the composition of cords and the mechanics and cellular dynamics of the cord formation process. First, time-lapse imaging of cells fluorescently labeled with calcein revealed that the small population of 10T1/2s remained randomly distributed within the mostly HUVEC cords throughout the contraction process

(Fig. 2.9A,B). Hematoxylin and eosin (H&E) and sirius red staining of fully contracted, paraffin embedded cords suggested that some clustering and wrapping of cells around a core of compacted collagen might also occur (Fig. 2.9C). These occasional clusters, however, were randomly distributed along the length of the cords.

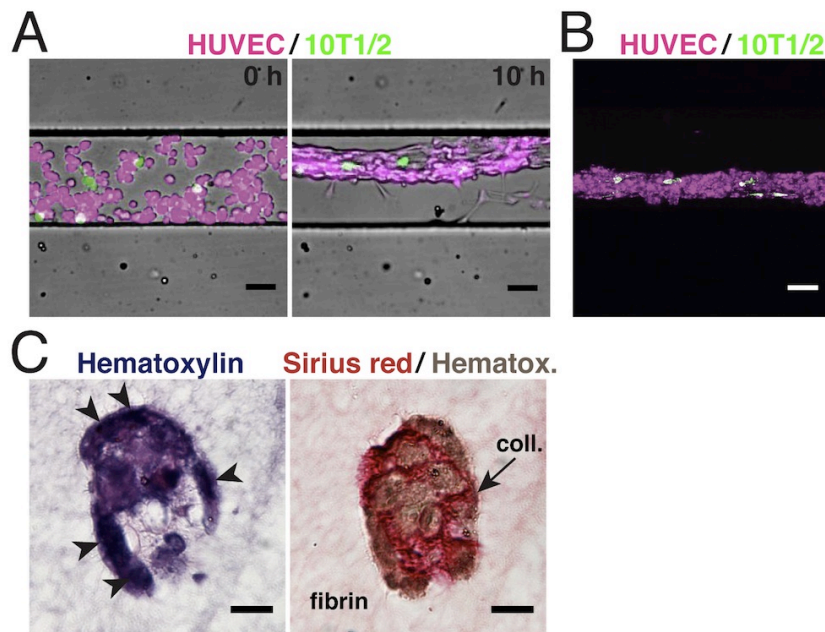


Figure 2.9 Relative distribution of HUVECs, 10T1/2s within collagen in EC cords. (A) Combined phase and fluorescence images of cord formation at 0 and 10 hours within PDMS microchannels (HUVECs: magenta, 10T1/2s: green, bars: 50 μ m). (C) Maximum intensity z-projection of fluorescently labeled HUVECs (magenta) and 10T1/2s (green) within fully formed cords (bar: 50 μ m). (bars: 20 μ m).

Once in culture, cords contracted to approximately 65% of their original diameter over a period of 10-12 hours (Fig. 2.10). To verify that this contraction is driven by cells exerting tractional forces against the surrounding ECM we treated cords with the myosin IIa inhibitor blebbistatin or the RhoA inhibitor Y27632. When treated with these inhibitors immediately after seeding, the cords remained in their uncontracted state (Fig. 2.10). Wash out of the inhibitors after 6.5 or 7.5 hours led to a rapid resumption of the contraction process. Within 6 hours of wash out, the cords had contracted to approximately 50-60% of their original diameter, which matched the contractility at 6 hours of cords treated with DMSO. These treatments confirmed our hypothesis that RhoA and myosin-mediated cytoskeletal tension are required for cord contraction.

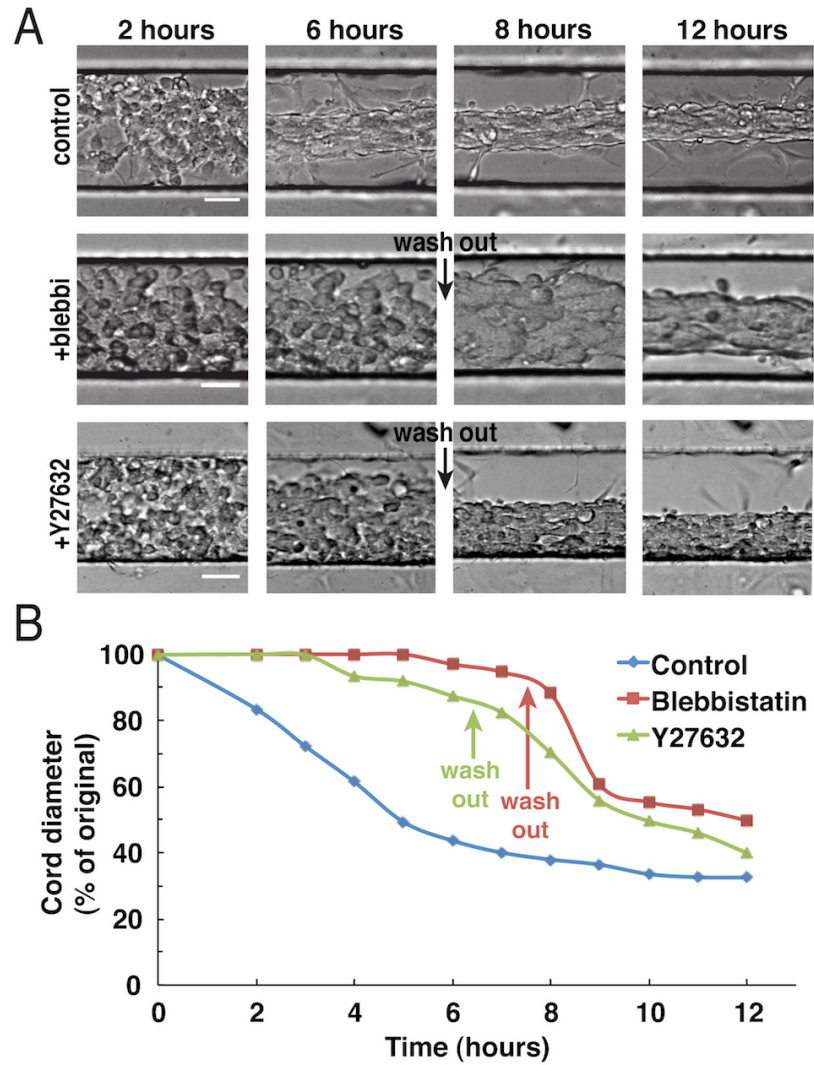


Figure 2.10 Cytoskeletal tension is required for cord contraction *in vitro*. (A) Time lapse imaging depicting cord formation in samples treated with vehicle, blebbistatin, or Y27632 (bars: 50 μ m). (B) Quantification of cord contraction reveals rapid increase in contraction after wash out of cytoskeletal tension inhibitors.

To determine whether the presence of 10T1/2 cells affected the dynamics of cord contraction, we generated HUVEC only cords and compared their contraction rate to that of HUVEC + 10T1/2 cords (Fig. 2.11). Given the contractile nature of mural cells *in vivo*, we predicted that cords containing 10T1/2s would contract more rapidly or to a higher degree than those containing HUVECs alone. Interestingly, both cord types exhibited similar contraction rates, suggesting that the contribution from 10T1/2 cells was negligible or not detectable in the presence of a high number of HUVECs.

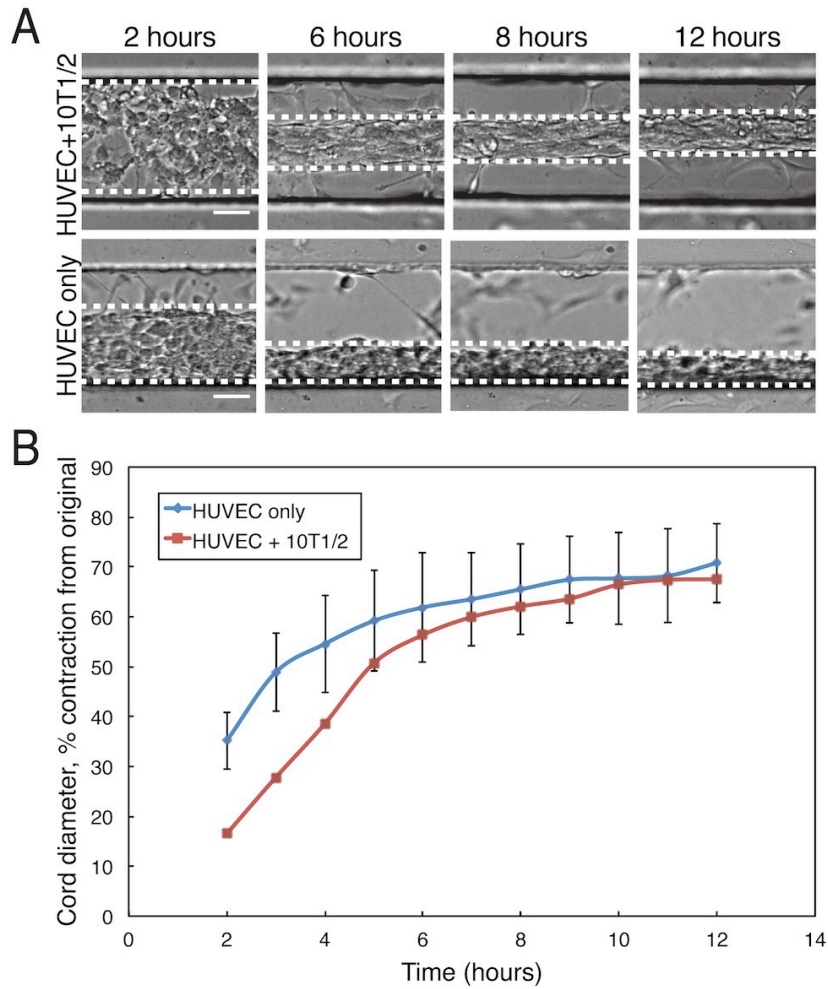


Figure 2.11 Contribution of C3H10T1/2 cells to cord contractility (A) Time-lapse phase contrast imaging shows contracting cords containing HUVECs + 10T1/2s or HUVECs only. Dashed lines delineate cord boundaries. (bars: 50 μ m) (B) Quantification of cord diameter indicates that the inclusion of 10T1/2 cells in cords has no significant impact on their contractility dynamics (error bars: sem, n=2).

To demonstrate the potential of using EC cords to pattern vasculature into a variety of geometries, we attempted to generate cords with a range of diameters and shapes. While in our previous work we demonstrated that varying collagen concentration could be used to alter final cord diameter, this approach is limited to a small range of diameters (Raghavan, Nelson, Baranski, Lim, & Chen, 2010a). Here, we chose to maintain a consistent collagen concentration while varying the PDMS microchannel width. To maintain a 1:1 aspect ratio for the various microchannel widths, separate wafers with matching heights were fabricated for each width. For cords with varying geometries, 150 μm wide and 150 μm deep microchannels were used. Several minor optimizations were necessary when generating cords of varying diameters. Cords smaller than 100 μm yielded a much-reduced volume of collagen within the PDMS microchannels than the typical 150 μm cords. Because such a small volume of collagen polymerized and dried out much more quickly, the polymerization time was reduced to just 2-3 minutes for smaller cords. In addition, the smaller microchannels exhibited a tendency to trap bubbles. After experimentation with a variety of techniques including vacuum degassing, we found that using a 1:20 rather than the typical 1:10 w/w ratio of PDMS base to curing agent resulted in much softer PDMS that could be more vigorously ‘scraped’ without damage to help remove trapped bubbles. Lastly, the technique for adding growth medium to the various cord shapes required adjustment. We found that in order to prevent the patterned cords floating out of the microchannels, it is necessary to add growth medium in a particular sequence: first to the areas most prone to damage such as vertices or junctions, second to the exposed ends of cords, and third to the remainder

of the cords and surrounding flat regions. These modifications allowed us to successfully generate cords with diameters that ranged from 25 μm to 500 μm (Fig. 2.12A) and a variety of architectures (Fig. 2.12B).

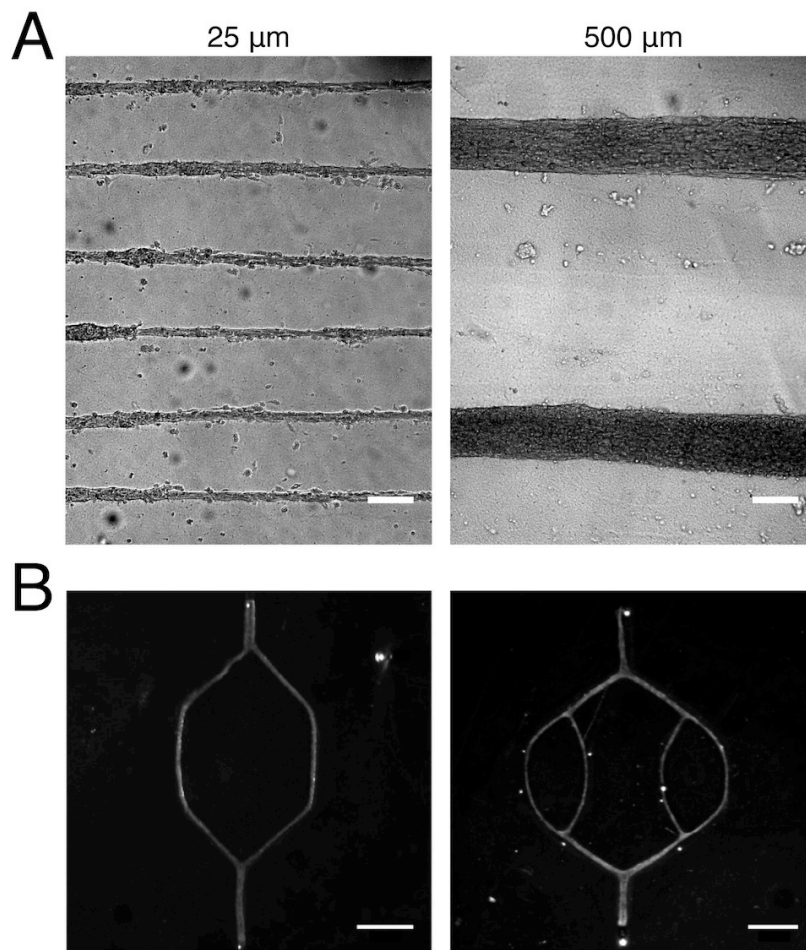


Figure 2.12 Generation of EC cords with varying diameters and geometries. (A) Phase contrast images of cords of varying diameters removed from PDMS templates and embedded in fibrin. (bars: 150 μm) (B) Brightfield images of cords with branching geometries removed from PDMS templates and embedded in fibrin. (bars: 1 mm)

2.3 Vascularizing engineered tissues *in vivo* via implantation of endothelial cell cords

2.3.1 Development of *in vivo* implantation model

To enable us to study the capability of EC cords to induce vascularization *in vivo*, we tried several surgical implantation models. We first attempted implantation of tissue constructs (fibrin gels containing EC cords) subcutaneously onto the backs of athymic mice. We found that constructs that were not sutured into place would never engraft properly into the host tissue. Seemingly, the unanchored constructs were always mobile within the subcutaneous space while the mice were active, which prevented them from engrafting. Next, we attempted to suture the tissue constructs in place to the subcutaneous tissue (hypodermis). While this approach effectively immobilized the constructs in place and seemed to improve engraftment, no vascular response was observed (Fig. 2.13A). We next attempted intra- and perimuscular implantation of our tissue constructs on the flanks of athymic mice. Both of these surgical sites required suturing to keep the construct properly immobilized. Neither site, however, resulted in a visible vascular response. Lastly, we implanted tissue constructs containing EC cords by suturing them directly to the parametrial fat pad within the intraperitoneal cavity. Gross observation of constructs harvested 5 days post implantation (PI) suggested proper engraftment and potential vascularization (Fig. 2.13). While observations of the gross anatomy of resected tissue constructs provided insights into the lack or presence of a response, histological techniques including hematoxylin and eosin (H&E) staining were used to verify the initial observations. Indeed, H&E staining of tissue constructs implanted adjacent to the

parametrial fat pad strongly suggested that blood was present within or near the implanted cords (Fig. 2.14).

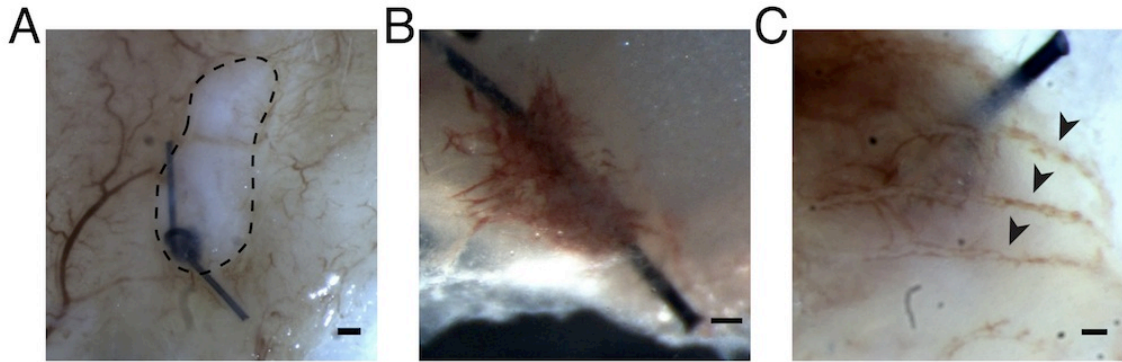


Figure 2.13 Gross anatomy of tissue constructs resected 5 days post-implantation (A) Tissue construct (dashed line) sutured to the hypodermis remained immobilized, but failed to become vascularized. (bar: 250 μm) (B) Tissue constructs sutured to the parametrial fat pad and exhibited a reddish appearance, which was suggestive of vascularization. (bar: 200 μm) (C) The patterns visible within these constructs sometimes mimicked those of the implanted cord architecture (arrowheads). (bar: 100 μm)

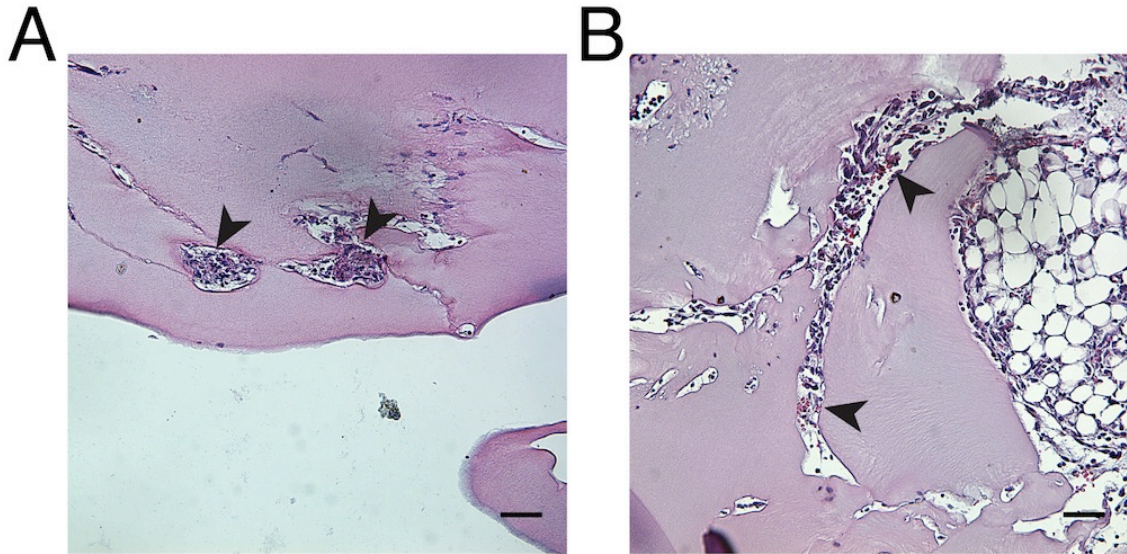


Figure 2.14 Early evidence of blood in implanted tissue constructs containing EC cords. H&E staining suggesting presence of blood in tissue constructs implanted adjacent to the parametrial fat pad. Fibrin gels containing EC cords directly sutured to the parametrial fat pad and resected 5 days PI. Arrowheads denote cords with evidence of red blood cells in transverse (left panel) or longitudinal cross section. (bars: 100 μm)

While histological examination of tissue constructs implanted adjacent to the fat pad indicated the presence of blood within cords, the overall architecture of the constructs and cords contained within was poorly preserved. This inability to maintain the originally patterned architecture within the tissue constructs made it difficult to properly assess the vascular response within the cords. To better preserve the geometry of the tissue constructs, we devised several approaches that utilized stiff and biocompatible materials to prevent the implanted constructs from losing their

shape upon implantation. First, we created our tissue constructs atop a thin (1 mm) layer of PDMS. The combined PDMS and fibrin gel with cords were cut into 6 mm discs using a biopsy punch. Small (0.75 mm) holes were punched near the periphery of the PDMS to allow for sutures to be passed through the structure for attaching to host tissue (Fig 2.15A). Without these holes near the discs' periphery, passing a suture needle through the PDMS discs led to tearing. This approach successfully maintained the shape/geometry of the constructs upon implantation. However, we found that the PDMS discs engrafted to the host adipose tissue making their removal without disrupting the implanted constructs extremely difficult. Because PDMS cannot be sectioned resecting the entire fat pad and implanted construct with the PDMS still attached would prohibit any subsequent histological analysis. Given these complications with PDMS, we next attempted to use a polypropylene mesh as a backing material for the tissue constructs. We cut small squares of mesh material (~1 cm²) and embedded them in fibrin. This procedure was performed atop a Pluronic-treated PDMS-coated petri dish to aid in the detachment of the fibrin prior to implantation. We next inverted cords onto the mesh/fibrin layer and removed them as before. The resulting assembly consisted of a layer of cords positioned immediately atop the polypropylene mesh with the entire assembly encased in fibrin (Fig. 2.15B). While it was possible to section the polypropylene mesh, we found that the mesh filaments prevented any imaging of the embedded cords. To enable potential intravital imaging of our tissue constructs, we utilized a 'donut'-shaped polypropylene mesh (Fig. 2.15B). These donut-shaped meshes were generated using

heated cork borers. The smooth outer edge facilitated their manipulation during surgery, while the inner hole would allow for direct imaging of the cords in the future. Use of a mesh material allowed for the needle and sutures to be passed directly through the periphery of the mesh without any further modifications during implantation (Fig. 2.15D).

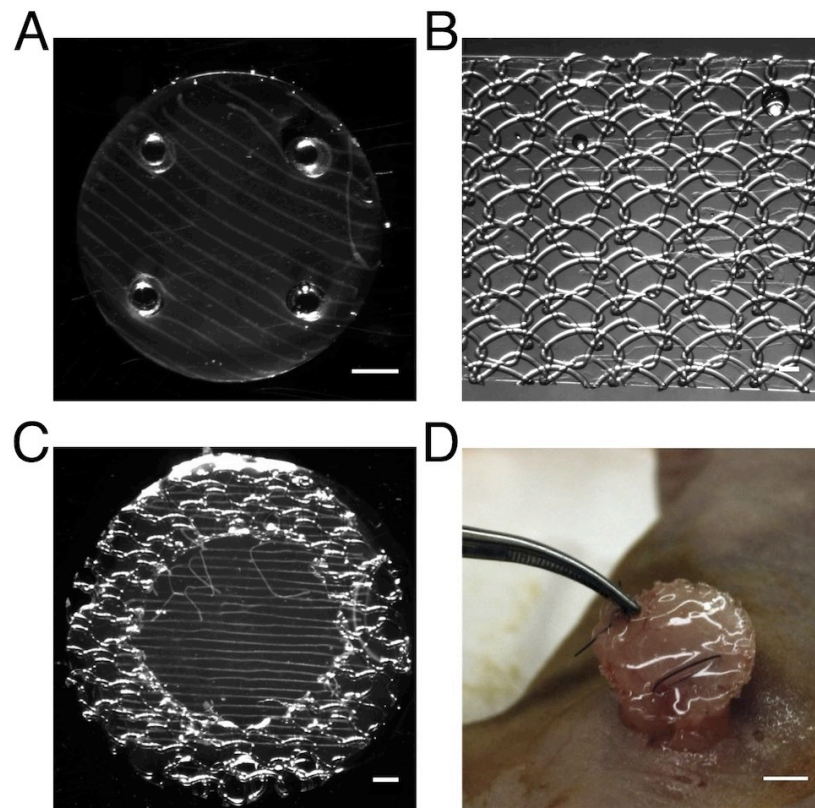


Figure 2.15 Development and implantation of a backing structure implantable tissue constructs. (A) Cords embedded in fibrin atop a PDMS backing structure containing holes for suturing. (bar: 1 mm) (B) Cords atop polypropylene mesh embedded in fibrin. Mesh structure allowed for suture and needle to be passed through the material without any additional modifications. (bar: 2 mm) (C) Cords

atop ‘donut-shaped’ mesh embedded in fibrin. Inner hole facilitated imaging of cords while smooth outer edge aided in implantation. (bar: 1 mm) (D) Mesh ring sutured atop the parametrial fat pad in preparation for implantation. (bar: 4 mm)

The polypropylene mesh incorporated into our design could be readily sectioned and successfully preserved the geometry of the implanted tissue constructs. These refinements to the implantation model allowed us to more thoroughly investigate whether cords were eliciting a vascularization response *in vivo*. H&E and sirius red staining of paraffin embedded tissues resected after 7 days indicated the presence of collagen-rich structures spatially organized in a pattern that mimicked the original position of the implanted cords (Fig. 2.16A). Higher magnification suggested the presence of blood in cell-rich regions that surrounded the periphery of the cords (Fig. 2.16B).

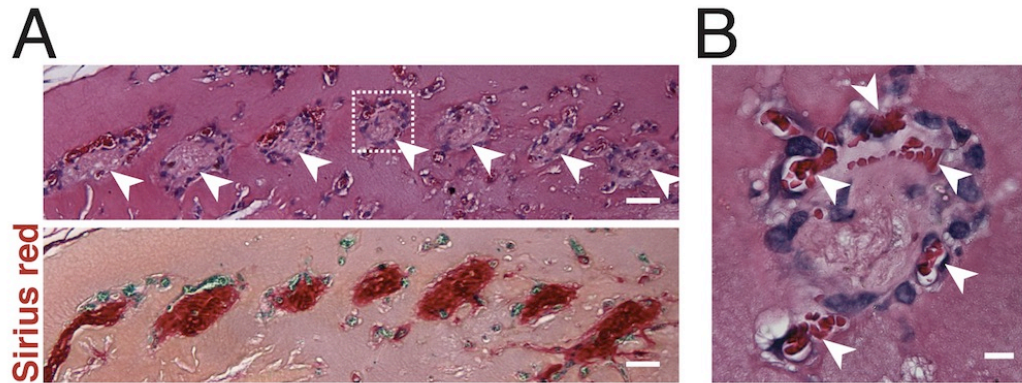


Figure 2.16 Preservation of geometry and presence of blood in EC cords resected 7 days post-implantation. (A) H&E and sirius red staining of cord-containing tissue constructs resected after 7 days *in vivo* suggests that original cord geometry was preserved upon implantation. Arrowheads indicate location of cords. (bar: 50 μm) (B) Higher magnification indicates areas of blood around the periphery of cords. (bars: 10 μm)

Our first analyses of vascularization within implanted EC cords relied solely on traditional histological stains such as H&E, sirius red and fast green. These stains were performed on sections cut from paraffin embedded tissue constructs. To facilitate immunohistochemical staining, we attempted to cut frozen sections of tissue constructs that were resected 5 days PI, briefly fixed and cryoembedded (Fig. 2.17). The cutting of tissue constructs via frozen section techniques, however, proved extremely difficult due to the heterogeneous nature of the tissues. While the optimal cutting temperature of the fibrin tissue constructs was relatively high ($-17\text{ }^{\circ}\text{C}$), the temperature required for properly cutting the surrounding adipose tissue was extremely low ($-35\text{ }^{\circ}\text{C}$). This incompatibility

in cutting temperatures resulted in smearing of the adipose tissue at higher temperatures and defects (likely due to cracking) in the fibrin tissue constructs at lower temperatures. Given these difficulties in cutting frozen sections, all immunohistochemical analyses described in this dissertation relied on paraffin embedded histological techniques, which yielded significantly improved preservation of tissue morphology (Fig. 2.17B).

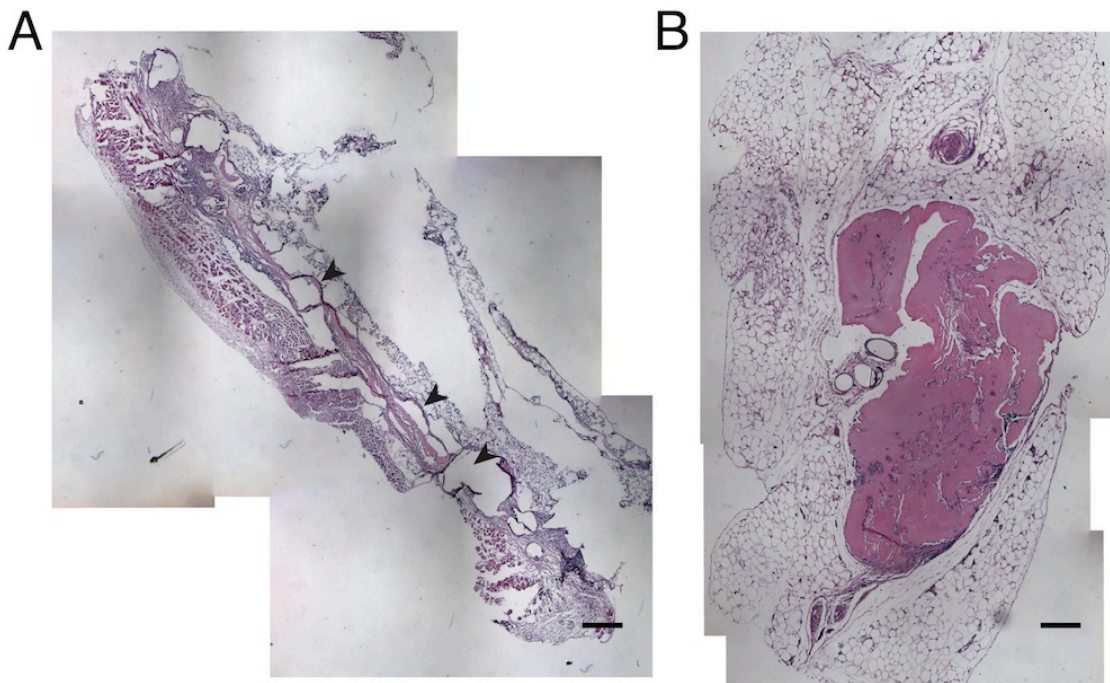


Figure 2.17 Frozen sectioning of tissue constructs. (A) Low magnification of H&E stained frozen section resected 5 days PI. Sections cut at low temperatures exhibited defects in the fibrin gels, while cutting at higher temperatures led to smearing of adipose tissue. Arrowheads indicate areas of cutting defects. (B) Sections cut from paraffin embedded tissue constructs showed no signs of defects and appeared to

exhibit improved preservation of morphology (tissue construct implanted without mesh support). (bars: 500 μm)

2.2.2 Implantation of endothelial cell cords drives formation of mature capillaries *in vivo*

To confirm whether implantation of endothelial cell cords resulted in the formation of blood vessels, we harvested tissue constructs at days 3, 5, 7, 14 and 28 post implantation (PI). H&E staining suggested the presence of red blood cells (RBCs) within cords as early as 3 days PI (Fig. 2.18A) with larger pools of blood also evident at both 3 and 5 days PI. These large areas of blood, suggestive of leaky vasculature, were replaced over time by smaller, vessel-like structures that persisted until 28 days PI. Sirius red/fast green staining indicated the persistence of a collagen core within cords for the duration of the entire time course (Fig. 2.18B). These collagen-rich areas showed no signs of degradation even at 28 days PI, and blood and surrounding cells were largely localized to the periphery of cords. To verify the presence of RBCs and endothelial cells of human origin, we performed immunohistochemical staining for Ter-119, an erythroid cell marker, and human-specific CD31 (Fig. 2.18C). Positive Ter-119 staining confirmed the presence of RBCs in all time points, and patterns matched those previously observed with H&E staining. Human-specific CD31 staining confirmed that the RBC-containing structures were blood vessels comprised of endothelial cells of human origin. These vessels appeared large and poorly organized at days 3 and 5 PI, but rapidly organized into smaller, lumenized capillaries as early as 7 days PI and persisted until at least 28 days PI.

Staining for alpha smooth muscle actin (α -SMA) revealed the presence of α -SMA-positive cells in a perivascular localization as early as day 3 (Fig. 2.18D). As nascent vessels reorganized into smaller capillaries, these α -SMA-positive cells became more tightly associated with adjacent endothelial cells indicating that they had adopted a pericyte phenotype.

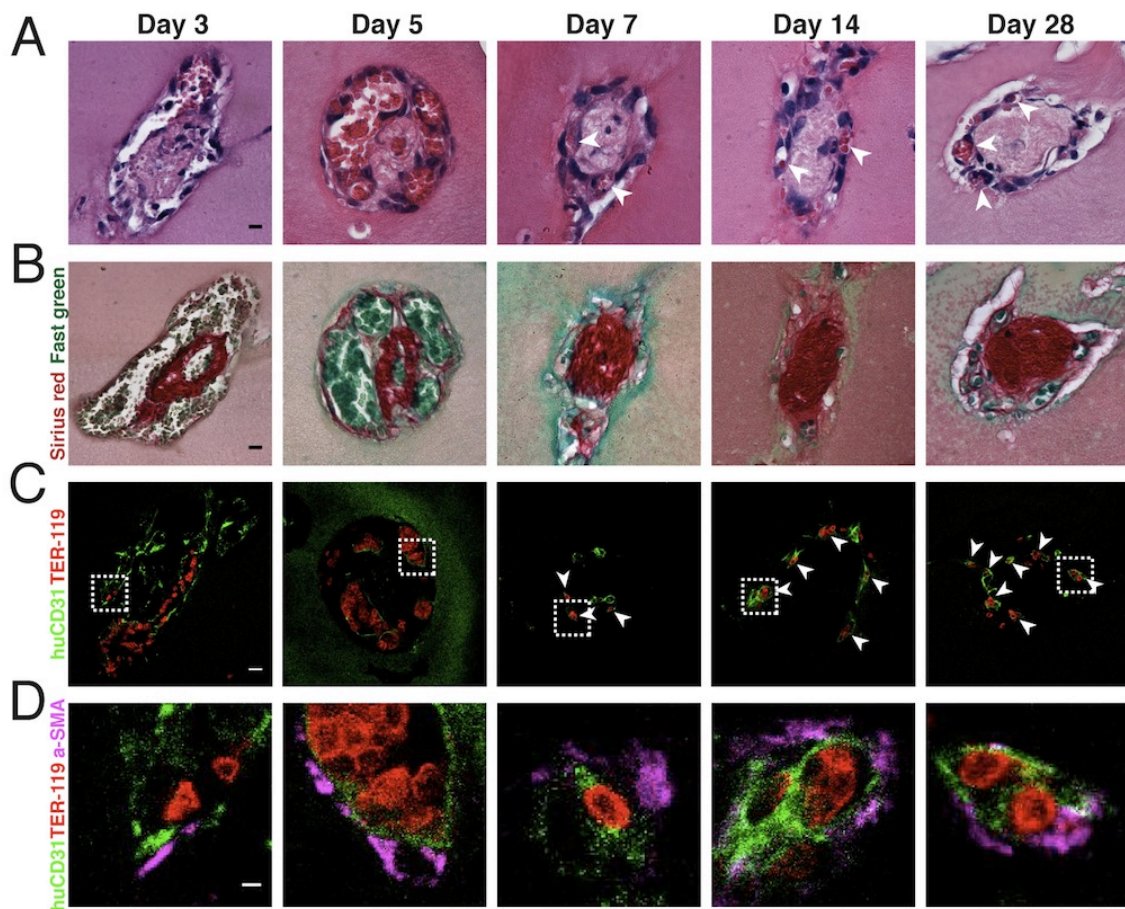


Figure 2.18 Implanted EC cords drive formation of mature capillaries. (A) H&E staining of tissue constructs containing EC cords resected at days 3, 5, 7, 14 and 28 PI suggests presence of blood within vessels that organize into small capillaries

(arrowheads) by day 7 (bar: 10 μm). (B) Sirius red/fast green staining confirms presence of collagen within implanted cords. (bar: 10 μm) (C) Ter-119 (red) and human-specific CD31 (green) staining identify RBCs and ECs, respectively. All areas containing RBCs also exhibited neighboring human ECs suggesting that vessels were patent (bar: 10 μm) (D) α -SMA staining (magenta) and higher magnification indicate the presence of α -SMA-positive cells with a perivascular localization. These cells appeared more tightly associated with capillaries at days 14 and 28 PI. (bar: 20 μm)

Quantification of vessels and blood in H&E stained sections further suggested the presence of mature capillaries within implanted tissue constructs (Fig. 2.19A). Namely, three trends were observed between days 5 and 7 PI: 1) the area of blood within cords decreased from approximately 65% to 25% of total cord area; 2) the number of vessels within cords increased from approximately 1.5 to 4.0; and 3) the average vessel diameter decreased from approximately 30 μm to 7 μm . All trends continued until at least 28 days PI and suggest that the cords quickly anastomose (day 3 PI) with the host vasculature to form nascent, leaky vessels that form lumens and reorganize into smaller, more numerous and mature capillaries (Fig. 2.19B).

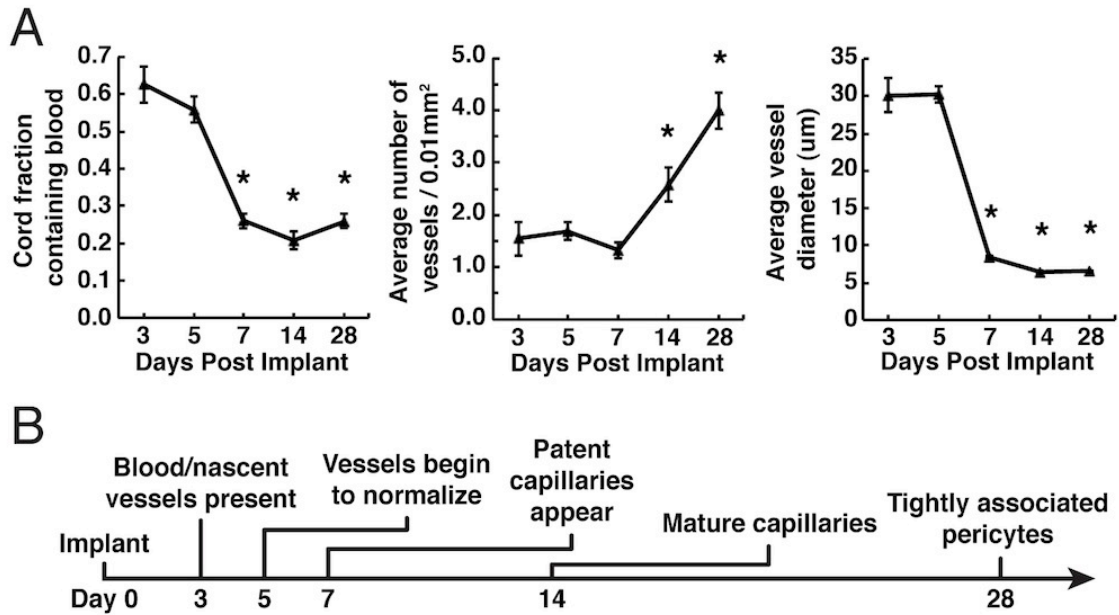


Figure 2.19 Quantification of the vascularization response (A) Quantification of blood area showed a sharp decrease in areas containing blood between 5 and 7 days PI. The average number of vessels per cord increased steadily after day 7, while the size of the vessels decreased and stabilized at a size of approximately 7.5 µm after day 5 PI (*: $p < 0.05$ for comparison of days 7, 14 and 28 vs. 3 and 5 in blood area measurements and vessel diameter measurements, days 14 and 28 versus 3, 5 and 7 in vessel number measurements, error bars: sem, $n \geq 5$). (B) Timeline with qualitative description of vascularization trends.

In addition to immunohistochemical techniques, we attempted to better track implanted endothelial cells by utilizing fluorescently labeled HUVECs. The labeled cells included HUVECs that were stably transduced with H2B:GFP via a lentiviral vector and commercially available cells that were also transduced using lentivirus (Angio-

Proteomie). We found that either population of labeled HUVECs failed to induce vascularization *in vivo* when patterned into cords and implanted. These cells spread to cover a larger surface area in culture and proliferated slower than unlabeled cells. Cords generated using the labeled HUVECs also appeared ‘frayed’ in appearance and contracted to a lesser degree than those generated with control cells. Given these abnormalities and lack of a vascularization response, we concluded that these means of labeling HUVECs placed too high of a metabolic burden on the cells and prevented them from functioning normally in our system. Additionally, successful immunohistochemical staining for human-specific CD31 (Fig. 2.18C,D) alleviated the need for labeled cells.

To gain additional insight into the mechanism of cord-host vessel anastomosis and the composition of newly formed capillaries, we injected a cocktail of fluorescently labeled human and mouse-specific lectins via the tail vein (Fig. 2.20). Subsequent Fluorescent imaging near the edge of implanted constructs following injection of a cocktail containing *Helix pomatia* agglutinin (HPA)-AlexaFluor488 and *Ulex europaeus* agglutinin I (UEA I)-TRITC indicated that perfused vessels extending beyond the boundary of the cords within tissue constructs were of mouse origin (Fig. 2.20A). Capillaries within the cords were comprised of a chimera of mouse and human endothelial cells. Imaging of host adipose tissue confirmed the lack of cross reactivity between UEA I and mouse vessels (Fig. 2.20B).

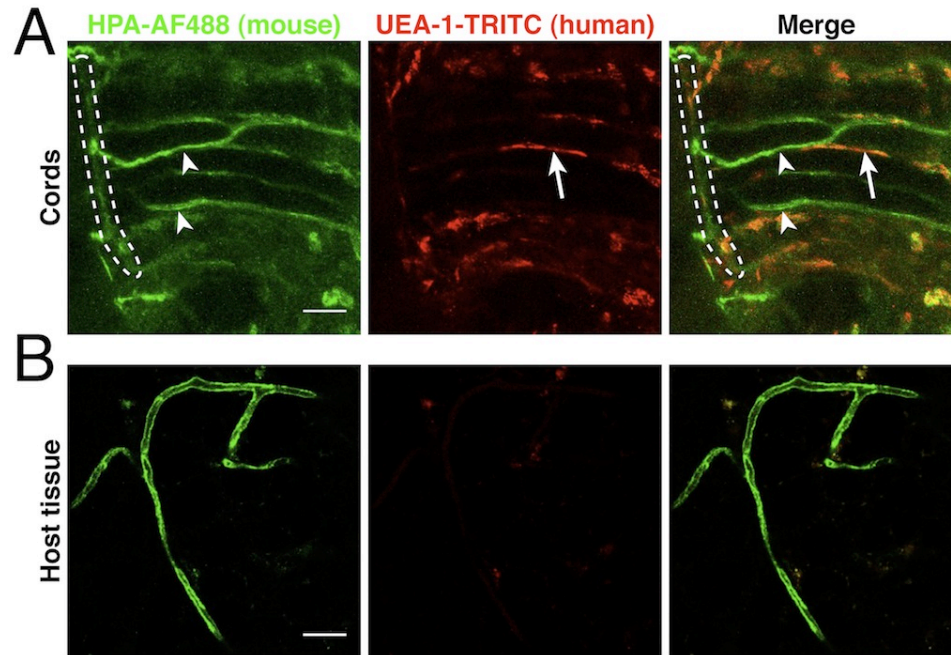


Figure 2.20 Composition of vessels at graft periphery. (A) Staining of constructs with mouse-specific (HPA) lectin revealed that vessels extending beyond the boundary of the cords were of mouse origin and appeared connected to several cord-associated capillaries (dashed line). Staining with human-specific (UEA-1) lectin further showed that capillaries within cords exhibited a chimeric composition (arrowheads: mouse, arrow: human). (B) Imaging of surrounding host adipose tissue confirmed the lack of cross reactivity between UEA I and mouse vessels. (bars: 25 μ m)

We next attempted to determine whether viable cells were a necessary for cord vascularization by implanting tissue constructs consisting of acellular fibrin gels, fibrin gels containing HUVECs and 10T1/2s randomly seeded and precultured for 2 days, or fibrin gels containing cords that had been ‘decellularized.’ To generate decellularized

cords, we patterned cells into cords as usual and subsequently induced cell death via snap freezing, exposure to hypo- and hypertonic solutions, and dissolution of the cell membrane in CHAPS or SDS detergents. Live/dead stains revealed that CHAPS buffer followed by 12 hours of PBS washing were most effective at removing cellular components without disturbing the surrounding matrix.

H&E staining of acellular fibrin gels indicated that they remained absent of cells and showed no evidence of blood at 7 days PI (Fig. 2.21A). In gels containing precultured HUVECs and 10T1/2s, small areas of blood near the periphery of the constructs suggested the formation of a small number of capillaries (Fig. 2.21B). Staining of ‘decellularized’ cords indicated the presence of small nuclei or DNA fragments near areas of collagen matrix, but no blood was evident (Fig. 2.21C). Overall, none of these control conditions yielded a vascularization response comparable to that seen upon implantation of viable EC cords.

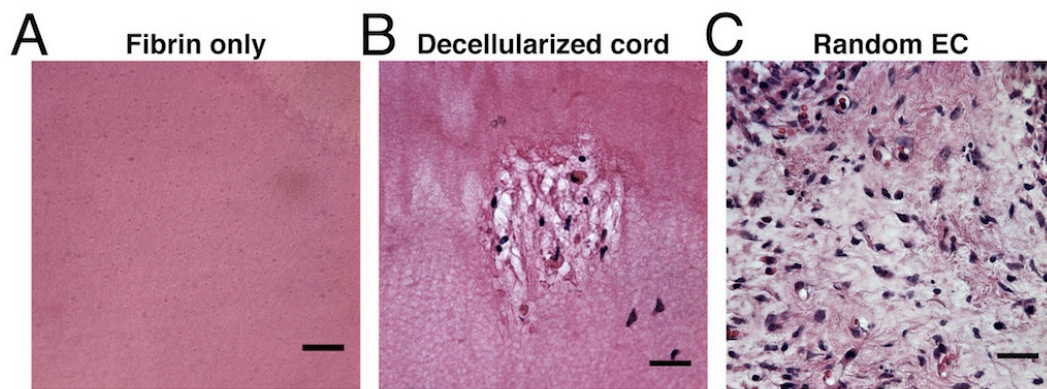


Figure 2.21 Cells are required for vascularization (A) H&E staining of acellular fibrin gel resected 7 days PI indicates lack of cells and blood. (B) H&E staining of fibrin gel containing mixture of HUVECs and 10T1/2s resected 7 days PI. Several

areas suggest the presence of RBCs within capillaries. (C) H&E staining of fibrin gel containing decellularized EC cords resected 5 days PI. Hematoxylin staining suggests the presence of several small nuclei or DNA fragments, but no blood. (bars: 25 μm)

The presence of 10T1/2 cells within cords had no effect on their contraction *in vitro* (Fig. 2.11). Here, we tested whether varying the relative proportions of 10T1/2s and HUVECs within implanted cords had an effect on the size of capillaries that form upon implantation. At 5 days PI, however, cords containing 2:1, 1:5, or 1:50 ratios of 10T1/2s to HUVECs did not seem to impact capillary diameter (Fig. 2.22). Given the known contributions of 10T1/2s to the vascularization process (Hirschi et al., 1998; Koike et al., 2004) and the lack of an observable effect upon their implantation in various ratios, we performed the remainder of studies with the originally established 1:50 ratio of 10T1/2s to HUVECs.

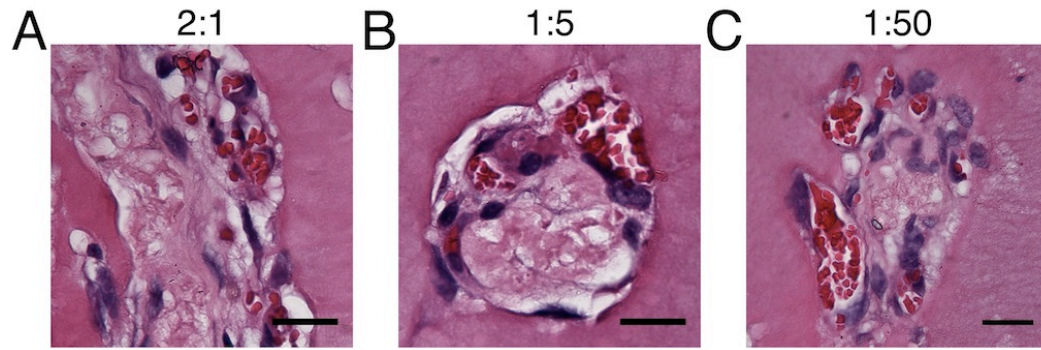


Figure 2.22 Effect of varying 10T1/2 to HUVEC ratios on *in vivo* capillary formation. No observable differences were seen in capillary size upon implantation of cords containing 2:1 (A, longitudinal cross-section), 1:5 or 1:50 10T1/2 to HUVEC ratios after 5 days *in vivo*. (bars: 25 μm)

To determine whether the diameter of the implanted cords could impact the size of the resultant capillaries, we implanted tissue constructs containing cords with 50 and 500 μm diameters (Fig. 2.23). Cells within the smaller cords were distributed randomly around the collagen core and contained pools of blood that appeared smaller than previously seen (Fig. 2.23A). Upon implantation of larger cords, the pools of blood appeared similar in size to those observed upon implantation of 150 μm cords, and the cells appeared localized to one side of the collagen core (Fig. 2.23B). Because the pools of blood observed in 150 μm cords reorganized into smaller capillaries after 7 days *in vivo*, we concluded that the same phenomenon would be observed in the 500 μm cords implanted here. All subsequent EC cord experiments described in this dissertation utilized 150 μm cords.

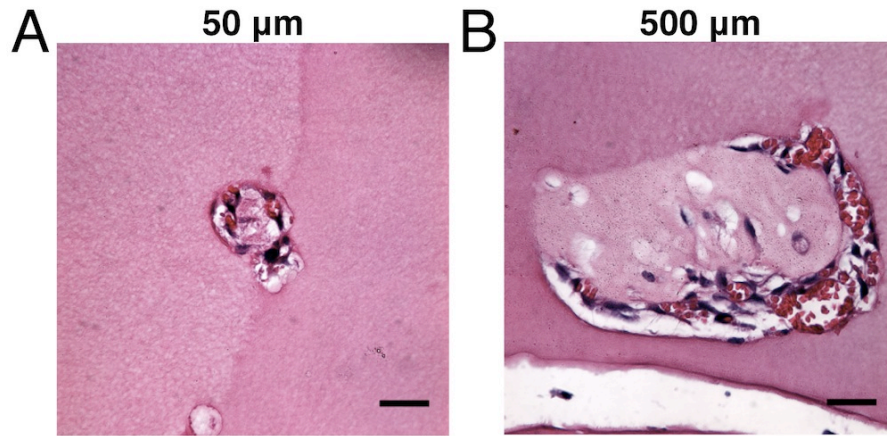


Figure 2.23 Effects of cord diameter on vascularization *in vivo*. H&E staining of tissue constructs containing 50 (A) and 500 µm (B) diameter cords resected 5 days PI. Smaller cords resulted in formation of small pools of blood at the periphery of the collagen core. Cells in the larger cords appeared localized to one side of the collagen core and indicated the presence of pools of blood similar in size to those seen upon implantation of 150 µm cords. (bars: 25 µm)

2.2.3 Implantation of patterned endothelial cell constructs yields a perfused *in vivo* vasculature with conserved geometry

Networks of implanted endothelial cells and fibroblasts can rapidly anastomose with the host circulation (X. Chen et al., 2010). To confirm that capillaries formed upon implantation of EC cords had anastomosed with the host vasculature, we performed injections of FITC-dextran via the tail vein at day 14 PI. Fluorescent imaging revealed the presence of a perfused network of capillaries with an architecture recapitulating that of the implanted cords (Fig. 2.24A,B middle panels). Capillaries spanned the entire length of the tissue constructs, and sprouts between adjacent capillaries within cords and

between capillaries in neighboring cords were also evident. Histological examination of tissue constructs resected 7 days PI additionally confirmed the presence of these sprouts and capillaries spanning the region between adjacent cords (Fig. 2.25). FITC-dextran injections of mice implanted with fibrin gels containing randomly seeded HUVECs and 10T1/2s did not result in comparable patterning of the vasculature and indicated that perfused vessels were present only near the periphery of implanted constructs (Fig. 2.24A,B middle panels). To investigate whether vascular architecture can be spatially patterned, we implanted tissue constructs that contained cords patterned into a Y-shaped topology (Fig. 2.24A, right panel). FITC-dextran injection 14 days PI indicated that these constructs resulted in the formation of vessels that anastomosed with the host vasculature and recapitulated the geometry of the implanted cord pattern (Fig. 2.24B, right panel).

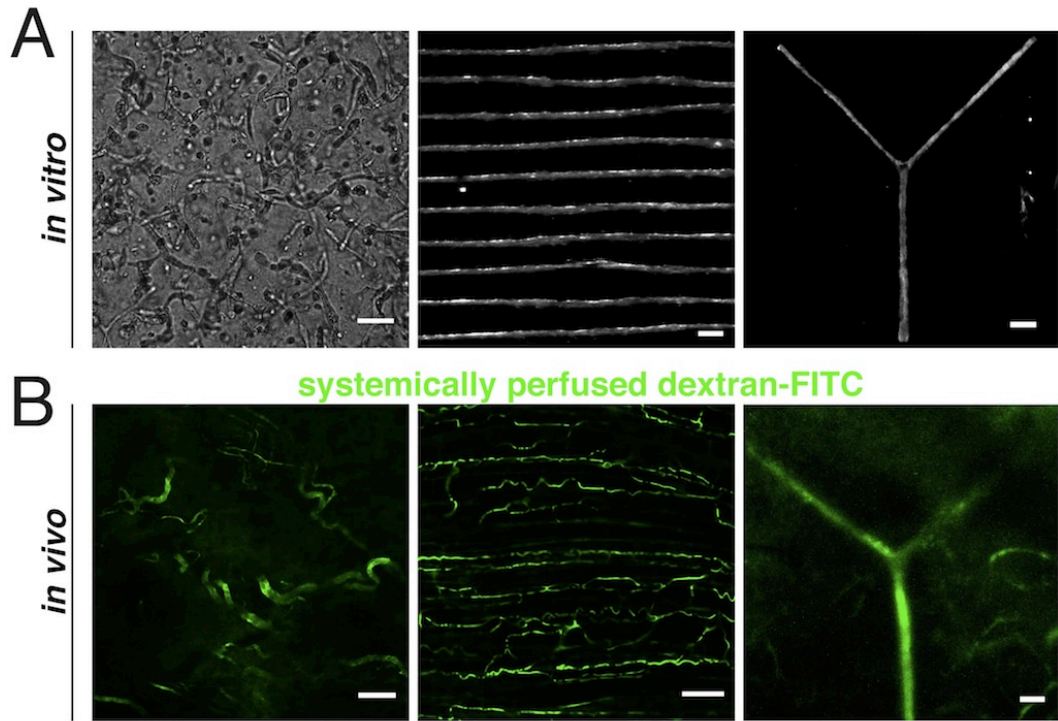


Figure 2.24 Perfusion with host blood and patterning of *in vivo* vasculature. (A) Brightfield images of non-implanted tissue constructs containing randomly seeded HUVECs and 10T1/2s, parallel EC cords or EC cords patterned into a Y-shaped topology (bars: 250 μm , 500 μm , 500 μm) (B) Confocal imaging following FITC-dextran injection via the tail vein shows vascular architecture following implantation of the tissue constructs shown in A. (bars: 100 μm)

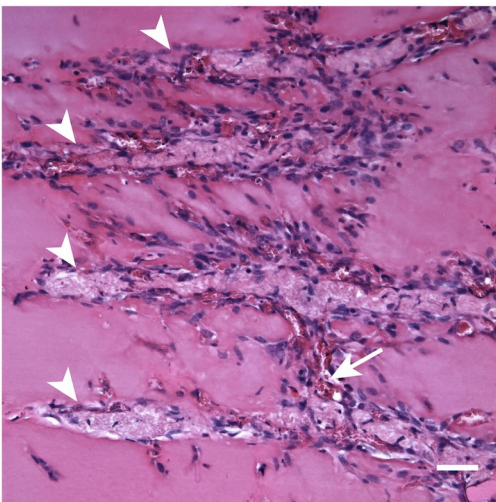


Figure 2.25 Capillary sprouting between adjacent cords. H&E staining of EC cords in longitudinal cross-section reveals presence of capillaries between adjacent cords (arrow). Arrowheads indicate locations of cords. (bar: 25 μ m)

2.2.4 Patterned vasculature within engineered hepatic tissues maintains hepatocyte function

Improved vascular organization enhances the integration of engineered and host tissues (Koffler et al., 2011). To test the ability of patterned EC cords to vascularize engineered tissues and improve their function *in vivo*, we generated tissue constructs that contained patterned EC cords and aggregates of primary rat liver hepatocytes (Fig. 2.26A). A lentiviral vector was used to transduce the hepatocytes to express luciferase under control of the albumin promoter. Bioluminescence imaging over 20 days following implantation revealed that hepatocyte constructs containing cords exhibited significantly higher levels of albumin promoter activity for at least 20 days (Fig 2.26C). Histological examination

revealed clusters of aggregates adjacent to vessels containing blood and deposits of collagen mimicking those previously found in the cords (Fig. 2.26B). Sirius red/fast green staining suggested that collagen previously present in the EC cords had been largely degraded and dense areas of elastin-rich matrix had been deposited by the hepatocyte aggregates. Immunofluorescent staining for Ter-119 and arginase 1, a hepatocyte marker, confirmed the presence of blood in areas directly adjacent to hepatocyte aggregates. These staining patterns suggested that the implanted hepatocytes remained viable for at least 20 days *in vivo* and had access to the host blood supply via capillaries that formed as a result of the implanted cords.

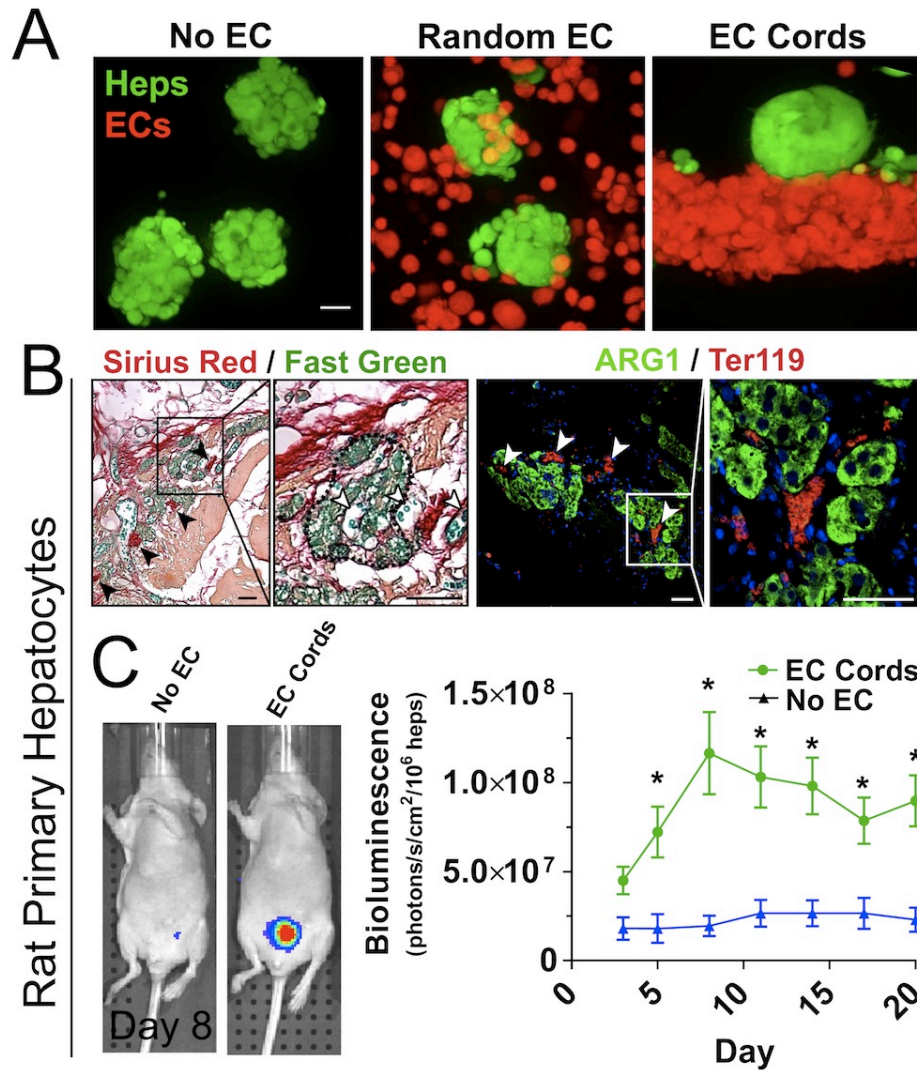


Figure 2.26 EC cords within engineered rat hepatic tissues improve function (A) Three types of tissue constructs containing varying combinations of primary hepatocyte aggregates and ECs were generated: 1) hepatocyte aggregates only, 2) hepatocyte aggregates with randomly seeded HUVECs and 10T1/2s, and 3) hepatocyte aggregates with EC cords (bar: 20 μ m). (B) H&E and sirius red/fast green staining revealed hepatocyte aggregates in close proximity to vessel-like structures that contained blood. Immunostaining for Ter-119 (green) and arginase

1 (red) confirmed the presence of RBCs in close proximity to viable hepatocyte aggregates at 20 days PI. (bars: 25 μm) (C) Luciferase activity showed significantly increased albumin promoter activity in the group of tissue constructs containing patterned rat hepatocyte aggregates and EC cords at least 20 days PI ($n \geq 5$, error bars: sem).

Next, we used primary human hepatocytes to investigate the effects of co-implanting patterned hepatocyte aggregates and EC cords. Histological analysis again showed that hepatocyte aggregates co-implanted with EC cords had access to host blood via adjacent capillaries (Fig. 2.27A). Luciferase imaging throughout the experiment indicated that hepatocyte aggregates co-implanted with EC cords exhibited significantly higher levels of albumin promoter activity (Fig. 2.27B). In an additional control condition, we ligated the host vessels within the parametrial fat pad immediately following implantation of the tissue constructs. Low albumin promoter activity within this group further suggested that the observed increases in hepatocyte function were a result of improved access to the vasculature rather than paracrine signaling alone. Measurements of serum albumin at day 18 PI supported the trends observed via luciferase imaging. Due to the low levels of serum albumin in all groups, however, these results were not statistically significant.

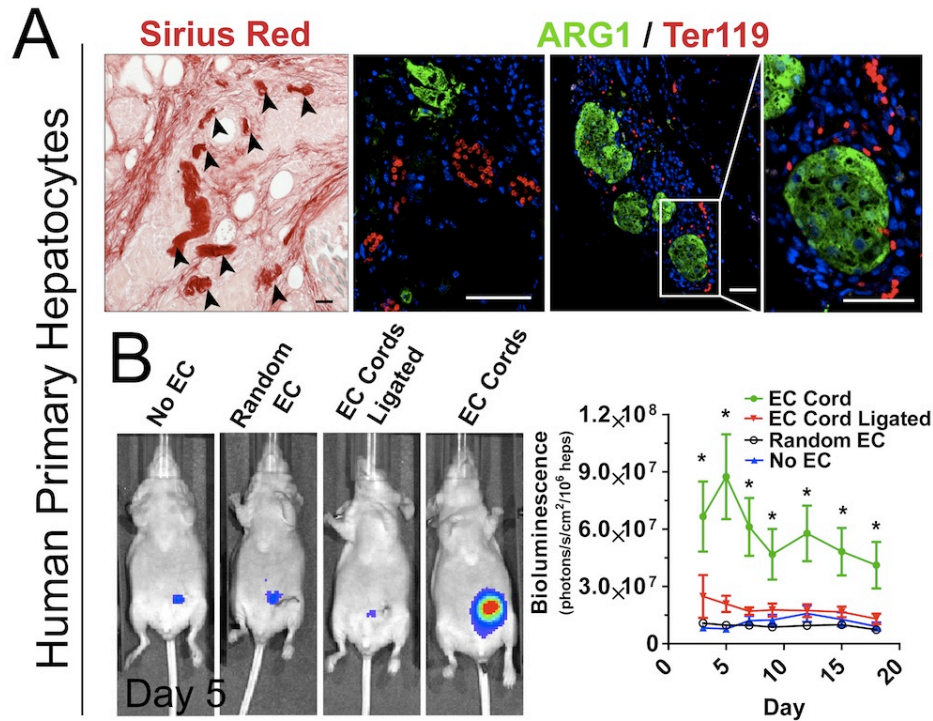


Figure 2.27 EC cords within engineered human hepatic tissues improve function. (A) H&E and sirius red/fast green staining suggested that hepatocyte aggregates were in close proximity to vessels that contained blood. Immunostaining for Ter-119 (green) and arginase 1 (red) confirmed the presence of RBCs in close proximity to viable hepatocyte aggregates at 18 days PI. (bars: 25 μ m) (B) Luciferase imaging revealed that constructs in the ‘no EC,’ ‘random EC,’ and ‘ligated’ control groups expressed similar levels of albumin expression. Constructs containing aggregates patterned with EC cords performed significantly better than control groups for at least 18 days PI ($n \geq 6$, error bars: sem). ELISA measurements suggested that serum albumin levels in all groups were comparable to those measured via luciferase imaging.

2.4 Materials and Methods

Cell culture

Primary human umbilical endothelial cells (HUVECs, Lonza) were cultured on 0.1% gelatin-coated dishes in EGM-2 (Lonza). C3H10T1/2 cells [American Type Culture Collection (ATCC)] were cultured in low glucose DMEM containing 10% fetal bovine serum (Atlanta Biologicals), 100 units/mL penicillin, and 100mg/mL streptomycin (Invitrogen). Primary human hepatocytes were cryopreserved and from a 1-yr-old female Caucasian donor (Lot Hu8085; CellzDirect). Human hepatocytes were cultured in high glucose DMEM (Cellgro) containing 10% fetal bovine serum (FBS; Gibco), 1% (vol/vol) ITS supplement (insulin, human transferrin, and selenous acid; BD Biosciences), 0.49 pg/ml glucagon, 0.08 ng/ml dexamethasone, 0.018 M HEPES, and 1% (vol/vol) penicillin-streptomycin (pen-strep; Invitrogen). J2-3T3 fibroblasts (gift of Dr. Howard Green; Harvard Medical School) were cultured in high glucose DMEM containing 10% bovine serum, and 1% penicillin-streptomycin.

Primary rat hepatocytes (2 – 3 month old adult female Lewis rats; Charles River) were isolated as described previously (A. A. Chen et al., 2011; Dunn, Tompkins, & Yarmush, 1991; Seglen, 1976). Each rat was anesthetized and the portal vein was cannulated. The liver was perfused with buffers followed by collagenase. Liver digest was purified using Percoll centrifugation, and hepatocyte viability was typically 85 – 95% using trypan blue exclusion. Rat hepatocytes were cultured in high glucose DMEM containing 10% (v/v) FBS, 0.5 U/ml insulin (Lilly), 7 ng/ml glucagon (Bedford Laboratories), 7.5 µg/ml hydrocortisone (Sigma), and 1% pen-strep.

Fabrication of PDMS templates and preparation of endothelial cell cords

Endothelial cell cords were micropatterned as previously described. Briefly, masters were prepared by photolithographically exposing silicon wafers coated with SU-8 photoresist (Shipley) to develop channel patterns at a height of 150 μ m. Liquid poly (dimethylsiloxane) (PDMS) pre-polymer was poured onto the silicon masters and cured to generate molded substrates. The PDMS substrates were sterilized with UV, and treated with 0.01% Pluronic F127 for 10 minutes prior to use as culture substrates. HUVECs and 10T1/2s were suspended at a ratio of 50:1 in 2.5mg/mL liquid collagen (BD Biosciences) and centrifuged into the PDMS channels. Excess unpolymerized collagen and cells were removed by dewetting the surface of the substrate. The collagen was polymerized, growth medium was added, and the constructs were incubated for 4-6 hours. The newly formed cords were removed from the PDMS substrates by inverting onto a drop of unpolymerized 7.5 mg/mL bovine fibrin (sigma). After the fibrin was polymerized at 37 °C, the constructs were submerged in PBS and the culture dish was gently agitated to dislodge the PDMS. The PBS was aspirated and a second layer of unpolymerized fibrin was added over the top and polymerized to fully encase the cords. The embedded cords were cut with a 6 mm biopsy punch prior to implantation.

Decellularization of cord constructs

Cord constructs were prepared as described above and subsequently decellularized using a solution containing 8 mM CHAPS, 1 M NaCl, 25 mM EDTA in PBS. During the

decellularization process, constructs were submerged in the decellularization solution and placed on an orbital shaker overnight. Excess cellular debris and detergent were then removed by soaking the constructs in PBS on an orbital shaker for several hours. Wash steps were repeated three times. The decellularized constructs were then cut with a 6 mm biopsy punch as described above.

Construction of hepatic engineered tissues

To enable noninvasive imaging of hepatocyte function and survival in engineered tissues, hepatocytes were transduced in suspension culture immediately after isolation (for rat hepatocytes) or thaw (for human hepatocytes) with a lentiviral vector expressing firefly luciferase under the human albumin promoter ((pTRIP.Alb.IVSb.IRES.tagRFP-DEST, gift of Charles Rice, The Rockefeller University). Hepatocytes and J2 fibroblasts were placed into Aggrewell micromolds overnight to form hepatic aggregates (average of 100 hepatocytes and 25 J2 fibroblasts per aggregate). Hepatic aggregates were removed from Aggrewell templates and suspended randomly in 7.5mg/mL unpolymerized bovine fibrin at a concentration of 15K/mL for the random aggregates condition. For the random aggregates plus random HUVEC condition, hepatic aggregates were suspended randomly in 7.5 mg/mL unpolymerized bovine fibrin at a concentration of 15k/mL along with 2 million HUVECs/mL and 10T1/2s at a 50:1 ratio. For the aggregates plus cords condition, cords were embedded in 7.5mg/mL bovine fibrin containing randomly suspended hepatic aggregates at a concentration of 15K/mL.

In vitro imaging of endothelial cell cords

HUVECs were labeled with 5 $\mu\text{g}/\text{mL}$ Calcein AM red-orange and 10T1/2s were labeled with 5 $\mu\text{g}/\text{mL}$ Calcein AM (invitrogen) prior to trypsinization. PDMS substrates were prepared and seeded as above. Cord contraction was imaged using an Eclipse epifluorescent microscope. Final cord morphology was imaged using a Zeiss 710 laser scanning confocal microscope. For measurements of cord contraction, cords were treated with 20 μM blebbistatin or 25 μM Y27632 at 7.5 or 6.5 hours after seeding, respectively.

For *in vitro* imaging of hepatic constructs, Huh7.5 cells were labeled with 5 $\mu\text{g}/\text{mL}$ calcein AM and placed into AggreWell micromolds overnight to form aggregates (approximately 100 cells per aggregate). Aggregates were removed from AggreWell templates and suspended in 7.5 mg/mL unpolymerized bovine fibrin at a concentration of 15K/ mL for the 'No EC' condition. For the 'random EC' condition, aggregates were suspended in 7.5 mg/mL unpolymerized bovine fibrin at a concentration of 15k/ mL along with 2 million HUVECs/ mL and 10T1/2s at a 50:1 ratio. HUVECs and 10T1/2s were labeled with 5 $\mu\text{g}/\text{mL}$ calcein red orange. For the 'EC cords' condition, cords were embedded in 7.5 mg/mL bovine fibrin containing randomly suspended hepatic aggregates at a concentration of 15K/ mL . Constructs were imaged using a Zeiss Axiovert 200m microscope equipped with a Yokogawa spinning disk confocal unit.

In vivo implantation of cords

For cord only experiments, all surgical procedures were conducted according to protocols approved by the University of Pennsylvania Institutional Animal Care and Use

Committee. Eight week old female Nu/Nu athymic mice (Charles River) were anesthetized using isoflurane and the constructs were sutured to the parametrial fat pad. The incisions were closed aseptically, and animals were administered 0.1 mg/ml buprenorphine every 12 hours for three days following surgery.

For hepatic engineered constructs, all animal procedures were approved by The Committee for Animal Care in the Department of Comparative Medicine at Massachusetts Institute of Technology. Immediately after engineered tissue fabrication, NCr nude mice (Taconic) were anesthetized using isoflurane, and engineered tissues were sutured to the mesenteric parametrial fat pad. For ‘cords + hepatocytes – excised’ animals, engineered tissue and attached mesentery were cut from the remainder of the mesentery via an upstream excision such that the tissue and attached mesentery were no longer directly connected to host circulation. The incisions were closed aseptically, and animals were administered 0.1 mg/ml buprenorphine every 12 hours for three days following surgery.

Bioluminescence imaging

For luminescence imaging, mice were injected intraperitoneally with 250 μ L of 15 mg/mL D-Luciferin (Caliper Life Sciences) and then imaged using the IVIS Spectrum (Xenogen) system and Living Image software (Caliper Life Sciences).

Dextran perfusion, lectin perfusion and imaging

To preserve geometry during implantation, cords were embedded in a gasket cut from a polypropylene surgical mesh (Davol). To visualize perfused vessels a 200uL solution of 20mg/mL fluorescein isothiocyanate (FITC)-labeled dextran (150 kDa) (Sigma) in PBS was injected intravenously via the tail vein. To visualize mouse versus human vessels, a 200uL solution of 500µg/ml lectin from *Helix pomatia* agglutinin (HPA) conjugated to Alexa 488 (Sigma), and 100µg/ml lectin from *Ulex europaeus* agglutinin (UEA-1) conjugated to TRITC (Vector labs) in PBS was injected intravenously via the tail vein. Animals were sacrificed and tissue was harvested from graft site immediately after injection. Perfused vessels were subsequently imaged using a Zeiss 710 laser scanning confocal microscope.

Tissue harvesting, processing and histology, and immunohistochemistry

Animals were sacrificed at various time points and tissue was harvested from the intraperitoneal space. Explants were fixed in 4% PFA for 48 hrs at 4°C , dehydrated in graded ethanol (50-100%), embedded in paraffin, and sectioned using a microtome (6µm) for immunohistochemical staining. For gross visualization of tissue, sections were stained with hematoxylin and eosin (H&E). For identification of cords composed partially of collagen, sections were stained with Sirius red (collagen) and fast green (other tissue elements).

For identification of vessels containing human endothelial cells, smooth muscle cells, and erythroid cells, sections were first blocked using M.O.M. blocking reagent

(Vector Labs) and normal goat serum and then immunostained using primary antibodies against human CD31 (1:20; DAKO), Ter-119 (1:100; BD Biosciences), and smooth muscle alpha-actin (1:100, Abcam). Signal was visualized after incubation with secondary goat anti-IgG1-Alexa 555, goat anti-rat-Alexa 488, and donkey anti-rabbit-Alexa 647 antibodies (Jackson ImmunoResearch). For identification of primary hepatocytes adjacent to vessels containing red blood cells, sections were blocked using normal donkey serum then incubated with primary antibodies against arginase-1 (ARG1, 1:400, Sigma) and Ter-119 and followed with species-appropriate secondary antibodies conjugated to Alexa 488 and 555. Images were obtained using a Zeiss 710 laser scanning confocal or Nikon 1AR Ultra-Fast Spectral Scanning Confocal Microscope.

Biochemical assays to assess hepatocyte function

Rat albumin in sampled media was quantified by enzyme-linked immunosorbent assay (ELISA) using a rat albumin ELISA kit (Bethyl labs; sheep anti-rat albumin antibody at 1:100).

Statistical Analysis and Quantification of Vascularization Parameters

Quantification was performed on H&E sections of fully engrafted cord constructs. Blood area was quantified by measuring the total area of tissue containing blood within a cord. This measurements was normalized to average cord area to compensate for oblique cutting angles. Vessel number was quantified by counting individual vessels within a cord and was normalized to the average cord area. Vessel diameter was quantified by

measuring the diameter of individual vessels within a cord. Sections for quantification were chosen from the center of the constructs, and a minimum of 3 sections at least 150 μ M apart were quantified per cord. All data are expressed as the mean \pm standard error. Statistical significance was determined using the one-way ANOVA followed by Tukey's post hoc test for group comparisons.

2.5 Conclusions

In the work described here, we have developed a novel technique for generating functional capillaries with spatially controlled geometry *in vivo*. Via adapting a previously described system for patterning cells into organized cords, we have created a strategy for embedding cords into implantable tissue constructs. The implantation of these constructs into mice led to the formation of functional capillaries that become perfused with blood within 3 days PI and remain stable and exhibit a mature phenotype for up to 28 days PI. The capillary networks are perfused with host blood, contain vessels that are largely comprised of implanted human cells, and exhibit a geometry that recapitulates that of the implanted EC cords. Previous studies have suggested that the ability to pattern vessels is essential for the function and proper engraftment of engineered tissues ((X. Chen et al., 2009; Koffler et al., 2011)). Here, we have further validated these findings by demonstrating that patterned EC cords used to vascularize engineered hepatic tissues were capable of significantly improving function.

Future studies in vascular tissue engineering will require the development of defined complex vessel architectures. Our data provide one of the first demonstrations of

capillary network patterning *in vivo* and further suggest that this approach is a viable strategy for vascularizing engineered solid tissues. We envision that the vascular patterning technique described here will enable future studies toward the design of optimal vessel architectures within a variety of tissue engineered contexts.

CHAPTER 3: Proliferative regulation by adhesion and RhoGTPases in smooth muscle cells is altered in idiopathic pulmonary arterial hypertension

3.1 Introduction

Organotypic models provide a powerful tool for studying disease processes *in vitro* while maintaining an added level of physiologic relevance that is not present in traditional tissue culture models. While angiogenic models that rely on tubes or channels coated with endothelial cells are common, more complex models of the arterial smooth muscle compartment have been seldom used in mechanistic studies (Chrobak et al., 2006; Zervantonakis et al., 2012). Niwa *et al.* and Fillinger *et al.* have previously described techniques for generating bilayers of endothelial and smooth muscle cells (Fillinger et al., 1997; Niwa et al., 2007). Here, we sought to generate an EC-SMC bilayer and utilize it in the study of cells isolated from patients with pulmonary hypertension. Given a lack of promising results, however, we continued with an investigation into the pathobiology of pulmonary hypertension using traditional tissue culture models.

Pulmonary arterial hypertension (PAH) is a disease characterized by hyperproliferation and remodeling within the small pulmonary arteries, which results in increased blood pressure within the lung vasculature (Gaine & Rubin, 1998; Ikeda et al., 2010; Rubin, 1997). In patients with PAH, the increased vascular resistance in the pulmonary circulation places a greater workload on the heart and ultimately leads to right

ventricular failure and premature death. Idiopathic pulmonary arterial hypertension (IPAH), which occurs in the absence of identifiable risks, is particularly difficult to diagnose (Chin & Rubin, 2008; Thyberg et al., 1990). Patients present with general symptoms and diagnosis is only made after the exclusion of other heart and lung diseases known to cause elevations in pulmonary arterial pressure. In patients with IPAH, the estimated survival rates for patients receiving treatment at 1, 2, and 3 years are 83, 67, and 58%, respectively (Aoyagi et al., 1997; Humbert et al., 2010; Jones & Rabinovitch, 1996; Monahan et al., 2007; Stouffer et al., 1998). Despite advances in the management of IPAH and increases in survival rates, patients' quality of life remains low and no further treatments outside of the realm of lung transplantation currently exist.

Histological examination of pulmonary arterioles in patients with IPAH shows neointimal thickening, pulmonary arteriolar occlusion, and plexiform lesions, suggesting that IPAH is a primarily vasoproliferative disease with accompanying vasoconstriction as well as catabolism and *de novo* synthesis of components of the extracellular matrix (ECM) (Burrige & Chrzanowska-Wodnicka, 1996; Chin & Rubin, 2008; Farber & Loscalzo, 2004; Guan & Shalloway, 1992; Humbert et al., 2004; Jones et al., 1997; Jones & Rabinovitch, 1996; Kornberg, Earp, Parsons, Schaller, & Juliano, 1992; Pietra et al., 1989). Studies into the mechanisms underlying abnormal PASMC proliferation in IPAH have only recently begun, however, and this area of research still remains largely unexplored (Chrzanowska-Wodnicka & Burrige, 1996; Ikeda et al., 2010; Lewis & Schwartz, 1995; Richardson, Malik, Hildebrand, & Parsons, 1997; Roovers & Assoian, 2003).

In vivo, the proliferation of SMCs is tightly regulated by many extracellular cues including cell adhesion to the extracellular matrix (ECM), the presence of soluble growth factors and cell-cell adhesion. In adult tissues, SMC proliferation is generally low and the cells exhibit a differentiated phenotype that enables proper maintenance of vascular tone and regulation of blood pressure. Upon injury and in the presence of the proper extracellular cues, however, SMCs can undergo a switch to a more synthetic, highly proliferative phenotype (Pirone et al., 2006; Thyberg et al., 1990). In this state, the SMCs become highly proliferative and exhibit increased migration and ECM production. Specifically, the production of ECM proteins including collagen, fibronectin, elastin, tenascin-C, and proteoglycans increases, and the expression of adhesion molecules such as integrins and cadherins is altered (Aoyagi et al., 1997; Danen, Sonneveld, Sonnenberg, & Yamada, 2000; Jones & Rabinovitch, 1996; Monahan et al., 2007; Ren & Schwartz, 2000; Stouffer et al., 1998; Welsh et al., 2001). Given the presence of a pathologic cellular microenvironment in the arteries of IPAH lungs, we sought to investigate whether adhesive signaling might be altered in PASMCS isolated from IPAH patients and whether this might impact proliferation of IPAH patient-derived PASMCS.

Adhesion-mediated proliferation in SMCs is facilitated by the binding and clustering of integrins to ECM proteins, ultimately forming focal adhesions. Mature focal adhesions serve dual roles as signaling hubs and as mechanical linkages between a cell and its extracellular environment. Focal adhesion kinase (FAK) is a key effector in focal adhesion signaling whose kinase activity is activated upon integrin ligation (Burrige & Chrzanowska-Wodnicka, 1996; Guan & Shalloway, 1992; Kornberg et al., 1992; Pirone

et al., 2006). FAK is involved in the development of focal adhesions allowing for cell spreading and the establishment of cytoskeletal tension (C. Chen, Mrksich, Huang, Whitesides, & Ingber, 1997; Chrzanowska-Wodnicka & Burridge, 1996; Lewis & Schwartz, 1995; Richardson et al., 1997; Roovers & Assoian, 2003). Notably, FAK has also been implicated as a key player in adhesion-mediated proliferative control via the RhoA signaling pathway, which is downstream of cell adhesion to the extracellular matrix (Chrzanowska-Wodnicka & Burridge, 1996; Pirone et al., 2006). Specifically, FAK regulates the activity of the Rho GTPase RhoA, which is required for sustained ERK signaling and cell cycle progression (C. Chen et al., 1997; Danen et al., 2000; Raines, 2000; Ren & Schwartz, 2000; Welsh et al., 2001).

Herein, we investigated the proliferative control mechanisms at work in PASMCs isolated from patients with advanced IPAH. We found that IPAH PASMCs showed significantly increased proliferation *in vitro* as compared to normal controls. While control cells exhibit a Rac-regulated proliferative control mechanism, IPAH cells appear to be Rho- dependent. Additionally, IPAH PASMCs exhibit several abnormalities in adhesion signaling including increased focal adhesion size, higher FAK phosphorylation levels, and loss of spreading-dependent proliferative control. Inhibition of FAK restored normal adhesion- mediated proliferation control suggesting that altered adhesion signaling might underlie the abnormal proliferation of PASMCs in IPAH.

3.2 Development of an organotypic arterial wall model

To generate an *in vitro* model of an arterial wall, we sought to create a bilayer structure consisting of endothelial cells (intima) grown atop a layer of smooth muscle cells and ECM (media). Treatment of SMCs with ascorbic acid leads to increased collagen production, decreased proliferation, and increased expression of smooth muscle markers (Arakawa et al., 2003; Niwa et al., 2007; Qiao, Bell, Juliao, Li, & May, 2009). By stimulating bovine pulmonary arterial smooth muscle cells (bPASCs) with ascorbic acid, we first attempted to create an ECM rich layer of smooth muscle cells.

Immunofluorescent staining suggested that treatment with 50 $\mu\text{g/ml}$ ascorbic acid of bPASCs cultured on fibronectin-coated glass increased expression of α -smooth muscle actin and decreased proliferation (Fig. 3.1A). Further culture of these cells in the presence of ascorbic acid, however, did not seem to affect their morphology or the rate at which they reached confluence (Fig. 3.1B). Additionally, confluent cells appeared growth arrested and did not continue proliferating to form a multilayered structure as expected.

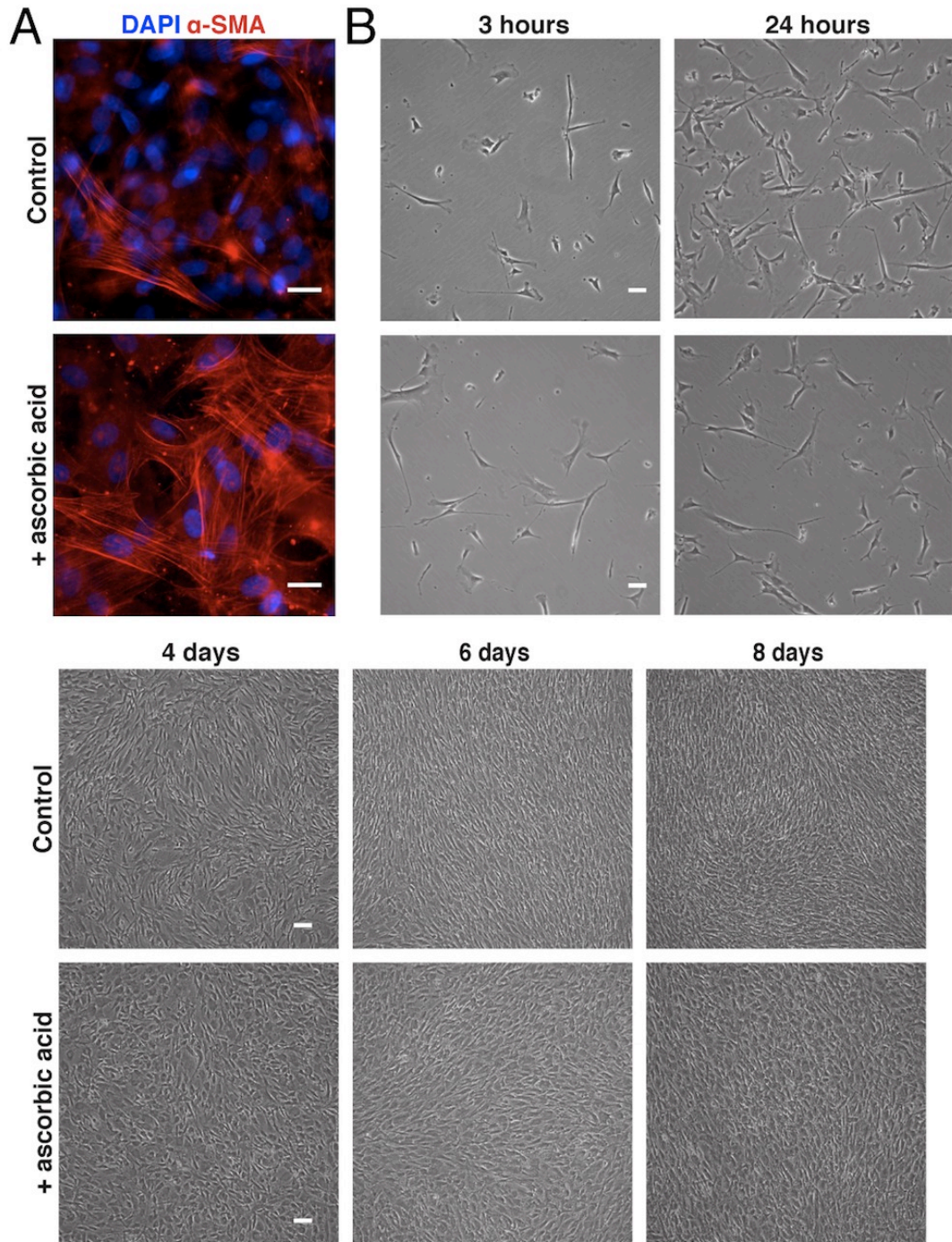


Figure 3.1 Ascorbic acid treatment of bPASCs (A) Immunostaining indicated that bPASCs cultures treated with ascorbic acid exhibited increased α -SMA expression (red) within 24 hours of seeding. Decreased numbers of nuclei (blue)

also suggested that ascorbic acid treatment decreased proliferation. (bars: 20 μm)

(B) Time lapse phase contrast imaging over 8 days did not show any observable differences in cultures of bPASCs treated with ascorbic acid and control cells.

(bars: 50 μm)

We next attempted to seed a monolayer of endothelial cells atop confluent layers of smooth muscle cells. We seeded bovine pulmonary arterial endothelial cells (bPAECs) at a density of 100,000 cells/cm² atop confluent layers of bPASCs treated with ascorbic acid (Fig. 3.2A, B). The bPAECs were labeled with CMTPX CellTracker dye and imaged for 10 hours. While the bPAECs appeared to attach and remain viable, they did not spread and proliferate to form a monolayer. Extended times in culture confirmed that the bPAECs did not proliferate and appeared to invade the layer of bPASCs underneath and adhere to the glass substrate below. Seeding bPAECs at a higher density (200,000 cells/cm²) yielded similar results (Fig. 3.3A, B). The higher density of endothelial cells present at the start of the experiment allowed for direct contact between neighboring cells. While we had hypothesized that this presence of cell-cell contacts might stimulate the bPAECs to remain as a monolayer, similar results to those utilizing the lower concentration of bPAECs were observed.

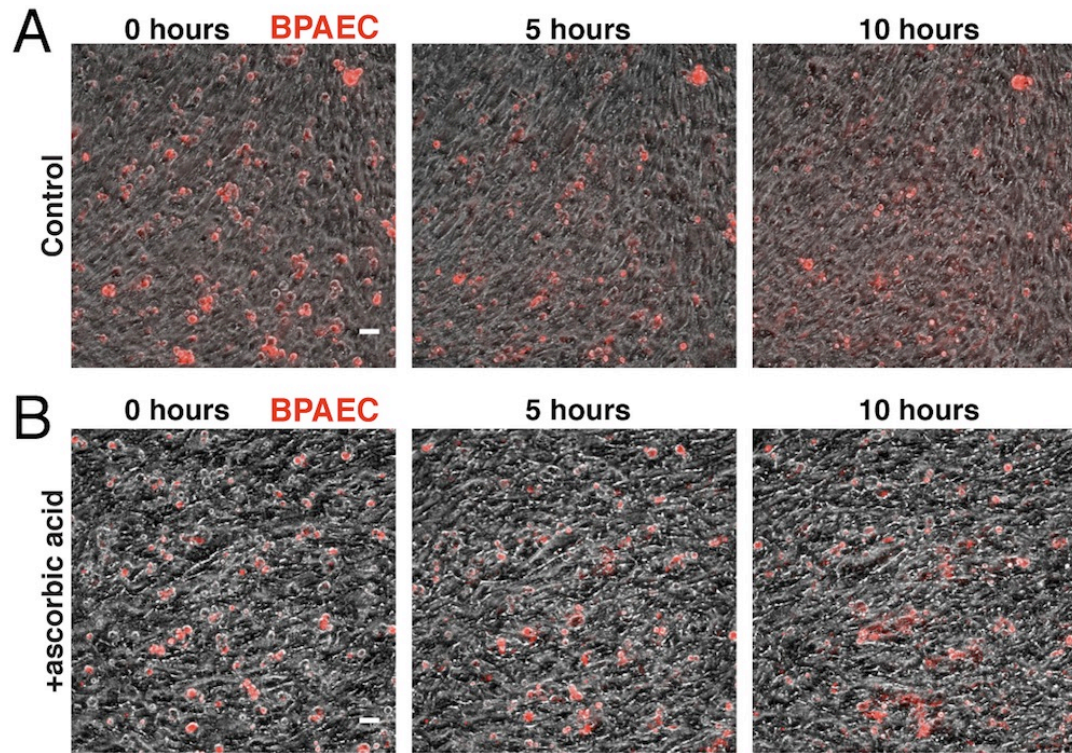


Figure 3.2 bPAECs ($100,000 \text{ cells/cm}^2$) grown atop a layer of bPASCs. Combined fluorescence and phase contrast imaging of $100,000$ bPAECs (red) seeded onto a confluent layer of bPASCs (unlabeled) that were either untreated (A) or treated with $50 \mu\text{g/ml}$ ascorbic acid (B). bPAECs attached, but remained rounded and failed to proliferate and form a monolayer. (bars: $100 \mu\text{m}$)

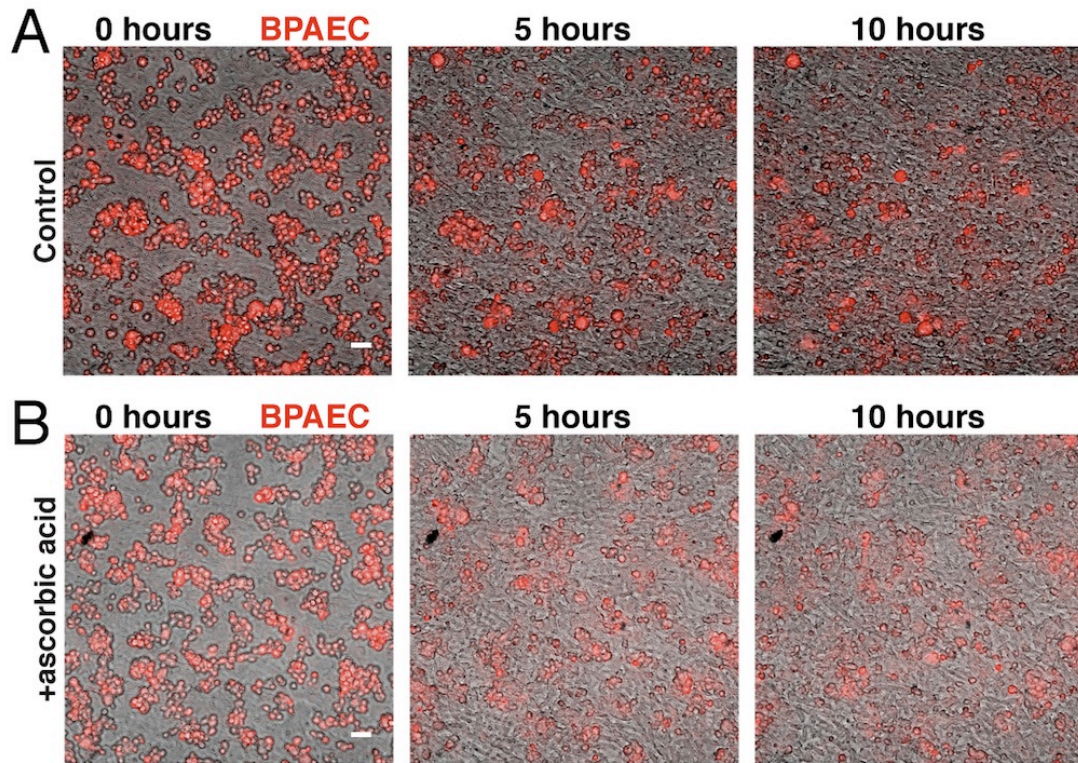


Figure 3.3 bPAECs ($200,000 \text{ cells/cm}^2$) grown atop a layer of bPASCs. Combined fluorescence and phase contrast imaging of $100,000$ bBPAECs (red) seeded onto a confluent layer of bPASCs (unlabeled) that were either untreated (A) or treated with $50 \mu\text{g/ml}$ ascorbic acid (B). bPAECs attached, but remained rounded and failed to proliferate and form a monolayer. (bars: $100 \mu\text{m}$)

Given the failure of bPAECs to spread atop layers of bPASCs, we sought to generate a ‘reversed’ aortic wall model by culturing smooth muscle cells atop endothelial cells. While such a model would be slightly less physiologically relevant, we hypothesized that it might still be useful for testing a variety of physiologically relevant

phenomena in an *in vitro* setting. To create this ‘reversed’ arterial model, we seeded bPASCs onto a monolayer of bPAECs. Imaging of bPASCs transduced with GFP via an adenoviral vector cultured atop bPAECs treated with DiI-AcLDL, however, indicated that the bPASCs did not remain on the top surface of the endothelial monolayer (Fig. 3.4). Rather, the ECs and SMCs seemed to mix randomly and failed to create a multilayered structure that might mimic arterial physiology.

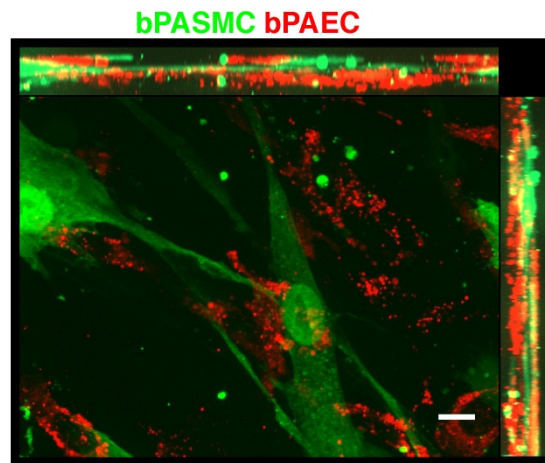


Figure 3.4 ‘Reverse’ arterial wall model. 15µm z-stack of bPASCs cultured atop a monolayer of bPAECs. bPASCs were transduced with GFP (green) via an adenoviral vector, bPAECs labeled with DiI-AcLDL. X-Z (top) and Y-Z (right) projections indicate that SMCs did not remain positioned on top of the EC monolayer. (bar: 10 µm)

3.3 Contractility measurements of IPAH PSMCs

Given the challenges in readily generating an arterial wall model, we performed a number of characterizations of PSMCs isolated from the lungs of patients with IPAH using more traditional tissue culture models. First, to determine whether these cells might be contributing to the hypertensive state via increased contractility, we examined the levels of myosin light chain (MLC) phosphorylation (Fig. 3.5). Comparison of donor cells from one IPAH lung versus control cells revealed only a minor increase in ppMLC expression. Treatment with several cytoskeletal tension inhibitors (Y27632: RhoA, ML-9: myosin light chain kinase, blebbistatin: myosin II, NSC 23766: Rac1) led to a differential response between the two cell populations when treated with ML-9. Treatment with blebbistatin, however, did not lead to decreased ppMLC expression in either cell population.

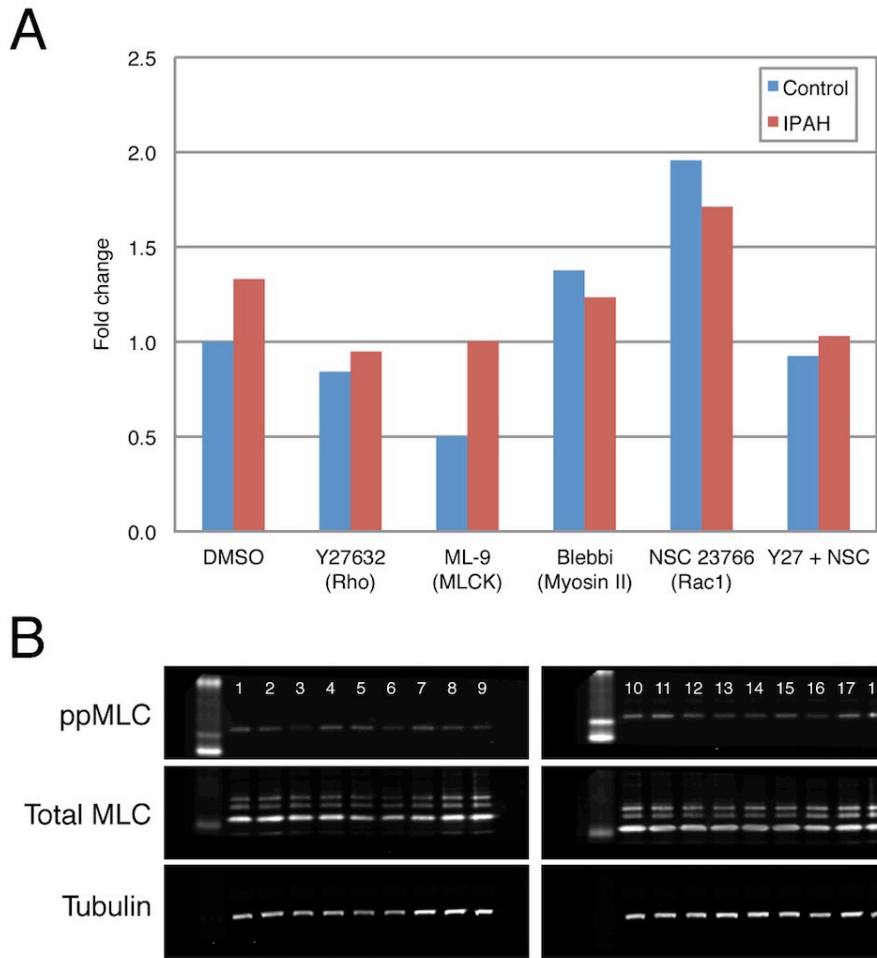


Figure 3.5 ppMLC expression levels in IPAH PSMCs. (A) Quantification of western blot for ppMLC in lysates from IPAH and control PSMCs. Lanes in B are 1) DMSO, 2) Y27632, 3) ML-9, 4) blebbistatin, 5) NSC 23766, 6) Y27632 + NSC 23766 in control cells, and 7) DMSO, 8) Y27632, 9) ML-9, 10) blebbistatin, 11) NSC 23766, 12) Y27632 + NSC 23766 in IPAH PSMCs isolated from lung #8.

The lack of a decrease in phosphorylation levels of MLC upon treatment with blebbistatin led us to pursue assays with direct functional read outs of contractility. We

employed a collagen gel contractility assay to compare the ability of IPAH and control SMCs to contract a free floating collagen gel (Fig. 3.5). IPAH PASMCs cultured for 4 days in 2.5 mg/ml collagen gels showed no clear trends in differences in contractility versus control PASMCs. Only cells isolated from IPAH Lung 1 exhibited decreased contractility. Cells from other donors exhibited contractility levels very similar to those observed in control PASMCs.

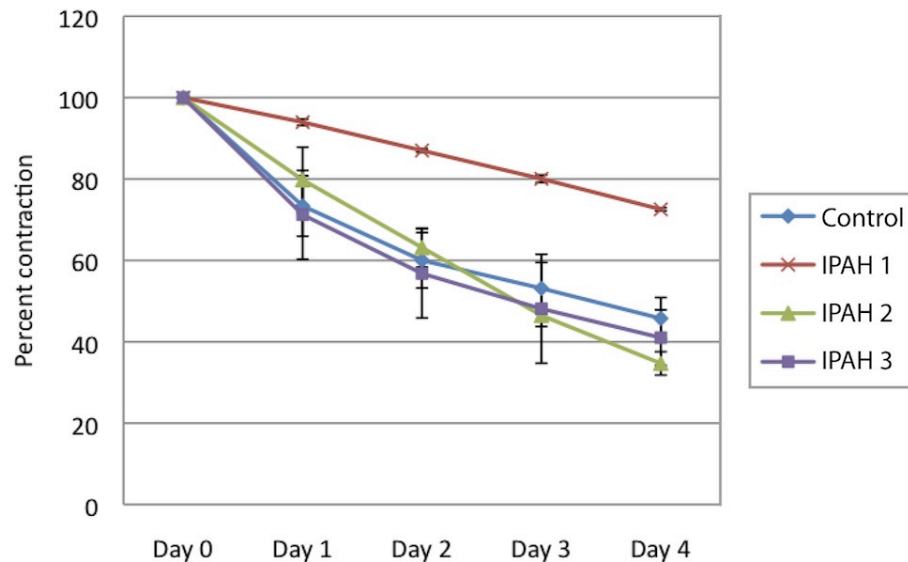


Figure 3.6 IPAH SMC contractility in collagen gels. Percent contraction of collagen gels containing IPAH and control PASMCs cultured for 4 days.

To better understand the contractile behavior of IPAH and control cells, we employed microfabricated post-array detectors (mPADs) to directly measure the traction forces exerted by individual cells (Fig. 3.7A) (Tan et al., 2003). Deflections measured upon seeding control and IPAH PASMCs onto mPADs showed only a moderate increase

in the IPAH cells (Fig. 3.7B). mPAD devices allowed us to make a variety of measurements including force per post, force per cell, and cell area. Measurements of cell area indicated that the IPAH SMCs spread to slightly larger areas. This increase in spread area contributed slightly to the total force per cell exerted by these cells. When cells with similar areas were compared, no differences in total traction force were observed. The most significant difference in traction forces were observed in measurements of traction force per post. These differences, however, were not statistically significant when compared via a student's t-test ($p > 0.05$).

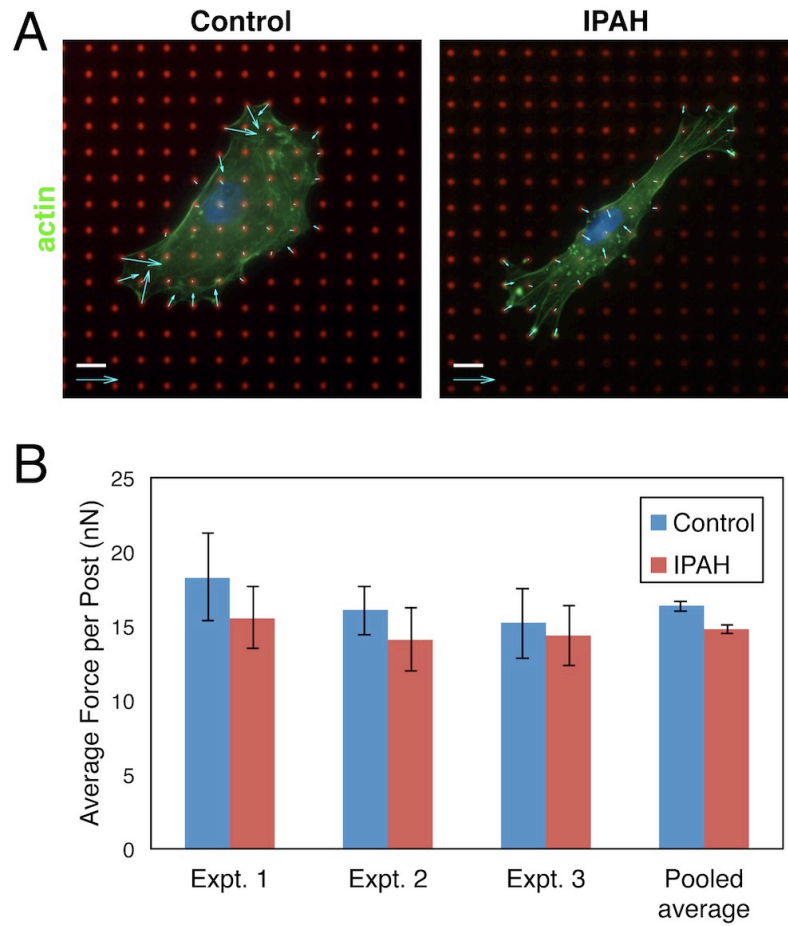


Figure 3.7 Measurements of traction forces generated by IPAH PSMCs. (A) Representative images of control and IPAH PSMCs seeded onto mPADs. (red: DiI, tops of PDMS posts, arrows: force vectors) (bar: 10 μ m) (B) Measurements of force exerted per post by control and IPAH PSMCs. (errors bars represent sd in expts. 1, 2, and 3 and sem in pooled data, measurements of at least 20 cells of each type were made in each experiment).

3.4 Further characterization of IPAH PSMCs

Observations of the IPAH PSMCs in routine culture suggested that they may exhibit an altered adhesive behavior. To test this hypothesis, we labeled control and IPAH SMCs with CyQUANT dye and determined the relative numbers of cells that remained attached to substrates coated with varying concentrations of fibronectin after 45 minutes. We performed this adhesion assay with 3 control and 3 IPAH cell lines, which were newly acquired. Results indicated that cells from all 6 cell lines were able to adhere in much larger quantities when the fibronectin concentration was increased to at least 1 $\mu\text{g/ml}$ Fig. 3.8). Differences between individual or pooled control and IPAH groups were not significant. Minor variations to this trend were observed at individual time points but no significant trends were observed overall.

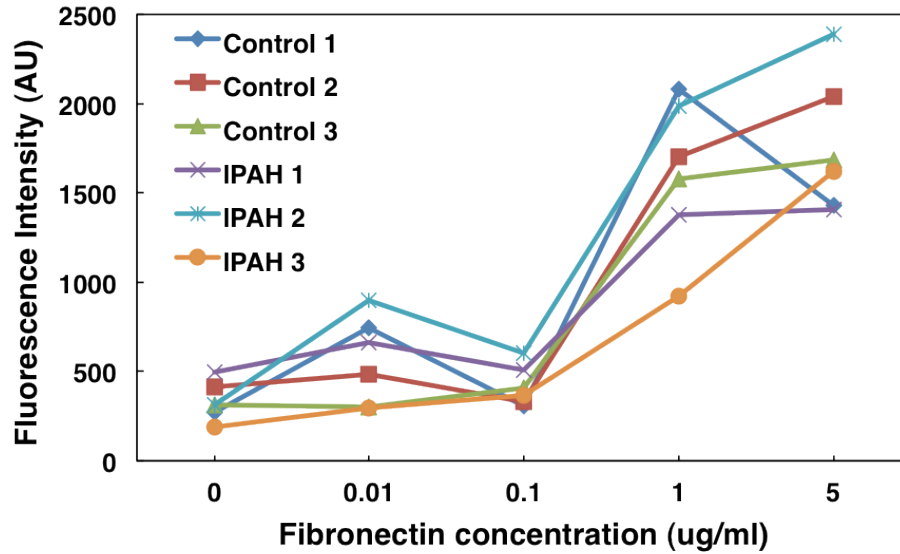


Figure 3.8 Adhesion of control and IPAH PSMCs to fibronectin-coated substrates. Quantification of control and IPAH cells labeled with CyQUANT and seeded onto polystyrene substrates coated with varying concentrations of fibronectin (measurements represent average of three replicate wells per condition).

Given that aberrant proliferation of vascular cells is a hallmark of pulmonary hypertension, we decided to investigate the proliferative behavior of IPAH SMCs (Chin & Rubin, 2008). First, we confirmed that both control and IPAH PSMCs grown to confluence and treated with serum free medium ceased proliferating and remained viable in culture. Once a successful synchronization protocol was established, we investigated the effects of seeding density on proliferation in both control and IPAH cells. IPAH and control cells both exhibited a biphasic response in proliferation rates when seeded at low, medium or high densities (Fig. 3.9A). Proliferation reached a maximum at medium

density (some cell-cell contact but not yet confluent) and a minimum at low (little to no cell-cell contacts) and high (near confluence) densities. In general, IPAH PASMCs were found to proliferate at rates approximately twice as high as those in control cells. To further investigate whether cell-cell contacts may be abnormal in IPAH cells, we assayed the basal expression levels of N-cadherin. Western blots indicated that N-cadherin expression in IPAH cells was significantly lower than in control cells. Additionally, we found that IPAH and control PASMCs transduced via an adenoviral vector with a dominant negative form of N-cadherin proliferated at similar rates. This result suggested that proliferation in IPAH SMCs could be lowered to normal levels by knockdown of N-cadherin. More extensive studies of proliferative regulation in IPAH PASMCs are described in section 3.5 below.

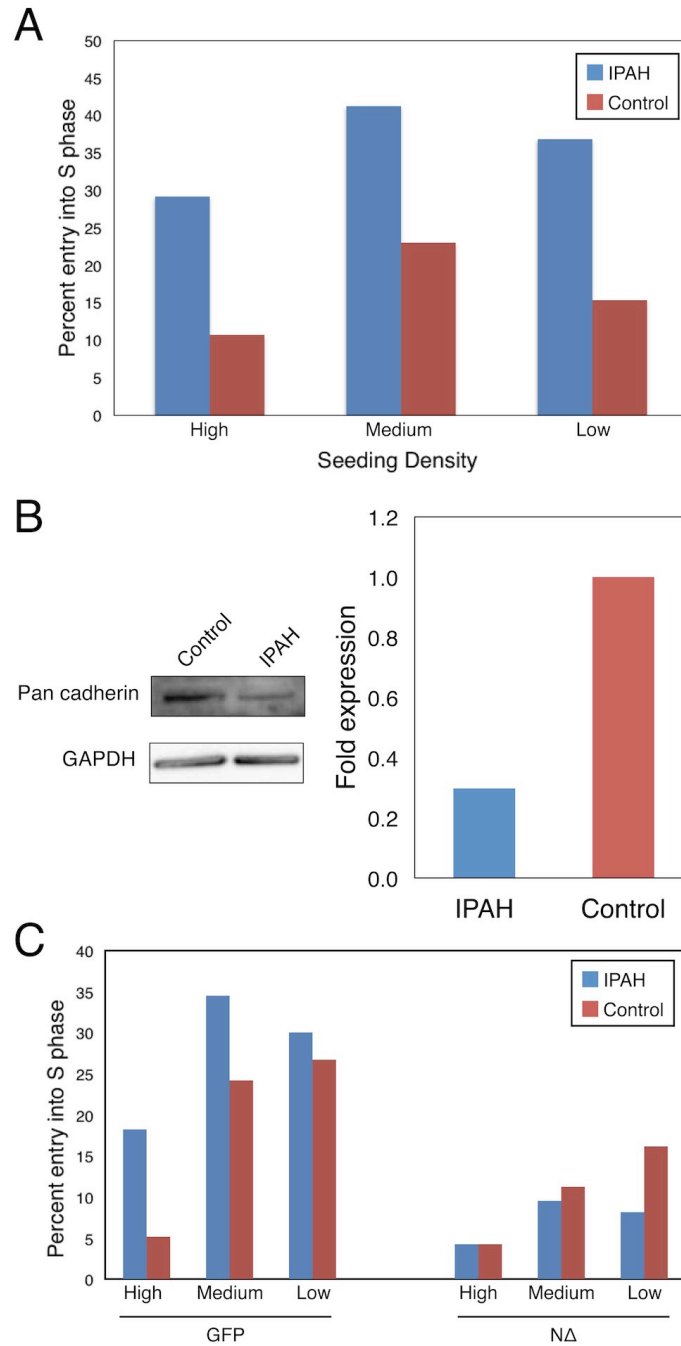


Figure 3.9 Effects of cell density and N-cadherin expression on IPAH PASMC proliferation (A) Both control and IPAH PASMCs exhibit a biphasic response in proliferation to varying levels of cell density. Overall proliferation rates were

approximately two-fold higher in IPAH cells (data represent at least 150 cells of each type counted from a single experiment). (B) IPAH PASMCs expression levels are approximately one-fourth lower than in control cells (data represents one experiment) (C) Expression of dominant negative N cadherin significantly lowered proliferation rates in both IPAH and control cells. Proliferation in IPAH PASMCs expressing N Δ dropped to levels below those in control cells (data represent average proliferation rates of at least 150 cells in each condition from a single experiment).

To further characterize the phenotype of IPAH PASMCs, we performed quantitative real-time PCR analysis for a panel of SMC differentiation markers. We found that all SMC differentiation markers examined (smooth muscle actin α -2, calponin, myocardin, SM22 α and smoothelin) were downregulated in the IPAH PASMCs (Figure 3.10). Taken together, the proliferation and gene expression data suggest that the IPAH PASMCs are likely to have undergone a switch from a differentiated to a less differentiated, highly proliferative phenotype. Subsequent analysis of additional IPAH donor cells, however, indicated that the observed trends were evident in only one IPAH PASMC cell line.

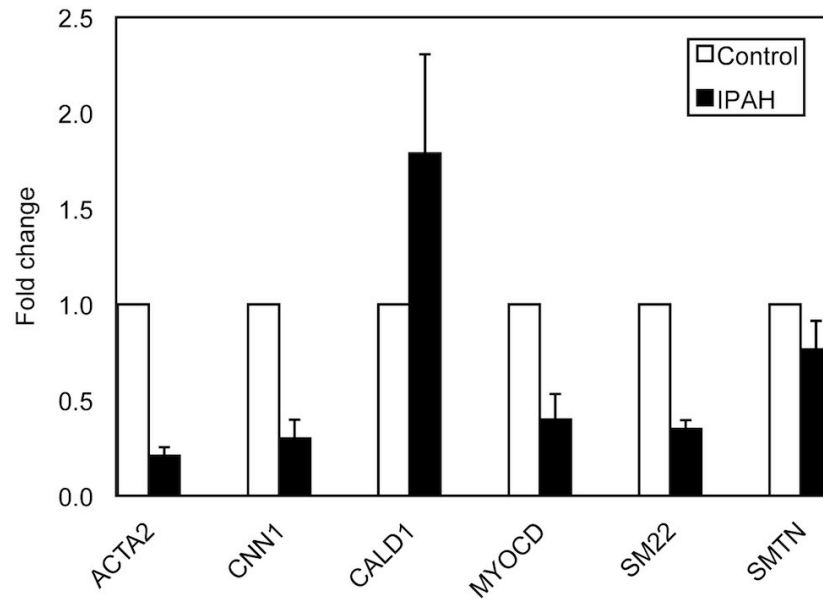


Figure 3.10 SMC marker expression levels of control versus IPAH PSMCs. SMC marker expression levels were measured by qRT-PCR. Cells were G0 synchronized, replated at a density of 5,000 cells/cm² prior to RNA isolation. (data are expressed as \pm SEM from at least 3 independent experiments. *, $p < 0.05$)

Previous studies have shown that decreased expression levels of the basement membrane protein perlecan might contribute to SMC hyperplasia *in vivo* (Tran et al., 2004). Immunofluorescent staining of IPAH PSMCs suggested that they might express reduced levels of perlecan in culture (Fig. 3.11). While it is plausible that IPAH PSMCs exhibit abnormal expression levels of ECM proteins in culture, these findings remain to be confirmed by western blot analysis and in a variety of donor cell lines.

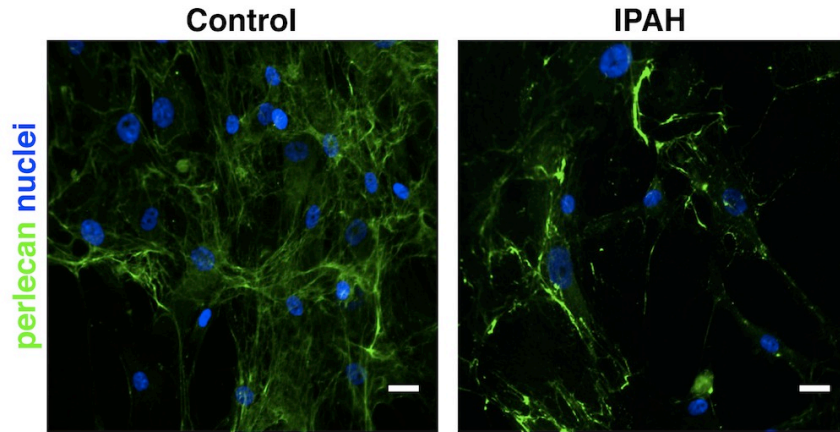


Figure 3.11 Perlecan deposition patterns in IPAH PASMC cultures. Cells were plated at a density of 5,000 cells/cm² and fixed 24 hours later. Staining patterns suggest that perlecan deposition by IPAH PASMCs may be lower than those in control cells. (bars: 25 μ m)

3.5 Proliferative regulation by adhesion and Rho GTPases is altered in IPAH PASMCs

3.5.1 Proliferation in IPAH SMCs is Rho-dependent

To test whether SMCs isolated from lungs of patients with IPAH exhibited a hyperproliferative phenotype *in vitro*, we cultured isolated PASMCs and measured their rate of S phase entry via a bromodeoxyuridine incorporation assay. PASMCs isolated from diseased lungs of multiple donors showed a significant increase in proliferation over control cells isolated from individuals without PAH (Fig. 3.12A). These results suggest that SMCs from patients IPAH retain their *in vivo* hyperproliferative phenotype when

isolated. Additionally, routine observation of control and IPAH SMCs in culture indicated the possibility of differences in adhesion between the IPAH and control cells. Specifically, the IPAH SMCs appeared to attach and spread more quickly than control cells (data not shown). Because the small GTPases RhoA and Rac 1 play known roles in cytoskeletal reorganization during cell spreading and in proliferative control, we investigated whether the RhoA or Rac 1 signaling pathways were involved in the proliferative control of IPAH PSMCs. After synchronizing control and IPAH PSMCs in G_0 , we replated the cells onto fibronectin in the presence of either the ROCK inhibitor Y-27632 or NSC-23766, to block Rac 1 signaling. We found that the hyperproliferation exhibited by IPAH PSMCs was reduced to levels comparable to those of the control cells via treatment with Y-27632. Control PSMCs were significantly less affected by Y-27632 treatment, but were particularly sensitive to NSC-23766 treatment (Fig. 3.12B). These data suggest that PSMCs of patients with IPAH may undergo a Rac-to-Rho proliferative control switch.

To further substantiate whether RhoA signaling might be higher in IPAH cells, we compared RhoA activity levels in PSMCs from a single diseased lung and a control lung. We found that the IPAH PSMCs have a greater than 2-fold higher RhoA activity as compared to the control cells (Fig. 3.12C). Taken together, these results suggest that RhoA signaling is altered in IPAH and that this may underlie the aberrant proliferation of IPAH PSMCs.

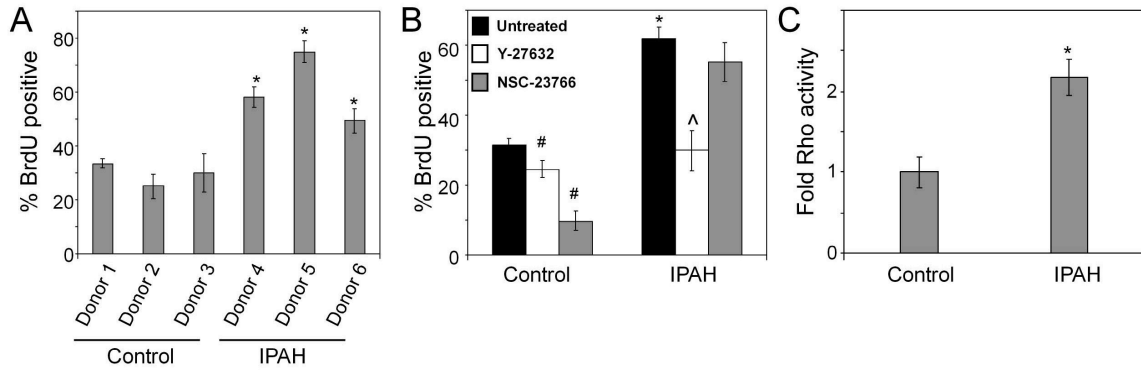


Figure 3.12 Proliferation rates of control and IPAH PASMCs in culture. (A) Baseline proliferation of isolated control and IPAH SMCs as measured by BrdU incorporation. *, $p < 0.05$. (B) Proliferation of control and IPAH SMCs after treatment with the RhoA inhibitor Y-27632 or the Rac inhibitor NSC-23766. Data represent pooled results from all control or IPAH donor cells. *, $p < 0.05$ for comparison of untreated control PASMC vs. IPAH PASMC. #, $p < 0.05$ for comparison of untreated control PASMC vs. drug-treated control PASMC. ^, $p < 0.05$ for comparison of untreated IPAH PASMC vs. NSC-23766-treated IPAH PASMC. (C) RhoA activity levels measured in a single control and IPAH donor cell population. *, $p < 0.05$. All data (panels A, B, and C) are expressed as \pm SEM from at least 3 independent experiments.

3.5.2 Adhesion signaling is altered in IPAH PASMCs

Focal adhesions are mechanical and biochemical linkages between the cell and its extracellular environment. Because focal adhesion size is known to be regulated by RhoA signaling (Chrzanowska-Wodnicka & Burridge, 1996), we sought to examine whether focal adhesion architecture or the expression levels of focal adhesion proteins might be

altered in IPAH PASMCs. We first investigated whether differences in the expression of vinculin, a key focal adhesion protein, existed in IPAH versus control cells. Indeed, we observed that IPAH PASMCs exhibited significantly higher vinculin expression than the control PASMCs (Fig. 3.13A). To visualize focal adhesion size and architecture, we performed vinculin immunostaining and found that focal adhesions appeared longer in IPAH cells versus controls (Fig. 3.13B). Quantification of focal adhesion length revealed that adhesions in cells from patients with IPAH were almost 50% larger than those in control PASMCs (Fig. 3.13C).

To investigate whether altered focal adhesion structure might also give rise to differences focal adhesion signaling, we measured the phosphorylation status of focal adhesion kinase (FAK), a key signaling molecule within focal adhesions. We found that IPAH SMCs expressed higher levels of FAK phosphorylated at Y397 (autophosphorylated FAK) than control cells (Fig. 3.13D). The aberrant focal adhesion size and signaling may contribute to the observed proliferation differences.

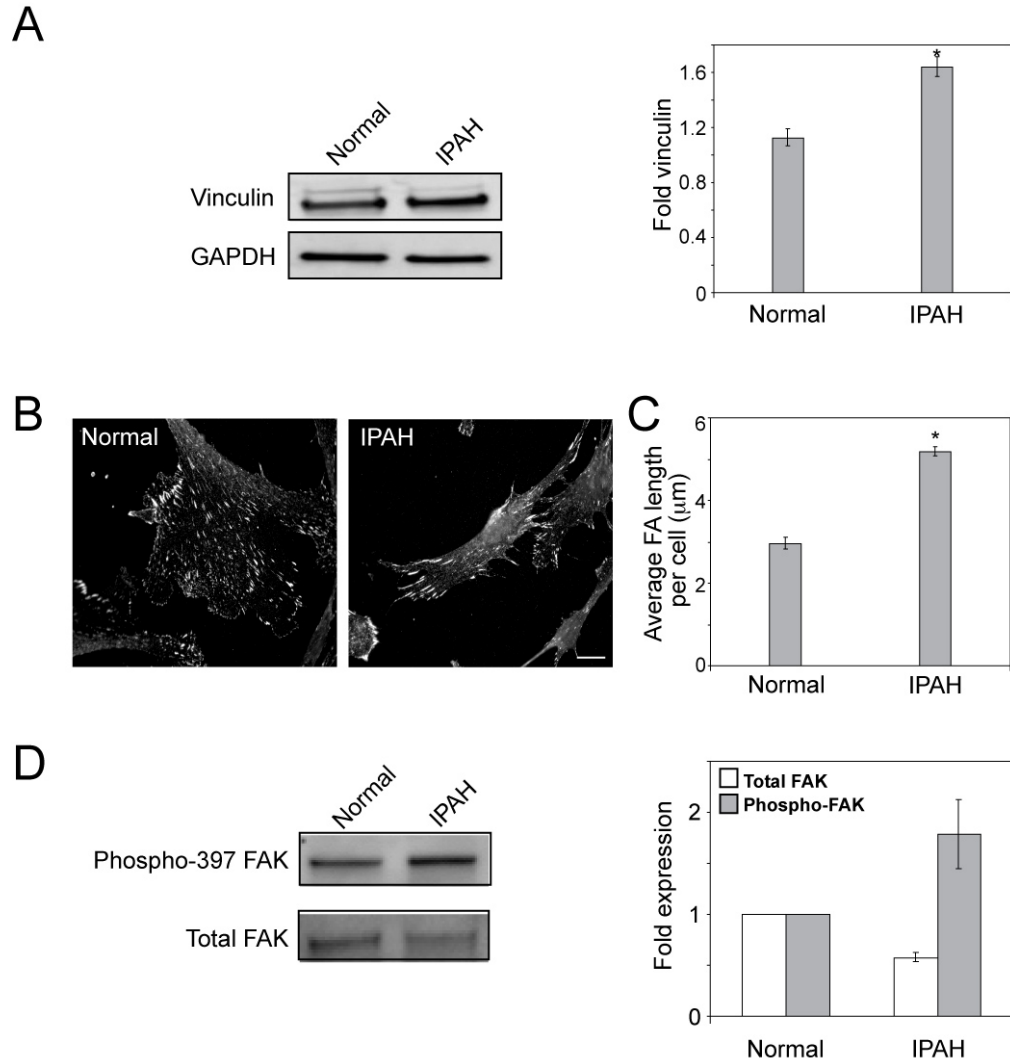


Figure 3.13 Focal adhesion size, structure, and FAK phosphorylation status in IPAH PSMCs. (A) Representative blots and quantification of vinculin expression in control and IPAH PSMCs. Quantification represents pooled data from all control and IPAH donors. *, $p < 0.05$. (B) Representative immunostaining for vinculin in control and IPAH PSMCs. Scale bar: 20 μm . (C) Quantification of average focal adhesion length in control and IPAH PSMCs. *, $p < 0.01$. (D) Representative blots and quantification of total and

phospho-397 FAK in control and IPAH PSMCs. Data are expressed as \pm SEM for panels A-C and \pm SD for panel D.

3.5.3 High proliferation in IPAH PSMCs is mediated by altered adhesion signaling

Cell adhesion to the extracellular matrix is a known regulator of cell growth and involves the physical spreading of cells against an underlying substrate (C. Chen et al., 1997; Raines, 2000). As expected, control PSMCs exhibited a nearly complete inhibition of proliferation when cultured on micropatterned substrates in which the geometry of the printed patterns limit the cell's ability to fully spread (Fig. 3.14A). Surprisingly, this adhesion-mediated growth control appears to be lost in IPAH PSMCs, which maintain their high proliferation rates even in a context of limited cell spreading (Fig. 3.14A). Because we have demonstrated that adhesion signaling through FAK is high in IPAH PSMC and that these cells exhibit altered adhesion-mediated growth control, we next investigated whether pharmacological inhibition of FAK would restore normal adhesion-mediated growth control in IPAH PSMC. We plated G0-synchronized IPAH PSMCs or control PSMCs onto micropatterned islands of fibronectin and treated with the FAK inhibitor PF-573,288. Blocking FAK signaling restored normal adhesion-mediated growth control mechanisms in the IPAH PSMCs (Fig. 3.14B). Together, these data suggest that IPAH PSMCs exhibit altered adhesion signaling, which appears to drive their hyperproliferation in culture.

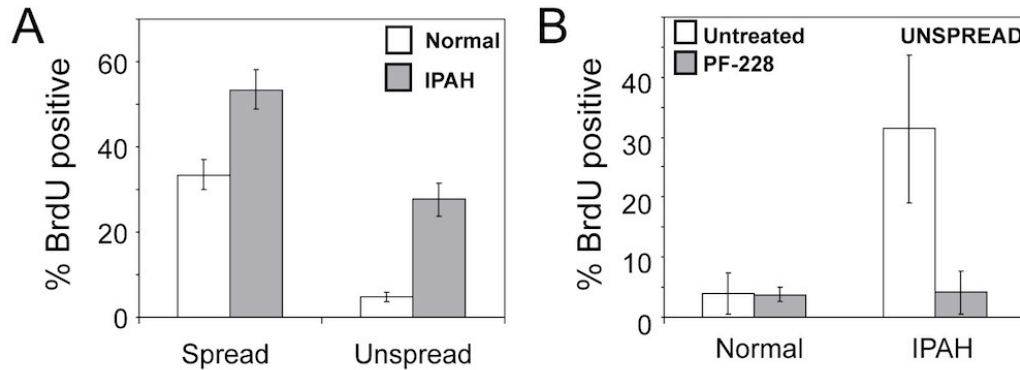


Figure 3.14 Adhesion-mediated proliferative control in IPAH PASMCs. (A) Proliferation of control and IPAH PASMCs on unpatterned (spread) and patterned (unspread) fibronectin-coated substrates. (B) Proliferation of control and IPAH PASMCs treated with PF-573,228 and seeded onto patterned fibronectin-coated substrates. All data are expressed as \pm SEM. *, $p < 0.05$ for comparison of control vs. IPAH PASMC under spread conditions. #, $p < 0.05$ for comparison of IPAH PASMC under spread vs. unspread conditions.

3.6 Materials and Methods

Cell Isolation

Lungs from IPAH patients were obtained through the Pulmonary Hypertension Breakthrough Initiative consortium. The lungs were grossly dissected by following the main pulmonary artery and subsequent branches until reaching the terminal vessels. The dissected arteries were then divided into three categories based on vessel diameter and the adventitia was removed by further dissection. For our studies, vessels with a diameter

of 1–5 mm were used. After isolation they were sectioned into approximately 30 mm long segments and placed into 100 mm tissue culture dishes with 10 mL SmGM-2 Smooth Muscle Growth Medium (Lonza). After two weeks, an additional 5 mL of growth medium was added, and a 50% change of growth medium was performed after a total of three weeks in culture. At this time, any remaining tissue was removed from the culture dish, and the remaining PASMCs were cultured under standard conditions as described below. Control PASMC were isolated from patients without pulmonary arterial hypertension using the same procedure.

Cell culture and reagents

PASMCs were cultured in Smooth Muscle Growth Medium-2 (Lonza) and were maintained at 37°C in a humidified CO₂ incubator. Y27632 and NSC23766 were purchased from EMD Biosciences. PF-573,228 was purchased from Tocris. All experiments were performed using cells at passage 8 or earlier.

Proliferation Assays

Control or IPAH diseased PASMC were G₀ synchronized by serum starvation for 24 hours. Cells were then trypsinized and replated in the presence of BrdU (GE Healthcare). Cells were fixed at 24 hours and stained for BrdU incorporation using a monoclonal antibody directed against BrdU (GE Healthcare) followed by incubation with an AlexaFluor-594-conjugated anti- mouse secondary antibody (Invitrogen). Cells were counterstained with Hoechst 33342 (Invitrogen). For inhibitor studies, cells were treated

with 25 μ M Y27632, 50 μ M NSC23766, or 5 μ M PF-573,228 at the time of plating after synchronization.

Quantitative Real-Time PCR Analysis of Smooth Muscle Cell Markers

Prior to lysis, cells were grown to confluence, cultured in the absence of serum for 24 h, and replated at a density of 5,000 cells/cm². The cells were then lysed and RNA was isolated using the RNeasy Micro Kit (Qiagen). 0.5 μ g of RNA from each sample was spotted in triplicates into a 96-well PCR plate (ISC BioExpress) along with nuclease-free water (Ambion) and oligo(dT) primer (Promega). The plate was heated to 70 °C for 2 min, after which a master RT-PCR mix containing 5x first strand buffer (Invitrogen), dNTP mix (Promega), RNasin RNase inhibitor (Promega) and M-MLV reverse transcriptase (Promega) was added. The RT reaction was run using an Eppendorf Mastercycler Gradient thermal cycler as follows: 42 °C for 1.5 h, 94 °C for 5 min, hold at 4 °C. 80 μ L water was added to the samples containing cDNA, and they were stored at -20 °C. Quantitative real-time PCR was performed in triplicate using TaqMan probes specific for ACTA2, CNN1, MYOCD, SM22, SMTN and GAPDH (Applied Biosystems) with the FAM dye label. The real-time PCR reaction was run using an Applied Biosystems 7300 Real-Time PCR System using standard conditions: 2 min at 45 °C, 30 sec at 95 °C, and 40 cycles of 2 sec at 95 °C denaturation and 60 °C annealing/extension. Results were quantified using the comparative CT method with GAPDH used as the reference amplification. Data for each marker were normalized to the control PSMC sample.

Immunocytochemistry, image analysis, and quantitative analysis of focal adhesions

Quantitative analysis of focal adhesions was performed as previously described (Pirone et al., 2006). Briefly, cells were incubated for 1 min with ice-cold cytoskeleton buffer (50 mM NaCl, 150 mM sucrose, 3 mM MgCl₂, 1 μg/mL of the following protease inhibitors: aprotinin, leupeptin, pepstatin, and 2 mM PMSF), followed by 1 min in ice-cold cytoskeleton buffer supplemented with 0.5% Triton-X 100. Detergent extracted cells were fixed in 4% formaldehyde in PBS, washed, and incubated with the hVin-1 primary antibody against vinculin (Sigma-Aldrich). Vinculin staining was visualized by incubation with an AlexaFluor-594-conjugated secondary antibody (Invitrogen). Quantitative microscopy of focal adhesions was performed using a SPOT camera (Diagnostic Instruments) attached to an inverted microscope (Zeiss, Axiovert 40 CFL) using a 63X oil immersion objective. Images were obtained and processed using SPOT software (Diagnostic Instruments) to measure the length of individual focal adhesions. Approximately 10 cells were analyzed per experimental condition.

RhoA activity assays

RhoA activity was quantified using an absorbance based G-LISA RhoA Activation Assay (Cytoskeleton) according to the manufacturer's instructions. Briefly, IPAH or normal control PSMCs were grown to confluence and serum starved for 24 hours. The cells were then plated into fibronectin coated (25 μg/mL) dishes at a density of 7,000 cells/cm² and lysed with the provided lysis buffer after 4 hours. Total protein concentration was

measured using the supplied reagents and each sample was added to duplicate wells of the provided 96-well plate. Following the manufacturer's protocol, antigen presenting buffer, primary antibody solution, secondary antibody solution and HRP detection solution were sequentially added to the wells. The signal was read by measuring absorbance at 490 nm using a multifunction microplate reader (TECAN GENios, TECAN).

Western Blots

Cells were washed in TBS and lysed in cold RIPA buffer. Proteins were separated by denaturing SDS-PAGE, electroblotted onto a PVDF membrane (Bio-Rad Laboratories), blocked with 5% milk in TBS, immunoblotted with specific primary antibodies, and detected using horseradish peroxidase-conjugated secondary antibodies (Jackson ImmunoResearch Laboratories) and SuperSignal West Dura (Pierce Chemical Co.) as a chemiluminescent substrate. Densitometric analysis was performed using a VersaDoc imaging system with QuantityOne software (Bio-Rad Laboratories).

Micropatterned Substrates

To generate stamps for microcontact printing of proteins, a prepolymer of poly(dimethylsiloxane) (PDMS; Sylgard 184; Dow Corning) was poured over a photolithographically generated master, as previously described (C. Chen et al., 1997). Stamps were immersed for 1 h in 50 µg/ml fibronectin, washed three times in water, and blown dry under nitrogen. Coated stamps were placed in conformal contact with a

surface-oxidized PDMS- coated glass coverslips. Stamped coverslips were immersed in 0.2% Pluronic F127 (Sigma-Aldrich) in PBS for 1 h and washed.

3.7 Conclusions

Organotypic models provide an important intermediate platform between traditional tissue culture models and *in vivo* studies for investigations into disease mechanisms in a physiologically relevant context. In previous studies, models of the arterial wall have been proposed that utilize sequentially seeded layers of SMCs and ECs to form a bilayer mimicking the intimal and medial compartments of arteries (Niwa et al., 2007; Ziegler et al., 1995). In the work described here, we have attempted to replicate a version of this model using bPAECs and bPASMCS with the eventual goal of employing ECs and SMCs derived from patients with IPAH. However, bPAECs seeded onto monolayers of bPASMCS treated with ascorbic acid failed to spread and form monolayers. As an alternative approach, we sought to generate layers of SMCs cultured atop confluent layers of ECs. However, failure to also generate this ‘inverse’ arterial wall model led us to abandon these approaches and focus on studying mechanisms regulating the proliferation of IPAH PASMCS using more traditional tissue culture models.

IPAH is characterized by an increase in SMC proliferation and subsequent occlusion of the luminal space. While we have a basic understanding of the pathophysiology of IPAH as it relates to vascular architecture, the underlying molecular etiology of the proliferative-driven thickening of the tunica media remains unclear. In the work presented here, we have demonstrated that the regulation of proliferation via Rho

GTPase activity and adhesion signaling pathways are dysfunctional in vascular SMCs isolated from patients with advanced IPAH.

Overall, our data presented here suggest the presence of a defect in the proliferative regulation mechanisms of SMCs obtained from patients with IPAH. These IPAH cells display a higher than normal expression of RhoA, increased focal adhesion size, and aberrant focal adhesion signaling, all of which are key in properly modulating proliferation. This lack of proliferative regulation via focal adhesions and cell spreading is reminiscent of an SMC phenotype found in neointimal lesions of IPAH patients (Chin & Rubin, 2008). Taken together, these findings suggest that the underlying etiology of IPAH is likely to have a mechanochemical basis.

CHAPTER 4: Discussion and Future Directions

4.1 Discussion of patterned endothelial cell cords for vascularizing engineered tissues

4.1.1. *In vitro* generation of endothelial cell cords

In the work described in Chapter 2, we have developed a novel strategy for generating functional capillaries with spatially controlled geometry *in vivo*. Our technique relies on the implantation of patterned endothelial cell cords into mice. The cords are formed using microfabricated PDMS templates to spatially arrange endothelial cells within collagen gels. We observed that HUVEC and 10T1/2 cells organized into cords through a contractility dependent process and have previously shown that they exhibit proper cell-cell junction formation (Raghavan, Nelson, Baranski, Lim, & Chen, 2010a).

Most *in vitro* approaches for generating constructs for the study of vascular biology have focused on creating endothelialized tubes (Chrobak et al., 2006; Miller et al., 2012). While these strategies are capable of generating increasingly complex architectures, their application has been limited to the creation of large diameter tubules. Other studies have demonstrated that endothelial cells seeded onto thin (10 μm) lines of patterned matrix also leads to the formation of cords (Dike et al., 1999). While this approach is capable of generating geometrically patterned cords, here we demonstrate the additional ability to alter cord diameter and, most importantly, the ability to embed the cords into implantable tissue constructs for further study *in vivo*. Our approach for

patterning cells into cords is capable of generating complex branched networks and geometries that mimic native vasculature within engineered tissues. In addition, because the cords in our system are formed in a separate step from their embedding into a surrounding material, they can be readily used to combine patterned vasculature with parenchymal or other cells. As an example, we demonstrate that aggregates of hepatocytes embedded into the matrix surrounding patterned cords exhibit improved function due to increased vascular access.

In the studies described in Chapter 2, EC cords were removed into fibrin, a natural ECM material that has been used extensively in angiogenic applications and one whose proangiogenic properties of have been well documented (X. Chen et al., 2009; Ghajar, Blevins, Hughes, George, & Putnam, 2006; Hall et al., 2001; Lesman et al., 2011). To study the effects of ECM properties on vascularization of engineered tissue constructs, one might envision embedding cords within ECMs such as PEG hydrogels that allow for independently varying material properties (Miller et al., 2010; Moon et al., 2011). Other natural ECMs such as Matrigel have been shown to elicit a strong angiogenic response *in vivo* (Passaniti et al., 1992). While our work has been limited to the use of fibrin as the proangiogenic scaffold for embedding cords, one could envision studies that utilize a variety of materials with different properties to gain better insights into the vascular response.

Our *in vitro* characterizations revealed that cords form via the cells' compaction of surrounding ECM using a contractility dependent process and that cells are distributed randomly throughout the fully formed cords. Over three decades ago, studies first showed

that fibroblasts embedded within a collagen gel progressively contract and reduce the diameter of the gel (E. Bell, Ivarsson, & Merrill, 1979). More recently, it has been shown that endothelial cells also exhibit similar contractile behavior in collagen gels (Vernon & Sage, 1996). Although the cords described here are geometrically different than the discs typically used in these contractility studies, it is likely that the contraction we observe in cords is driven by the same mechanisms. In their study Sage and colleagues observed that endothelial cells contracted collagen gels similarly to dermal fibroblasts. Although the traction forces generated by C3H10T1/2 cells have never been assayed directly, it is likely that they exhibit similar contractile forces to that of other cells of mesenchymal origin such as fibroblasts. Given comparable levels of contraction to that of HUVECs and the relatively low abundance of 10T1/2s in our cords, it is not surprising that their absence has no measurable effect on the rate or degree of cord formation. To precisely tease out the relative contributions of each cell type, one might envision experiments involving the direct measurements of traction forces exhibited by each cell type as well as measuring the contraction rates of gels formed with varying proportions of the two cell types. However, the formation of cell-cell contacts and juxtaposition of neighboring cells rather than contractility likely contribute most to the vascularization process *in vivo* (discussed below).

4.1.2 The vascularization response to implanted endothelial cell cords

Implantation of tissue constructs containing cords of endothelial cells led to the formation of functional capillaries *in vivo*. We observed that the capillary walls were comprised of implanted endothelial cells and became perfused with blood within 3 days PI. Previous

studies of engineered vasculature have shown that implanted endothelial cells contribute directly to the formation of vessels and persist for up to one year *in vivo* (X. Chen et al., 2010; Koike et al., 2004). Our findings that viable cells within cords are required for the vascularization response suggest that similar mechanisms of cells organizing into lumenized vessels take place within the vascularization strategy described here.

While our analyses here have been limited to post-sacrifice histology and imaging, one might envision the use of longitudinal intravital imaging techniques to directly observe the cellular dynamics within implanted cords (Au, Daheron, Duda, Cohen, Tyrrell, et al., 2008a; White et al., 2012). Histological studies of implanted EC cords indicate that cells of human origin persist within the capillaries for at least 28 days. We also observe, however, that these vessels remodel significantly upon formation, becoming smaller, invested by pericytes, and more numerous. While no notable differences exist between capillaries within cords and the host vasculature, the formation process of the engineered is likely unique. Interestingly, events in vascularization upon implantation of EC cords resemble early processes in both vasculogenesis and angiogenesis. In vasculogenesis, aggregates of angioblasts, or endothelial precursor cells, organize around blood islands to form nascent vessels (Risau & Flamme, 1995). In angiogenesis, prior to forming a lumen sprouting endothelial cells migrate collectively as a ‘cord’ (Adams & Alitalo, 2007). Patterned cords of endothelial cells likely become vascularized utilizing a combination of mechanisms that underlie these two physiological processes. To shed light on some of the underlying mechanisms that drive the vascularization process, one might envision adapting our vascularization strategy for use

with longitudinal intravital imaging techniques. Questions particularly worthy of investigation using such a system might be: 1) how do implanted ECs sort and migrate to form lumenized vessels? 2) what is the fate of implanted ECs that do not become incorporated into the walls of capillaries? 3) do implanted 10T1/2 cells contribute to the pericyte population observed in mature capillaries? While our data demonstrate the successful formation of spatially controlled capillary networks *in vivo*, further studies such as those described above will undoubtedly herald manipulations that allow an additional level of control over the vascularization process.

4.1.3 Role of cell type in the vascularization response upon implantation of endothelial cell cords

A variety of cell types have successfully been used in various strategies for engineering microvasculature (Au, Daheron, Duda, Cohen, Tyrrell, et al., 2008a; Au, Tam, Fukumura, & Jain, 2008b; X. Chen et al., 2010; Ghajar et al., 2006; Melero-Martin et al., 2008). Findings by George and colleagues indicate that cell networks formed prior to implantation lead to a more robust vascularization response *in vivo* (X. Chen et al., 2009). Here, we confirmed that a 1:50 combination of C3H10T1/2s:HUVECs exhibits extensive networking behavior when embedded within collagen gels *in vitro*. Additionally, previous studies have demonstrated that 10T1/2s are capable of contributing to the vascularization process by differentiating into smooth muscle cells or pericytes (Hirschi et al., 1998). Based on these findings, the majority of studies described here were conducted using a combination of 1:50 10T1/2s and HUVECs. Our data suggest that nearly all capillaries formed in the implanted cords exhibited the presence of α -

SMA-positive cells immediately adjacent to the vessel walls. While the HUVECs could be readily identified using immunohistochemical techniques due to their human origin, we were unable to immunostain the murine-derived 10T1/2s. A study utilizing labeled 10T1/2 cells (e.g. with GFP) is needed to definitively elucidate their contribution to the vascularization process. It could be postulated that alternative mechanisms could be responsible for recruiting α -SMA-positive of host origin to the forming vessels. Studies have shown that circulating perivascular progenitor cells can contribute to tumor angiogenesis (Mancuso et al., 2011). While unlikely, sources of pericytes such as these cannot be ruled out until more detailed studies are conducted. Despite lacking knowledge on the exact role of 10T1/2s in implanted EC cords, our data and other studies suggest that they play a direct role in driving the maturation of newly formed capillaries.

Previous studies have shown that endothelial cells of various origins exhibit different levels of angiogenic potential *in vivo* (Barclay et al., 2012). While the HUVECs employed in our studies have a verified endothelial phenotype including the expression of CD31 and von Willebrand factor, their capability to contribute to angiogenesis was not directly tested. Vascularization strategies employed by others have utilized a variety of cell types including human adult and cord blood derived endothelial progenitor cells and human embryonic endothelial cells (Levenberg et al., 2005; Melero-Martin et al., 2008). Future studies should focus on the ability of these and other cell types to contribute to the vascularization process in implanted EC cords.

4.1.4 Role of growth factor signaling in the vascularization response upon implantation of endothelial cell cords

Previous studies have shown that production of growth factors such as VEGF by pericytes is associated with endothelial cell survival (Darland et al., 2003). Additionally, PDGF produced by endothelial cells works to recruit and maintain pericytes in a differentiated state (Hirschi et al., 1998). Such VEGF/VEGFR and PDGF/PDGFR paracrine loops between HUVECs and 10T1/2 cells are likely at the heart of growth factor signaling within EC cords. While not directly measured in our studies, previous of angiogenic mechanisms have demonstrated that HUVECs respond to canonical proangiogenic growth factors such as VEGF (Angulo et al., 2011). Additionally, it has been shown that HUVECs modulate the proliferation and differentiation of 10T1/2 via PDGF when cultured together (Hirschi, Rohovsky, Beck, Smith, & D'Amore, 1999). While these signaling pathways help to regulate HUVEC and 10T1/2 angiogenic behavior within cords *in vitro*, they are subject to an additional milieu of growth factors upon implantation. Differentiated 10T1/2s are known to produce VEGF and maintain endothelial cell survival (Darland et al., 2003). Likely, 10T1/2s embedded within cords signal not only to adjacent HUVECs but also to the surrounding host tissue. Indeed, our data suggest that angiogenic activity leads to capillary formation between adjacent cords (Fig. 2.25), a phenomenon that is likely driven by secretion of growth factors from adjacent cords.

Host tissue is undoubtedly affected by growth factor signaling from implanted cords. Likely, factors including VEGF and PDGF stimulate angiogenic sprouting from

otherwise quiescent host vessels and help to recruit mural cells to forming capillaries, respectively. Indeed, it has been shown that implanted endothelial cells elicit a wound healing response in host tissue that is regulated by growth factors including VEGF and PDGF among others (Soejima, Negishi, Nozaki, & Sasaki, 1998). While our histological analyses do not suggest that a host angiogenic response reaches the center of implanted constructs, we do observe vessels of host origin near the periphery. Likely, this angiogenic response from host vessels is driven in large part by secreted growth factors. Localization of growth factor signaling to the periphery of implanted constructs is further supported by evidence that secreted VEGF is largely cell- or matrix-bound, effectively limiting its ability to signal over large distances (Darland et al., 2003).

In vivo, growth factors are secreted into the surrounding matrix and form complex spatiotemporal gradients within tissues, making their detection and characterization particularly challenging (Guo et al., 2012). Additional study into the role of growth factor signaling in the vascularization response upon implantation of EC cords could be undertaken by loss- or gain-of-function studies and pharmacological inhibition. Namely HUVECs or 10T1/2s lacking VEGF, PDGF, or their receptors might be used to generate cords. Subsequent implantation and histological analyses would shed light on the requirements of these angiogenic factors in the vascularization response. Specifically, it might be hypothesized that VEGF production by the implanted cells is required to elicit a proper angiogenic response from the surrounding host tissue. Thus, it would be interesting to investigate whether implantation of VEGF-null cells would still result in proper anastomosis and connection with the host vasculature. Additionally, one might

envision the use of pharmacological inhibitors of growth factor receptors to probe their roles in different stages of the vascularization response. For example, PDGF inhibitors could be introduced at day 5 post-implantation to determine whether it is required for capillary maturation. Lastly, materials with controlled-release properties might be employed to gain a degree of control over the delivery of the growth factors (Laham et al., 1999; Lin & Anseth, 2008). Use of such materials, however, would first require a thorough characterization of their capabilities in driving vascularization in tissue constructs containing EC cords.

4.1.5 Role of the extracellular matrix in the vascularization response upon implantation of endothelial cell cords

To date, a variety of natural and synthetic matrices have been used for generating vasculature *in vivo* (Lovett et al., 2009; Moon et al., 2011; Peters et al., 2002; Phelps & García, 2010). In the system described here, the combination of type I collagen and fibrin provides a permissive environment for vessel formation that consists of natural ECM materials that can be remodeled by cells over time. Both fibrin and collagen have been extensively used in tissue-engineered vascularization strategies and the proangiogenic activity of fibrin is well documented (X. Chen et al., 2009; Hall et al., 2001; Lesman et al., 2011; Oh, Lu, Kawazoe, & Chen, 2011; A. Y. Wang et al., 2008). The regulation of angiogenesis by ECM is largely manifested through its degradation by matrix metalloproteinases (Ghajar, George, & Putnam, 2008b). Here, we observed signs of fibrin degradation as early as 7 days PI. Likely, this degradation is a required and permissive cue for the sprout formation that we observed between capillaries in adjacent cords and at

the edges of implanted constructs. While these findings suggest that cells within cords actively remodel the fibrin matrix upon implantation, it is not clear whether MMP activity is required for the vascularization process. Indeed, because the ends of EC cords are often exposed near the edges of the encapsulating fibrin gel, matrix degradation may not be required for the host vasculature to enter into contact with the implanted cords. Given the rapid rate of vascularization that we observed, it is plausible that MMPs may only become upregulated over time as newly formed vessels begin to remodel. Interestingly, we observed no signs of collagen degradation within the cords. Studies have shown that specific MMPs, namely MT1-MMP, play a pivotal role in angiogenic processes both *in vitro* and *in vivo* (Collen et al., 2003). Given that various MMPs act selectively on the various ECM components, it would be especially interesting to examine their secretion patterns within tissue constructs containing EC cords. Ultimately, more elaborate studies employing MMP-resistant synthetic materials or genetic manipulations of MMP expression within implanted cells could be used to gain further insights into their role in the vascularization response described here.

When cultured cells are placed in a three dimensional environment such as within a gel of ECM, their proliferation rates typically decrease significantly (Cukierman, Pankov, & Yamada, 2002; Cukierman, Pankov, Stevens, & Yamada, 2001). In addition, quiescent endothelial cells, whether in a monolayer on a tissue culture dish or in patent vessel wall, exhibit very low rates of proliferation (S. M. Schwartz & Benditt, 1977). These trends suggest that cells within the EC cords used in our studies also proliferate at relatively low levels upon implantation. Accordingly, histological analysis did not reveal

cell numbers within cords that appeared to be dramatically higher than those originally implanted. This observation, however, is strictly qualitative and the question of proliferation has not yet been fully explored within our system. Immunostaining for proteins involved in cell cycle progression such as Ki-67 could be used as a simple for increased proliferation in the implanted cells.

4.1.6 Role of cell-cell contacts in the vascularization response upon implantation of endothelial cell cords

We have demonstrated that implanted cords of ECs become rapidly perfused with host blood upon implantation and form mature capillaries after just 7 days. While our results show that these capillaries are comprised of juxtaposed endothelial cells, the precise role of cell-cell contacts during capillary formation remains to be fully explored. Endothelial cell-cell contacts are known to play a vital role in angiogenesis and vessel homeostasis (Adams & Alitalo, 2007; Nguyen & D'Amore, 2001). In the context of engineered vasculature, previous studies have shown that increasing the amount of cell-cell contact between endothelial cells by 'preculturing' them for one week prior to implantation leads to enhanced vascularization *in vivo* (X. Chen et al., 2009). These studies led us to hypothesize that increased cell-cell contacts between ECs patterned into cords would allow them to rapidly form patent vessels while maintaining the geometry of the cords. In a previous study, we have shown that extensive CD31 cell-cell junctions form between adjacent ECs within cords (Raghavan, Nelson, Baranski, Lim, & Chen, 2010a). It is likely that the densely packed arrangement of HUVECs within cords allows them to form numerous other types of cell-cell contacts including adherens and gap junctions.

Formation of such contacts might allow cells within cords to act as a collective unit, much like an angiogenic sprout, and quickly form patent vessels upon the introduction of blood. While we have already shown that cords contain CD31 cell-cell junctions, the presence of adherens and gap junctions could be confirmed via immunostaining for their components including VE-cadherin and connexin 43, respectively. Such characterization would pave the way for subsequent loss-of-function studies that might be used to directly test the requirements for the presence of established cell-cell junctions during capillary formation. Viral delivery of dominant negative mutants of VE-cadherin, N-cadherin (for interfering with EC-10T1/2 interactions) or connexin 43 prior to cord formation could be utilized for this purpose. Because cord formation appears to be driven by cytoskeletal contractility, it is not likely that knockout of these proteins would interfere with this process *in vitro*. Indeed, one might hypothesize that the relatively high cell density even in uncontracted cords might be sufficient for extensive cell-cell contacts to rapidly form. Consequently, the contraction phase of cord formation might not be required for the vascularization response that follows their implantation.

Further histological studies such as those described in Chapter 2 will provide insights into whether mature cell-cell junctions within cords are required for their ability to drive capillary formation *in vivo*. Quantifiable outputs of these studies should include the rate of vascularization (time required until evidence of blood, lumenized vessels), vessel patency/leakiness, and long-term vessel stability. Implantation of heterologous cells or tissues such as EC cords requires the use of immunodeficient host animals. This requirement combined with lethal defects in animals whose cells are unable to form

proper adherens or gap junctions limits loss of function studies to the realm of manipulations of the implanted materials (Carmeliet et al., 1996; Radice et al., 1997; Reaume et al., 1995). Additional insights into the role of cell-cell contacts in driving the vascularization response could be achieved via gain of function experiments. Specifically, one might test whether overexpression of junctional proteins could be used to speed up or otherwise alter the vascularization response. If such manipulations were to speed up vascularization, a particularly interesting follow-up experiment would be to transiently overexpress the implicated junctional proteins. In such a model, one might hypothesize while initially higher expression levels help to drive a rapid and robust vascularization response that quickly produces patent vessels, the eventual return of the expression levels to baseline might be necessary to ensure proper vessel function over the long term. Overall, given the importance of cell-cell contacts in angiogenesis and homeostasis in quiescent vessels, it is likely that they play a significant role in the mechanisms underlying vascularization in our system.

4.1.7 Anastomosis with the host vasculature

Studies by George and colleagues have suggested that engineered capillary networks can anastomose with host vasculature within 1 day of implantation (X. Chen et al., 2010). Here, we have observed that implanted EC cords become perfused with blood within 3 days of implantation. Venous introduction of fluorescent dextran further confirmed that capillaries within the cords are perfused with host blood after 2 weeks. The underlying mechanisms of host-graft anastomosis in our system have not been fully elucidated, however. Findings by Jain and colleagues have suggested a ‘wrapping-and-tapping’

mechanism of anastomosis in engineered tissues (Cheng et al., 2011). Here, injections of lectins specific for mouse or human endothelium have suggested that some cells of mouse origin are present within the vessel walls near the edges of implanted constructs. These data suggest that an angiogenic response from the host tissue is elicited, causing typically quiescent host vessels to sprout and eventually connect with capillaries forming within the implanted cords. Presence of solely this mechanism, however, seems unlikely and would contradict the findings by Jain and colleagues. While not yet directly observed, we predict that a ‘wrapping-and-tapping’ mechanism of anastomosis might also play a role in the vascularization response described here.

Over the last several years, advanced methods for longitudinal intravital imaging of angiogenic processes in rodents have been developed (Koike et al., 2004; White et al., 2012). These imaging methodologies must now be adapted for use with the vascularization strategy described here in order to better understand the mechanisms that underlie host-graft anastomosis. Correctly predicting and imaging areas where anastomosis might occur remains difficult in current vascularization approaches. Interestingly, employing longitudinal intravital imaging techniques in conjunction with our vascularization strategy might not only provide insights into mechanisms of anastomosis within our system, but also enable investigators to more readily observe anastomotic events. We have recently been able to elicit a vascularization response in tissue constructs implanted subcutaneously by utilizing a mesh backing material. These results suggest that monitoring of cellular dynamics and subsequent anastomosis within an implanted window chamber is feasible.

In addition to the canonical interactions between tip cells in anastomosing angiogenic sprouts, research has recently shown that macrophages also play a role in guiding the sprouting tips (Fantin et al., 2010). The studies described here were performed in athymic mice, which, despite decreased immune function, possess the ability to recruit macrophages to sites of injury. It is plausible that these cells might be directly involved in the anastomosis of EC cords with host circulation. Experiments including longitudinal in situ imaging described above and immunostaining for host macrophages would shed additional light on this hypotheses.

4.1.8 Patterning of vasculature via implantation of endothelial cell cords

Spatial patterning of vessel architecture is necessary for the design of complex functional vasculatures in engineered tissues (Vacanti, 2012). Previous studies have utilized physical constraints such as PDMS templates or patterns of ECM-bound VEGF to guide the host angiogenic response (Oh et al., 2011; Zheng et al., 2011). Additionally, general approaches for vascularizing engineered tissues are limited to prevascularization of constructs via self assembly of randomly distributed cells into rudimentary capillary networks (X. Chen et al., 2009; Koffler et al., 2011; Koike et al., 2004; Melero-Martin et al., 2008).

Here, via implantation of patterned EC cords, we have demonstrated one of the first strategies for directly patterning capillaries *in vivo*. The geometry of the vasculature is determined by directly patterning EC cords using a PDMS template that can be fabricated to take a variety of shapes. Perfusion of the vasculature with fluorescent dextran showed that spatial organization is preserved following implantation of either parallel arrays or Y

shaped networks of cords. We hypothesize that *in vivo*, the shape of the resulting capillary network is determined by both the initial topology of EC cords and the persistence of collagen. Histological analyses suggest that the collagen ‘cores’ within implanted cords showed no signs of degradation even 28 days PI. These findings suggest that the collagen cores, by providing persistent adhesive cues to the implanted cells, allow them to better maintain their original conformation and form capillaries *in situ*.

Attempts at controlling vessel diameter by implanting EC cords with varying diameters did not result in vessels that varied in size. Instead, numerous capillaries adjacent to the collagen core were evident in cords of all sizes. These data suggest that vessel diameter cannot be controlled via the implantation of larger cords. Indeed, large vessels formed during development grow over a period of time rather than forming spontaneously via vasculo- or angiogenesis (Adams & Alitalo, 2007). Additionally, current approaches to engineer large vessels rely on complex methods that rely on the generation of a physiologically accurate vessel *in vitro* (Matsumura, Hibino, Ikada, Kurosawa, & Shin'oka, 2003). Thus, it is likely that future integration of larger vessels into constructs with patterned EC cords will require a hybrid approach that combines two distinct strategies for generating both larger caliber vessels and small capillaries.

Histological analyses revealed that implantation of EC cords fabricated using 150 μm wide microchannels results in the formation of several capillaries in each cord. Given these results, one might hypothesize that an excess of implanted cells is driving the formation of these multiple capillaries and that formation of single capillaries might be possible by utilizing smaller microchannels (e.g. 10 μm) for generating cords. While such

an approach would yield much greater control of the fidelity of the final vascular architecture, it is also possible that the smaller number of cells per cord would result in a less robust response upon implantation. Ultimately, studies such as these will be necessary to better understand the extent of control that is possible over capillary network geometry.

4.1.9 Remaining challenges for vascularization of engineered tissues via implantation of endothelial cell cords

Perhaps the biggest challenge in tissue engineering today is the generation of properly vascularized solid tissues (Vacanti, 2012). In the study presented here, we have demonstrated the ability to generate a functional, patterned capillary network within engineered hepatic tissues. While capillaries generated within the hepatic constructs significantly increased albumin promoter activity over hepatocyte-only controls, the overall levels of albumin produced were below physiologically relevant level. One of the next steps in developing clinically viable engineered therapies is the scale up of the vascularization technique to generate tissues that can replace or augment tissue function in the host. Indeed, as many as 2×10^9 isolated hepatocytes are currently used in human transplantation trials (Baccarani et al., 2005). In the hepatic constructs described here, which contained at most one hundred thousand hepatocytes, the amount of albumin secreted into the blood stream was very low. Next, we plan to generate constructs with an increased number of hepatocytes and potential to augment liver function. A challenge associated with this goal is that of successfully integrating patterned EC cords within a

larger hepatic construct. We anticipate overcoming this goal by generating multilayered tissue constructs.

Another challenge in the further development of our vascularization strategy is that of implantation into non-immunosuppressed hosts. Most likely, an ‘all-rat’ model could be used to demonstrate effectiveness in wildtype animals. Specifically, EC cords could be generated using isolated rat endothelial and smooth muscle cells. While the angiogenic potential of various endothelial cell lines may be different, we do not foresee any additional complications in demonstrating feasibility in non-immunosuppressed hosts. Ideally, cell-free approaches will ultimately ameliorate the need for cells and overcome this challenge altogether.

Lastly, long-term studies must be performed to better understand the stability of the vessels over time. Jain and colleagues have demonstrated the persistence of an engineered vasculature up to one year *in vivo* (Koike et al., 2004). Here, the current end point of 28 days does not allow for extensive remodeling and long-term function of the vasculature. While capillaries formed within cords appear to recruit pericytes and are non-leaky after 7 days, their prolonged function in an engineered tissue remains to be tested. A potential complication in these types of studies may be the effectiveness of the ECM material to provide proper structural support to the vessels. It is possible that degradation of the surrounding fibrin matrix might compromise the integrity of the entire tissue construct. Synthetic materials with controlled mechanical properties and degradation rates may prove helpful in addressing these issues.

4.2 Discussion of studies on proliferative regulation in IPAH SMCs

4.2.1 Generation of an *in vitro* arterial wall model

The mature arterial wall consists of an inner layer of endothelial cells surrounded by a contractile smooth muscle layer, and abnormal cell behavior within the media contribute to the pathogenesis of many vascular diseases including atherosclerosis and hypertension (Chin & Rubin, 2008; Lusis, 2000). Most studies of diseased smooth muscle cells, however, are limited to simple tissue culture models that utilize SMCs alone or animal models that severely limit the scope of possible manipulations. Previous work has shown that treatment of smooth muscle cells in culture with ascorbic acid stimulates the expression of smooth muscle-specific markers and increases the synthesis of collagen (Arakawa et al., 2003; Barone et al., 1985; Qiao et al., 2009). Based on these findings, we sought to generate an *in vitro* arterial wall model by culturing a monolayer of endothelial cells atop smooth muscle cells embedded within a collagen matrix. While an EC-SMC bilayer is itself not novel, few studies have reported the use this model in studies of vascular disease (Fillinger et al., 1997; Niwa et al., 2007).

Our findings indicated that endothelial cells, even when seeded at high densities, did not attach and spread to form monolayers. Instead, our results suggest they do not spread extensively and intergrade into the confluent layer of smooth muscle cells, perhaps even attaching directly to the underlying glass substrate. Although we did not perform imaging of the EC-SMC layers in cross section, it is likely that the amount of ECM deposited by SMCs at the time of EC seeding was not high enough to prevent the ECs from making contact with the glass substrate. Indeed, previous studies describing the

development of arterial wall models relied on an exogenous collagen gel to fully encapsulate the SMC layer prior to seeding ECs (Niwa et al., 2007; Ziegler et al., 1995). In addition to the quantity of ECM deposited by SMCs, its identity must also be considered. Endothelial cells have been shown to form monolayers when cultured on type I collagen gels and this method is a routinely used model of angiogenic sprouting (Bayless, Kwak, & Su, 2009; W. Koh, Stratman, Sacharidou, & Davis, 2008). Culture of endothelial cells atop other matrices such as reconstituted basement membrane (Matrigel), however, elicits networking behavior (Goodwin, 2007). It is plausible that the more complex matrix secreted by SMCs treated with ascorbic acid contains components that prevent the ECs from forming a fully confluent monolayer. It could be hypothesized that one such component of the secreted matrix might be elastin, whose deposition has also been shown to be increased upon stimulation with ascorbic acid (Barone et al., 1985). Lastly, the source of the cells used in the generation of an arterial wall model must be considered. While in our studies we have used bPAECs, the studies previously mentioned in this section have mostly utilized HUVECs. Given that endothelial cells from different sources possess various levels of angiogenic potential, the studies described here should be tested using HUVECs (Auxenfans et al., 2011). The initial goal of our studies was to develop an arterial wall model in which ECs and SMCs derived from the lungs of patients with IPAH could be used. Because of the potential for different responses due to cell source, such a system will have to be thoroughly tested for robustness with endothelial cells from a variety of sources including human adult lungs.

Given the inability to recreate the published arterial wall models described here, we decided to pursue an understanding of IPAH SMC pathology in more traditional tissue culture models. If future attempts at using these cells to generate EC-SMC bilayers is to be made, several considerations must be taken. First, a more thorough characterization of confluent SMCs treated with ascorbic acid is necessary. Immunofluorescent staining of cultures for collagen I and elastin should be performed to better understand the composition of the secreted matrix, while sectioning and histological should be used to observe the physical properties of the cell layers in cross section. Second, the use of exogenous collagen matrix should be considered. While allowing the cells to deposit their own ECM is preferable due to physiological relevance, production of type I collagen within the medial compartment has been observed *in vivo* (Rattazzi, Bertacco, Puato, Faggini, & Pauletto, 2012; Wolinsky, 1970). Thus, inclusion of exogenous collagen might not have a negative impact on the physiological relevance of an arterial wall model and should not be ruled out. Lastly, parameters for seeding cells within the system such as numbers of cells used and the length of ascorbic acid treatment should be further explored. Namely, the number of endothelial cells used and length of culture should be extended. By utilizing DiI-AcLDL and seeding larger numbers of ECs seeded atop SMCs, more favorable results are likely to be achieved. In summary, with the incorporation of these changes we predict that an arterial wall model could be used to better study IPAH PASMC biology in an *in vitro* setting.

4.2.2 Mechanisms underlying abnormal proliferation in IPAH smooth muscle cells

Results described in Chapter 3 indicate that PASMCs isolated from lungs of patients with IPAH exhibit increased proliferation when cultured *in vitro*. While hyperproliferation in PAH SMCs has previously been documented (Chin & Rubin, 2008), our insights into the underlying abnormal regulation of proliferative control in IPAH SMCs provide a novel insight into the pathobiology of the disease.

Here, we show that IPAH SMCs exhibit increased RhoA activity and larger focal adhesions. These findings are likely explained by previous studies, which have shown that increases in Rho-dependent contractility lead to the aggregation of integrins into focal adhesions (Chrzanowska-Wodnicka & Burridge, 1996). While not statistically significant, data presented here also suggest that myosin light chain phosphorylation might be increased in the IPAH cells. More in depth studies of MLC phosphorylation in conjunction with immunostaining for integrins would help clarify whether similar mechanisms underlie the hyperproliferative behavior in IPAH SMCs.

Next, our investigation into focal adhesion signaling showed that higher levels of FAK are phosphorylated in IPAH SMCs as compared with control cells. This finding is consistent with studies that demonstrate that overexpression of FAK leads to G1/S cell cycle progression (Gilmore & Romer, 1996; Zhao, Reiske, & Guan, 1998). Our findings also suggest that increased FAK activity in the IPAH PASMC prevent their ability to normally regulate adhesion-mediated proliferative control. FAK, a key effector in focal adhesion signaling, is involved in their formation, which allows for cell spreading and the establishment of cytoskeletal tension (Burridge & Chrzanowska-Wodnicka, 1996; C.

Chen et al., 1997; Chrzanowska-Wodnicka & Burridge, 1996; Guan & Shalloway, 1992; Kornberg et al., 1992; Lewis & Schwartz, 1995; Pirone et al., 2006; Richardson et al., 1997; Roovers & Assoian, 2003). Notably, FAK has been implicated as a key player in adhesion-mediated proliferative control via the RhoA signaling pathway, which is downstream of cell adhesion to the extracellular matrix (Chrzanowska-Wodnicka & Burridge, 1996; Pirone et al., 2006). Additionally, FAK has been shown to regulate the activity of RhoA, which is required for sustained ERK signaling and cell cycle progression (C. Chen et al., 1997; Danen et al., 2000; Raines, 2000; Ren & Schwartz, 2000; Welsh et al., 2001). Given the central role of FAK as a signaling hub between the extracellular environment and intracellular signaling, it is not surprising that it may play a role in the abnormal proliferative regulation observed in SMCs in a disease that involves significant mechanical and biochemical changes to the extracellular environment. To better understand the role of adhesion signaling in IPAH, we suggest that subsequent studies focus on investigating whether proliferation of IPAH PASMCs can be controlled via changes to their adhesive microenvironment. Specifically, cells could be plated on compliant gels or even embedded in a three dimensional arterial wall model such as that described above. Measurements of FAK and Rho activity in these contexts of altered adhesion might shed further light on the causative agents in the hyperproliferative phenotype previously observed. In the more immediate future, our experimental plans focus on confirming that FAK inhibition via genetic manipulations leads to a restoration of normal proliferative behavior in the IPAH SMCs.

4.2.2 Assessing the phenotype of IPAH smooth muscle cells

One of the biggest challenges in studies of rare diseases such as IPAH is the ability to acquire reliable source material. Due to the relatively low prevalence of PAH, approximately 1300 cases per million, the number of patients with the potential to donate tissue or other source material is extremely limited (McDonnell, Toye, & Hutchins, 1983). The resection of lung tissue is a highly invasive procedure that cannot be justified for the purpose of acquiring research material. Thus, the majority of human lung tissue used in the study of IPAH is obtained from patients who have undergone lung transplantation. Because transplantation is a treatment option of last resort, however, cells in these lungs have often been subjected to a variety of treatments for several years. Ultimately, human cells isolated and used in any *in vitro* study of IPAH mechanisms are likely to exhibit considerable levels of heterogeneity. We acquired cells from IPAH patients via laboratories at the University of Pennsylvania participating in the Pulmonary Hypertension Breakthrough Initiative. Using cells from this single source insured a consistent level of quality control – all SMCs were isolated, propagated and frozen using identical protocols. Factors such as age, sex and clinical history, however, were not controlled due to the scope of the study. Indeed, the data presented in Chapter 3 represents findings from at most 3 diseased and 3 control samples. In future studies, larger cohorts will be necessary to ensure no bias is introduced due to donor variability.

Similar challenges are faced when selecting control cells for use in these studies. While commercially available sources of human pulmonary artery smooth muscle cells ensure a high level of consistency and quality control, their methods of isolation

(including source within the lungs), propagation, maintenance and cryopreservation do not match that of the independently acquired PAH cells. In order to mitigate some of this bias here, we have used control cells that were obtained through both commercial sources and isolated at the same laboratories as the IPAH cells. Our findings, however, should be independently validated as additional donor cells become available.

4.2.3 Clinical translation of findings

The insights into abnormal proliferative regulation in IPAH SMCs presented in Chapter 3 require additional validation to have direct applications in the clinic. First and foremost, our findings must be validated in a larger study. Such a study should include several additional lines of donor control and IPAH cells and should include additional manipulations not performed here. While we have shown initial evidence that inhibition of FAK in an unspread context results in the return of proliferation to normal levels in IPAH SMCs, additional studies utilizing genetic manipulations in larger donor cell populations might help to solidify the link between FAK and proliferation in IPAH. Specifically, overexpression of dominant negative FAK or Rho in additional donor cells might be used to validate our proposed mechanism of proliferative misregulation.

Next, potential drug targets must be identified in animal models of pulmonary hypertension such as hypoxia or monocrotaline treatment in rats (Stenmark, Meyrick, Galie, Mooi, & McMurtry, 2009). While our data suggest that FAK inhibition has the potential to restore proliferation in IPAH SMCs to normal levels, its inhibition must be tested *in vivo*. Recently, the inhibition of smooth muscle myosin and RhoA, both downstream effectors of focal adhesion signaling, have shown promise in animal models

(Ho et al., 2012; E. Z. Xu et al., 2010). While these treatments offer to reduce pulmonary arterial pressure via vasodilatory effects, our work suggests that further studies into their potential antiproliferative effects might also be warranted. Given that our data have demonstrated a mechanosensitive component to the abnormal proliferation in IPAH SMCs, an eventual cure might involve inhibition of molecules such as FAK or integrins, which act as signaling hubs between the extracellular environment and intracellular pathways.

4.3 Future directions

4.3.1 Applications of vascularization via patterned EC cords

Vascularization of engineered tissues is perhaps the biggest obstacle that we face toward the development of clinically viable tissue engineered therapies (Jain et al., 2005; Rouwkema et al., 2008; Vacanti, 2012). Here, we have demonstrated the ability of our vascularization strategy to be incorporated into engineered hepatic microtissues. While much work still remains to be done in order to scale this approach up to larger tissues, we believe that this is largely an engineering problem and expect no significant biological barriers. Ultimately, we propose that large scale versions of our technique might be employed to rapidly and effectively vascularize complex tissues such as liver, kidney and pancreas. As a first step in achieving clinical efficacy, such engineered tissues are likely to only augment failing tissue function rather than provide a complete organ replacement. Challenges including cell source, immunogenicity, and host-graft integration must be overcome on the road to true organ replacement therapy.

Additionally, we envision vascularization via implantation of patterned EC cords as having the ability to vascularize wounds or areas of ischemic tissues. Specifically, gels containing cords could be used as a dressing in applications such as diabetic ulcers and infarcted cardiac tissue. A particular challenge in the area of wound treatments will be that of source material. In situations requiring the revascularization of ischemic tissues, the length of time until initiating the treatment is critical for ensuring the best clinical outcomes. To overcome these challenges, future research should focus on identifying sources of autologous cells that are amenable to rapid isolation, expansion, and use in implantable tissue constructs/wound healing materials.

In a research setting, we propose that vascularization via EC cords might be used as a model to study the effects of vascular architecture on the efficiency of nutrient delivery and waste removal via the circulation. Currently, much is known about the mechanisms underlying vascular patterning (LaRue et al., 2003). Studies have also shown that an increased level of vascular patterning in engineered tissue improves the engraftment and vascularization rates of those tissues (X. Chen et al., 2009; Koffler et al., 2011). However, it is not currently well understood what is the optimal topology of vascular architecture in tissue engineered contexts. This area has been poorly studied largely due to the lack of an experimental technique that allows for the patterning of vessel networks *in vivo*. We propose that the method of patterning capillaries described here could be used to study how different vascular architectures affect the delivery of oxygen and nutrients to surrounding tissues *in vivo*. It would be of particular interest to embed cells containing reporters of metabolic activity within the parenchyma of

engineered tissues containing varying topologies of EC cords. Combined with *in vivo* imaging, these types of experiments could be used to test a variety of models of optimal tissue architecture.

Lastly, we envision the development of diagnostic tools that utilize tissue engineered constructs at their core. While these types of technologies will surely require years of research to reach the clinic, vascularization techniques such as the one described here might lie at the core of these approaches. Real-time monitoring of various circulating biomarkers is an area of particular interest (Ardill & O'Dorisio, 2010; De Mattos-Arruda, Olmos, & Taberero, 2011; Masson, Latini, & Anand, 2010). Rather than externally tapping into existing vessels, we envision implantable devices or sensor-laden tissue constructs that become vascularized independently. In such an application, predicting areas that will become vascularized will be of key importance. Thus, strategies for patterning vessels such as the one described here could be used in the development of these technologies.

4.3.2 Future understanding of proliferative regulation in IPAH

Management of PAH has improved significantly over the last decade, and patients now experience a higher quality of life (Agarwal & Gomberg-Maitland, 2011). New treatments, however, continuously rely on the same categories of drugs to treat symptoms of the disease with no clear signs of an emerging cure. We believe that mechanistic studies such as the work presented in Chapter 3 are critical to further uncovering the pathogenesis of IPAH. Here, our data suggest that abnormal SMC proliferation in IPAH has a mechanical or adhesive component. Identifying the source of these extracellular

cues should will be the focus of our future studies in this area. Elucidating the causative factors that create a permissive microenvironment for abnormal proliferative regulation in PASMCs could lead to the discovery of an underlying cause of IPAH and pave the way for the development of future therapies. Lastly, it should be noted that efforts that implicate other signaling factors such as PDGF in the etiology of IPAH are currently underway (Ikeda et al., 2010). Future investigations into whether these pathways overlap with the proliferative misregulation we report here will be key to identifying drug targets and gaining a broader understanding of the pathobiology of IPAH.

BIBLIOGRAPHY

- Adams, R. H., & Alitalo, K. (2007). Molecular regulation of angiogenesis and lymphangiogenesis. *Nature Reviews Molecular Cell Biology*, 8(6), 464–478. doi:10.1038/nrm2183
- Agarwal, R., & Gomberg-Maitland, M. (2011). Current therapeutics and practical management strategies for pulmonary arterial hypertension. *American heart journal*, 162(2), 201–213. doi:10.1016/j.ahj.2011.05.012
- American Diabetes Association. (2007). Economic Costs of Diabetes in the U.S. in 2007. *Diabetes Care*, 31(3), 596–615. doi:10.2337/dc08-9017
- Angulo, J., Peiró, C., Romacho, T., Fernández, A., Cuevas, B., González-Corrochano, R., Giménez-Gallego, G., et al. (2011). Inhibition of vascular endothelial growth factor (VEGF)-induced endothelial proliferation, arterial relaxation, vascular permeability and angiogenesis by dobesilate. *European journal of pharmacology*, 667(1-3), 153–159. doi:10.1016/j.ejphar.2011.06.015
- Aoyagi, M., Yamamoto, M., Azuma, H., Niimi, Y., Tajima, S., Hirakawa, K., & Yamamoto, K. (1997). Smooth muscle cell proliferation, elastin formation, and tropoelastin transcripts during the development of intimal thickening in rabbit carotid arteries after endothelial denudation. *Histochemistry and cell biology*, 107(1), 11–17.
- Arakawa, E., Hasegawa, K., Irie, J., Ide, S., Ushiki, J., Yamaguchi, K., Oda, S., et al. (2003). L-ascorbic acid stimulates expression of smooth muscle-specific markers in smooth muscle cells both in vitro and in vivo. *Journal of cardiovascular pharmacology*, 42(6), 745–751.

- Ardill, J. E. S., & O'Dorisio, T. M. (2010). Circulating biomarkers in neuroendocrine tumors of the enteropancreatic tract: application to diagnosis, monitoring disease, and as prognostic indicators. *Endocrinology and metabolism clinics of North America*, 39(4), 777–790. doi:10.1016/j.ecl.2010.09.001
- Arima, S., Nishiyama, K., Ko, T., Arima, Y., Hakozaiki, Y., Sugihara, K., Koseki, H., et al. (2011). Angiogenic morphogenesis driven by dynamic and heterogeneous collective endothelial cell movement. *Development (Cambridge, England)*, 138(21), 4763–4776. doi:10.1242/dev.068023
- Arroyo, A. G., & Iruela-Arispe, M. L. (2010). Extracellular matrix, inflammation, and the angiogenic response. *Cardiovascular research*, 86(2), 226–235. doi:10.1093/cvr/cvq049
- Assoian, R. K., & Marcantonio, E. E. (1997). The extracellular matrix as a cell cycle control element in atherosclerosis and restenosis. *Journal of Clinical Investigation*, 100(11 Suppl), S15–8.
- Athanasίου, K. A., Niederauer, G. G., & Agrawal, C. M. (1996). Sterilization, toxicity, biocompatibility and clinical applications of polylactic acid/polyglycolic acid copolymers. *Biomaterials*, 17(2), 93–102.
- Au, P., Daheron, L. M., Duda, D. G., Cohen, K. S., Tyrrell, J. A., Lanning, R. M., Fukumura, D., et al. (2008a). Differential in vivo potential of endothelial progenitor cells from human umbilical cord blood and adult peripheral blood to form functional long-lasting vessels. *Blood*, 111(3), 1302–1305. doi:10.1182/blood-2007-06-094318
- Au, P., Tam, J., Fukumura, D., & Jain, R. K. (2008b). Bone marrow-derived

- mesenchymal stem cells facilitate engineering of long-lasting functional vasculature. *Blood*, 111(9), 4551–4558. doi:10.1182/blood-2007-10-118273
- Augustin, H. G., Koh, G. Y., Thurston, G., & Alitalo, K. (2009). Control of vascular morphogenesis and homeostasis through the angiopoietin-Tie system. *Nature Reviews Molecular Cell Biology*, 10(3), 165–177. doi:10.1038/nrm2639
- Auxenfans, C., Lequeux, C., Perrusel, E., Mojallal, A., Kinikoglu, B., & Damour, O. (2011). Adipose-derived stem cells (ASCs) as a source of endothelial cells in the reconstruction of endothelialized skin equivalents. *Journal of Tissue Engineering and Regenerative Medicine*. doi:10.1002/term.454
- Avraamides, C. J., Garmy-Susini, B., & Varner, J. A. (2008). Integrins in angiogenesis and lymphangiogenesis. *Nature reviews. Cancer*, 8(8), 604–617. doi:10.1038/nrc2353
- Baccarani, U., Adani, G. L., Sanna, A., Avellini, C., Sainz-Barriga, M., Lorenzin, D., Montanaro, D., et al. (2005). Portal vein thrombosis after intraportal hepatocytes transplantation in a liver transplant recipient. *Transplant international : official journal of the European Society for Organ Transplantation*, 18(6), 750–754. doi:10.1111/j.1432-2277.2005.00127.x
- Bader, B. L., Rayburn, H., Crowley, D., & Hynes, R. O. (1998). Extensive vasculogenesis, angiogenesis, and organogenesis precede lethality in mice lacking all alpha v integrins. *Cell*, 95(4), 507–519.
- Barclay, G. R., Tura, O., Samuel, K., Hadoke, P. W., Mills, N. L., Newby, D. E., & Turner, M. L. (2012). Systematic assessment in an animal model of the angiogenic

- potential of different human cell sources for therapeutic revascularization. *Stem cell research & therapy*, 3(4), 23. doi:10.1186/scrt114
- Barone, L. M., Faris, B., Chipman, S. D., Toselli, P., Oakes, B. W., & Franzblau, C. (1985). Alteration of the extracellular matrix of smooth muscle cells by ascorbate treatment. *Biochimica et biophysica acta*, 840(2), 245–254.
- Barst, R. J., Gibbs, J. S. R., Ghofrani, H. A., Hoeper, M. M., McLaughlin, V. V., Rubin, L. J., Sitbon, O., et al. (2009). Updated evidence-based treatment algorithm in pulmonary arterial hypertension. *Journal of the American College of Cardiology*, 54(1 Suppl), S78–84. doi:10.1016/j.jacc.2009.04.017
- Barst, R. J., Rubin, L. J., Long, W. A., McGoon, M. D., Rich, S., Badesch, D. B., Groves, B. M., et al. (1996). A comparison of continuous intravenous epoprostenol (prostacyclin) with conventional therapy for primary pulmonary hypertension. The Primary Pulmonary Hypertension Study Group. *The New England journal of medicine*, 334(5), 296–302. doi:10.1056/NEJM199602013340504
- Bayless, K. J., Kwak, H.-I., & Su, S.-C. (2009). Investigating endothelial invasion and sprouting behavior in three-dimensional collagen matrices. *Nature Protocols*, 4(12), 1888–1898. doi:10.1038/nprot.2009.221
- Bazzoni, G., & Dejana, E. (2004). Endothelial cell-to-cell junctions: molecular organization and role in vascular homeostasis. *Physiological reviews*, 84(3), 869–901. doi:10.1152/physrev.00035.2003
- Beenken, A., & Mohammadi, M. (2009). The FGF family: biology, pathophysiology and therapy. *Nature reviews. Drug discovery*, 8(3), 235–253. doi:10.1038/nrd2792

- Bell, E., Ivarsson, B., & Merrill, C. (1979). Production of a tissue-like structure by contraction of collagen lattices by human fibroblasts of different proliferative potential in vitro. *Proceedings of the National Academy of Sciences of the United States of America*, 76(3), 1274–1278.
- Bergers, G., Brekken, R., McMahon, G., Vu, T. H., Itoh, T., Tamaki, K., Tanzawa, K., et al. (2000). Matrix metalloproteinase-9 triggers the angiogenic switch during carcinogenesis. *Nature Cell Biology*, 2(10), 737–744. doi:10.1038/35036374
- Berra, E., Diaz-Meco, M. T., Dominguez, I., Municio, M. M., Sanz, L., Lozano, J., Chapkin, R. S., et al. (1993). Protein kinase C zeta isoform is critical for mitogenic signal transduction. *Cell*, 74(3), 555–563.
- Boniface, S., & Reynaud-Gaubert, M. (2011). Endothelin receptor antagonists -- their role in pulmonary medicine. *Revue des maladies respiratoires*, 28(8), e94–e107. doi:10.1016/j.rmr.2009.07.001
- Bottomley, M. J., Webb, N. J., Watson, C. J., Holt, P. J., Freemont, A. J., & Brenchley, P. E. (1999). Peripheral blood mononuclear cells from patients with rheumatoid arthritis spontaneously secrete vascular endothelial growth factor (VEGF): specific up-regulation by tumour necrosis factor-alpha (TNF-alpha) in synovial fluid. *Clinical and experimental immunology*, 117(1), 171–176.
- Brooks, P. C., Silletti, S., Schalscha, von, T. L., Friedlander, M., & Chersesh, D. A. (1998). Disruption of angiogenesis by PEX, a noncatalytic metalloproteinase fragment with integrin binding activity. *Cell*, 92(3), 391–400.
- Burridge, K., & Chrzanowska-Wodnicka, M. (1996). Focal adhesions, contractility, and

- signaling. *Annual review of cell and developmental biology*, 12, 463–518.
doi:10.1146/annurev.cellbio.12.1.463
- Cadena, D. L., & Gill, G. N. (1992). Receptor tyrosine kinases. *The FASEB journal : official publication of the Federation of American Societies for Experimental Biology*, 6(6), 2332–2337.
- Carmeliet, P. (2003). Angiogenesis in health and disease. *Nature Medicine*, 9(6), 653–660. doi:10.1038/nm0603-653
- Carmeliet, P., & Jain, R. K. (2000). Angiogenesis in cancer and other diseases. *Nature*, 407(6801), 249–257. doi:10.1038/35025220
- Carmeliet, P., & Jain, R. K. (2011). Molecular mechanisms and clinical applications of angiogenesis. *Nature*, 473(7347), 298–307. doi:10.1038/nature10144
- Carmeliet, P., Ferreira, V., Breier, G., Pollefeyt, S., Kieckens, L., Gertsenstein, M., Fahrig, M., et al. (1996). Abnormal blood vessel development and lethality in embryos lacking a single VEGF allele. *Nature*, 380(6573), 435–439.
doi:10.1038/380435a0
- Carmeliet, P., Moons, L., Luttun, A., Vincenti, V., Compernelle, V., De Mol, M., Wu, Y., et al. (2001). Synergism between vascular endothelial growth factor and placental growth factor contributes to angiogenesis and plasma extravasation in pathological conditions. *Nature Medicine*, 7(5), 575–583. doi:10.1038/87904
- Chamley, J. H., Campbell, G. R., McConnell, J. D., & Gröschel-Stewart, U. (1977). Comparison of vascular smooth muscle cells from adult human, monkey and rabbit in primary culture and in subculture. *CELL AND TISSUE RESEARCH*, 177(4), 503–

522.

- Chen, A. A., Thomas, D. K., Ong, L. L., Schwartz, R. E., Golub, T. R., & Bhatia, S. N. (2011). Humanized mice with ectopic artificial liver tissues. *Proceedings of the National Academy of Sciences of the United States of America*, *108*(29), 11842–11847. doi:10.1073/pnas.1101791108
- Chen, C., Mrksich, M., Huang, S., Whitesides, G., & Ingber, D. (1997). Geometric control of cell life and death. *Science (New York, N.Y.)*, *276*(5317), 1425–1428.
- Chen, R. R., & Mooney, D. J. (2003). Polymeric growth factor delivery strategies for tissue engineering. *Pharmaceutical research*, *20*(8), 1103–1112. doi:10.1023/A:1025034925152
- Chen, R. R., Silva, E. A., Yuen, W. W., & Mooney, D. J. (2006). Spatio-temporal VEGF and PDGF Delivery Patterns Blood Vessel Formation and Maturation. *Pharmaceutical research*, *24*(2), 258–264. doi:10.1007/s11095-006-9173-4
- Chen, X., Aledia, A. S., Ghajar, C. M., Griffith, C. K., Putnam, A. J., Hughes, C. C. W., & George, S. C. (2009). Prevascularization of a fibrin-based tissue construct accelerates the formation of functional anastomosis with host vasculature. *Tissue Engineering Part A*, *15*(6), 1363–1371. doi:10.1089/ten.tea.2008.0314
- Chen, X., Aledia, A. S., Popson, S. A., Him, L., Hughes, C. C. W., & George, S. C. (2010). Rapid anastomosis of endothelial progenitor cell-derived vessels with host vasculature is promoted by a high density of cotransplanted fibroblasts. *Tissue Engineering Part A*, *16*(2), 585–594. doi:10.1089/ten.TEA.2009.0491
- Cheng, G., Liao, S., Wong, H. K., Lacorre, D. A., di Tomaso, E., Au, P., Fukumura, D.,

- et al. (2011). Engineered blood vessel networks connect to host vasculature via wrapping-and-tapping anastomosis. *Blood*. doi:10.1182/blood-2011-02-338426
- Chin, K. M., & Rubin, L. J. (2008). Pulmonary arterial hypertension. *Journal of the American College of Cardiology*, *51*(16), 1527–1538. doi:10.1016/j.jacc.2008.01.024
- Chrobak, K. M., Potter, D. R., & Tien, J. (2006). Formation of perfused, functional microvascular tubes in vitro. *Microvascular Research*, *71*(3), 185–196. doi:10.1016/j.mvr.2006.02.005
- Chrzanowska-Wodnicka, M., & Burridge, K. (1996). Rho-stimulated contractility drives the formation of stress fibers and focal adhesions. *The Journal of Cell Biology*, *133*(6), 1403–1415.
- Chun, T., Sabeh, F., Ota, I., Murphy, H., McDonagh, K., Holmbeck, K., Birkedal-Hansen, H., et al. (2004). MT1-MMP-dependent neovessel formation within the confines of the three-dimensional extracellular matrix. *The Journal of Cell Biology*, *167*(4), 757.
- Cleary, M. A., Geiger, E., Grady, C., Best, C., Naito, Y., & Breuer, C. (2012). Vascular tissue engineering: the next generation. *Trends in Molecular Medicine*, 1–11. doi:10.1016/j.molmed.2012.04.013
- Clowes, A. W., Reidy, M. A., & Clowes, M. M. (1983). Kinetics of cellular proliferation after arterial injury. I. Smooth muscle growth in the absence of endothelium. *Laboratory investigation; a journal of technical methods and pathology*, *49*(3), 327–333.
- Coffer, P. J., Jin, J., & Woodgett, J. R. (1998). Protein kinase B (c-Akt): a multifunctional

- mediator of phosphatidylinositol 3-kinase activation. *The Biochemical journal*, 335 (Pt 1), 1–13.
- Collen, A., Hanemaaijer, R., Lupu, F., Quax, P. H. A., van Lent, N., Grimbergen, J., Peters, E., et al. (2003). Membrane-type matrix metalloproteinase-mediated angiogenesis in a fibrin-collagen matrix. *Blood*, 101(5), 1810–1817.
doi:10.1182/blood-2002-05-1593
- Contois, L., Akalu, A., & Brooks, P. C. (2009). Integrins as “functional hubs” in the regulation of pathological angiogenesis. *Seminars in cancer biology*, 19(5), 318–328.
doi:10.1016/j.semcancer.2009.05.002
- Corpataux, J.-M., Naik, J., Porter, K. E., & London, N. J. M. (2005). The effect of six different statins on the proliferation, migration, and invasion of human smooth muscle cells. *Journal of Surgical Research*, 129(1), 52–56.
doi:10.1016/j.jss.2005.05.016
- Corsini, A., Bellosta, S., Baetta, R., Fumagalli, R., Paoletti, R., & Bernini, F. (1999). New insights into the pharmacodynamic and pharmacokinetic properties of statins. *Pharmacology & therapeutics*, 84(3), 413–428.
- Cukierman, E., Pankov, R., & Yamada, K. M. (2002). Cell interactions with three-dimensional matrices. *Current opinion in cell biology*, 14(5), 633–639.
- Cukierman, E., Pankov, R., Stevens, D. R., & Yamada, K. M. (2001). Taking cell-matrix adhesions to the third dimension. *Science (New York, N.Y.)*, 294(5547), 1708–1712.
doi:10.1126/science.1064829
- D'Amore, P. A., & Thompson, R. W. (1987). Mechanisms of angiogenesis. *Annual*

review of physiology, 49, 453–464. doi:10.1146/annurev.ph.49.030187.002321

Danen, E. H., Sonneveld, P., Sonnenberg, A., & Yamada, K. M. (2000). Dual stimulation of Ras/mitogen-activated protein kinase and RhoA by cell adhesion to fibronectin supports growth factor-stimulated cell cycle progression. *The Journal of Cell Biology*, 151(7), 1413–1422.

Darland, D. C., Massingham, L. J., Smith, S. R., Piek, E., Saint-Geniez, M., & D'Amore, P. A. (2003). Pericyte production of cell-associated VEGF is differentiation-dependent and is associated with endothelial survival. *Developmental biology*, 264(1), 275–288.

De Mattos-Arruda, L., Olmos, D., & Tabernero, J. (2011). Prognostic and predictive roles for circulating biomarkers in gastrointestinal cancer. *Future oncology (London, England)*, 7(12), 1385–1397. doi:10.2217/fon.11.122

Dejana, E., & Giampietro, C. (2012). Vascular endothelial-cadherin and vascular stability. *Current opinion in hematology*, 19(3), 218–223.
doi:10.1097/MOH.0b013e3283523e1c

Dejana, E., Tournier-Lasserre, E., & Weinstein, B. M. (2009). The control of vascular integrity by endothelial cell junctions: molecular basis and pathological implications. *Developmental Cell*, 16(2), 209–221. doi:10.1016/j.devcel.2009.01.004

Desgrosellier, J. S., & Cheresch, D. A. (2010). Integrins in cancer: biological implications and therapeutic opportunities. *Nature reviews. Cancer*, 10(1), 9–22.
doi:10.1038/nrc2748

Dike, L. E., Chen, C. S., Mrksich, M., Tien, J., Whitesides, G. M., & Ingber, D. E.

- (1999). Geometric control of switching between growth, apoptosis, and differentiation during angiogenesis using micropatterned substrates. *In vitro cellular & developmental biology. Animal*, 35(8), 441–448. doi:10.1007/s11626-999-0050-4
- Dunn, J. C., Tompkins, R. G., & Yarmush, M. L. (1991). Long-term in vitro function of adult hepatocytes in a collagen sandwich configuration. *Biotechnology progress*, 7(3), 237–245. doi:10.1021/bp00009a007
- Eddahibi, S., Guignabert, C., Barlier-Mur, A.-M., Dewachter, L., Fadel, E., Dartevielle, P., Humbert, M., et al. (2006). Cross talk between endothelial and smooth muscle cells in pulmonary hypertension: critical role for serotonin-induced smooth muscle hyperplasia. *Circulation*, 113(15), 1857–1864. doi:10.1161/CIRCULATIONAHA.105.591321
- Fantin, A., Vieira, J. M., Gestri, G., Denti, L., Schwarz, Q., Prykhozhij, S., Peri, F., et al. (2010). Tissue macrophages act as cellular chaperones for vascular anastomosis downstream of VEGF-mediated endothelial tip cell induction. *Blood*, 1–32. doi:10.1182/blood-2009-12-257832
- Farber, H. W., & Loscalzo, J. (2004). Pulmonary arterial hypertension. *The New England journal of medicine*, 351(16), 1655–1665. doi:10.1056/NEJMra035488
- Ferns, G. A., Raines, E. W., Sprugel, K. H., Motani, A. S., Reidy, M. A., & Ross, R. (1991). Inhibition of neointimal smooth muscle accumulation after angioplasty by an antibody to PDGF. *Science (New York, N.Y.)*, 253(5024), 1129–1132.
- Ferrara, N., & Kerbel, R. S. (2005). Angiogenesis as a therapeutic target. *Nature*, 438(7070), 967–974. doi:10.1038/nature04483

- Ferrara, N., Gerber, H.-P., & LeCouter, J. (2003). The biology of VEGF and its receptors. *Nature Medicine*, 9(6), 669–676. doi:10.1038/nm0603-669
- Fillinger, M. F., Sampson, L. N., Cronenwett, J. L., Powell, R. J., & Wagner, R. J. (1997). Coculture of endothelial cells and smooth muscle cells in bilayer and conditioned media models. *Journal of Surgical Research*, 67(2), 169–178. doi:10.1006/jsre.1996.4978
- Folkman, J. (2007). Angiogenesis: an organizing principle for drug discovery? *Nature reviews. Drug discovery*, 6(4), 273–286. doi:10.1038/nrd2115
- Fong, G. H., Rossant, J., Gertsenstein, M., & Breitman, M. L. (1995). Role of the Flt-1 receptor tyrosine kinase in regulating the assembly of vascular endothelium. *Nature*, 376(6535), 66–70. doi:10.1038/376066a0
- Friedlander, M., Brooks, P. C., Shaffer, R. W., Kincaid, C. M., Varner, J. A., & Chersesh, D. A. (1995). Definition of two angiogenic pathways by distinct alpha v integrins. *Science (New York, N.Y.)*, 270(5241), 1500–1502.
- Fuentes, A., Coralic, A., & Dawson, K. L. (2012). A new epoprostenol formulation for the treatment of pulmonary arterial hypertension. *American journal of health-system pharmacy : AJHP : official journal of the American Society of Health-System Pharmacists*, 69(16), 1389–1393. doi:10.2146/ajhp110687
- Gaengel, K., Genové, G., Armulik, A., & Betsholtz, C. (2009). Endothelial-mural cell signaling in vascular development and angiogenesis. *Arteriosclerosis, Thrombosis, and Vascular Biology*, 29(5), 630–638. doi:10.1161/ATVBAHA.107.161521
- Gainé, S. P., & Rubin, L. J. (1998). Primary pulmonary hypertension. *The Lancet*,

- 352(9129), 719–725. doi:10.1016/S0140-6736(98)02111-4
- Galie, N., Brundage, B. H., Ghofrani, H. A., Oudiz, R. J., Simonneau, G., Safdar, Z., Shapiro, S., et al. (2009). Tadalafil therapy for pulmonary arterial hypertension. *Circulation*, *119*(22), 2894–2903. doi:10.1161/CIRCULATIONAHA.108.839274
- Gambillara, V., Thacher, T., Silacci, P., & Stergiopoulos, N. (2008). Effects of reduced cyclic stretch on vascular smooth muscle cell function of pig carotids perfused ex vivo. *American journal of hypertension*, *21*(4), 425–431. doi:10.1038/ajh.2007.72
- Garlick, J. A. (2007). Engineering skin to study human disease--tissue models for cancer biology and wound repair. *Advances in biochemical engineering/biotechnology*, *103*, 207–239.
- Gärtner, C., Ziegelhöffer, B., Kostelka, M., Stepan, H., Mohr, F.-W., & Dhein, S. (2012). Knock-down of endothelial connexins impairs angiogenesis. *Pharmacological Research*, *65*(3), 347–357. doi:10.1016/j.phrs.2011.11.012
- Ghajar, C. M., Blevins, K. S., Hughes, C. C. W., George, S. C., & Putnam, A. J. (2006). Mesenchymal stem cells enhance angiogenesis in mechanically viable prevascularized tissues via early matrix metalloproteinase upregulation. *Tissue engineering*, *12*(10), 2875–2888. doi:10.1089/ten.2006.12.2875
- Ghajar, C. M., Chen, X., Harris, J. W., Suresh, V., Hughes, C. C. W., Jeon, N. L., Putnam, A. J., et al. (2008a). The effect of matrix density on the regulation of 3-D capillary morphogenesis. *Biophysical Journal*, *94*(5), 1930–1941. doi:10.1529/biophysj.107.120774
- Ghajar, C. M., George, S. C., & Putnam, A. J. (2008b). Matrix metalloproteinase control

of capillary morphogenesis. *Critical reviews in eukaryotic gene expression*, 18(3), 251–278.

- Ghofrani, H. A., Wiedemann, R., Rose, F., Schermuly, R. T., Olschewski, H., Weissmann, N., Gunther, A., et al. (2002). Sildenafil for treatment of lung fibrosis and pulmonary hypertension: a randomised controlled trial. *Lancet*, 360(9337), 895–900. doi:10.1016/S0140-6736(02)11024-5
- Gilmore, A. P., & Romer, L. H. (1996). Inhibition of focal adhesion kinase (FAK) signaling in focal adhesions decreases cell motility and proliferation. *Molecular biology of the cell*, 7(8), 1209–1224.
- Goodwin, A. M. (2007). In vitro assays of angiogenesis for assessment of angiogenic and anti-angiogenic agents. *Microvascular Research*, 74(2-3), 172–183. doi:10.1016/j.mvr.2007.05.006
- Greenberg, J. I., Shields, D. J., Barillas, S. G., Acevedo, L. M., Murphy, E., Huang, J., Scheppke, L., et al. (2008). A role for VEGF as a negative regulator of pericyte function and vessel maturation. *Nature*, 456(7223), 809–813. doi:10.1038/nature07424
- Griga, T., Werner, S., Köller, M., Tromm, A., & May, B. (1999). Vascular endothelial growth factor (VEGF) in Crohn's disease: increased production by peripheral blood mononuclear cells and decreased VEGF165 labeling of peripheral CD14+ monocytes. *Digestive diseases and sciences*, 44(6), 1196–1201.
- Guan, J. L., & Shalloway, D. (1992). Regulation of focal adhesion-associated protein tyrosine kinase by both cellular adhesion and oncogenic transformation. *Nature*,

358(6388), 690–692. doi:10.1038/358690a0

Guignabert, C., Izikki, M., Tu, L. I., Li, Z., Zadigue, P., Barlier-Mur, A.-M., Hanoun, N., et al. (2006). Transgenic mice overexpressing the 5-hydroxytryptamine transporter gene in smooth muscle develop pulmonary hypertension. *Circulation research; Circulation research*, *98*(10), 1323–1330.
doi:10.1161/01.RES.0000222546.45372.a0

Guo, X., Elliott, C. G., Li, Z., Xu, Y., Hamilton, D. W., & Guan, J. (2012). Creating 3D Angiogenic Growth Factor Gradients in Fibrous Constructs to Guide Fast Angiogenesis. *Biomacromolecules*, 120904134656001. doi:10.1021/bm301029a

Hall, H., Baechi, T., & Hubbell, J. A. (2001). Molecular properties of fibrin-based matrices for promotion of angiogenesis in vitro. *Microvascular Research*, *62*(3), 315–326. doi:10.1006/mvre.2001.2348

Heineken, F. G., & Skalak, R. (1991). Tissue Engineering - a Brief Overview. *Journal of Biomechanical Engineering-Transactions of the Asme*, *113*(2), 111–112.

Hellberg, C., Ostman, A., & Heldin, C.-H. (2010). PDGF and vessel maturation. *Recent results in cancer research. Fortschritte der Krebsforschung. Progrès dans les recherches sur le cancer*, *180*, 103–114. doi:10.1007/978-3-540-78281-0_7

Hellström, M., Phng, L.-K., Hofmann, J. J., Wallgard, E., Coultas, L., Lindblom, P., Alva, J., et al. (2007). Dll4 signalling through Notch1 regulates formation of tip cells during angiogenesis. *Nature*, *445*(7129), 776–780. doi:10.1038/nature05571

Henry, T. D., Annex, B. H., McKendall, G. R., Azrin, M. A., Lopez, J. J., Giordano, F. J., Shah, P. K., et al. (2003). The VIVA trial: Vascular endothelial growth factor in

- Ischemia for Vascular Angiogenesis. *Circulation*, 107(10), 1359–1365.
- Henry, T. D., Rocha-Singh, K., Isner, J. M., Kereiakes, D. J., Giordano, F. J., Simons, M., Losordo, D. W., et al. (2001). Intracoronary administration of recombinant human vascular endothelial growth factor to patients with coronary artery disease. *American heart journal*, 142(5), 872–880. doi:10.1067/mhj.2001.118471
- Hibino, N., Villalona, G., Pietris, N., Duncan, D. R., Schoffner, A., Roh, J. D., Yi, T., et al. (2011). Tissue-engineered vascular grafts form neovessels that arise from regeneration of the adjacent blood vessel. *The FASEB journal : official publication of the Federation of American Societies for Experimental Biology*. doi:10.1096/fj.11-182246
- Hill, C. E., Rummery, N., Hickey, H., & Sandow, S. L. (2002). Heterogeneity in the distribution of vascular gap junctions and connexins: implications for function. *Clinical and experimental pharmacology & physiology*, 29(7), 620–625.
- Hirschi, K. K., Rohovsky, S. A., Beck, L. H., Smith, S. R., & D'Amore, P. A. (1999). Endothelial cells modulate the proliferation of mural cell precursors via platelet-derived growth factor-BB and heterotypic cell contact, 84(3), 298–305.
- Hirschi, K., Rohovsky, S., & D'Amore, P. (1998). PDGF, TGF-beta, and heterotypic cell-cell interactions mediate endothelial cell-induced recruitment of 10T1/2 cells and their differentiation to a smooth muscle fate. *The Journal of Cell Biology*, 141(3), 805–814.
- Hlushchuk, R., Ehrbar, M., Reichmuth, P., Heinemann, N., Styp-Rekowska, B., Escher, R., Baum, O., et al. (2011). Decrease in VEGF expression induces intussusceptive

- vascular pruning. *Arteriosclerosis, Thrombosis, and Vascular Biology*, 31(12), 2836–2844. doi:10.1161/ATVBAHA.111.231811
- Ho, D., Chen, L., Zhao, X., Durham, N., Pannirselvam, M., Vatner, D. E., Morgans, D. J., et al. (2012). Smooth muscle myosin inhibition: a novel therapeutic approach for pulmonary hypertension. *PLoS ONE*, 7(5), e36302. doi:10.1371/journal.pone.0036302
- Hodivala-Dilke, K. (2008). alphavbeta3 integrin and angiogenesis: a moody integrin in a changing environment. *Current opinion in cell biology*, 20(5), 514–519. doi:10.1016/j.cecb.2008.06.007
- Huang, X., Griffiths, M., Wu, J., Farese, R. V., & Sheppard, D. (2000). Normal development, wound healing, and adenovirus susceptibility in beta5-deficient mice. *Molecular and cellular biology*, 20(3), 755–759.
- Humbert, M., Morrell, N. W., Archer, S. L., Stenmark, K. R., MacLean, M. R., Lang, I. M., Christman, B. W., et al. (2004). Cellular and molecular pathobiology of pulmonary arterial hypertension. *Journal of the American College of Cardiology*, 43(12 Suppl S), 13S–24S. doi:10.1016/j.jacc.2004.02.029
- Humbert, M., Sitbon, O., Chaouat, A., Bertocchi, M., Habib, G., Gressin, V., Yaïci, A., et al. (2010). Survival in patients with idiopathic, familial, and anorexigen-associated pulmonary arterial hypertension in the modern management era. *Circulation*, 122(2), 156–163. doi:10.1161/CIRCULATIONAHA.109.911818
- Ikeda, T., Nakamura, K., Akagi, S., Kusano, K. F., Matsubara, H., Fujio, H., Ogawa, A., et al. (2010). Inhibitory effects of simvastatin on platelet-derived growth factor

- signaling in pulmonary artery smooth muscle cells from patients with idiopathic pulmonary arterial hypertension. *Journal of cardiovascular pharmacology*, 55(1), 39–48. doi:10.1097/FJC.0b013e3181c0419c
- Inamdar, N. K., & Borenstein, J. T. (2011). Microfluidic cell culture models for tissue engineering. *Current opinion in biotechnology*, 22(5), 681–689. doi:10.1016/j.copbio.2011.05.512
- Iruela-Arispe, M. L., & Davis, G. E. (2009). Cellular and molecular mechanisms of vascular lumen formation. *Developmental Cell*, 16(2), 222–231. doi:10.1016/j.devcel.2009.01.013
- Ishibashi, H., Nakamura, M., Komori, A., Migita, K., & Shimoda, S. (2009). Liver architecture, cell function, and disease. *Seminars in immunopathology*, 31(3), 399–409. doi:10.1007/s00281-009-0155-6
- Jain, R. K. (2003). Molecular regulation of vessel maturation. *Nature Medicine*, 9(6), 685–693. doi:10.1038/nm0603-685
- Jain, R. K., Au, P., Tam, J., Duda, D. G., & Fukumura, D. (2005). Engineering vascularized tissue. *Nature Biotechnology*, 23(7), 821–823. doi:10.1038/nbt0705-821
- Jakobsson, L., Franco, C. A., Bentley, K., Collins, R. T., Ponsioen, B., Aspalter, I. M., Rosewell, I., et al. (2010). Endothelial cells dynamically compete for the tip cell position during angiogenic sprouting. *Nature Cell Biology*, 12(10), 943–953. doi:10.1038/ncb2103
- Jiang, L., Zhou, T., & Liu, H. (2012). Combined effects of the ATP-sensitive potassium channel opener pinacidil and simvastatin on pulmonary vascular remodeling in rats

- with monocrotaline-induced pulmonary arterial hypertension. *Die Pharmazie*, 67(6), 547–552.
- Jones, P. L., & Rabinovitch, M. (1996). Tenascin-C is induced with progressive pulmonary vascular disease in rats and is functionally related to increased smooth muscle cell proliferation. *Circulation research; Circulation research*, 79(6), 1131–1142.
- Jones, P. L., Cowan, K. N., & Rabinovitch, M. (1997). Tenascin-C, proliferation and subendothelial fibronectin in progressive pulmonary vascular disease. *AJPA*, 150(4), 1349–1360.
- Kamat, N., Nguyen-Ehrenreich, K. L.-T., Hsu, S. H., Ma, A. P., Sinn, I., Coleman, L., & Tai, J. (2011). Characterization of vascular injury responses to stent insertion in an ex-vivo arterial perfusion model. *Journal of vascular and interventional radiology : JVIR*, 22(2), 193–202. doi:10.1016/j.jvir.2010.10.006
- Kamei, M., Saunders, W. B., Bayless, K. J., Dye, L., Davis, G. E., & Weinstein, B. M. (2006). Endothelial tubes assemble from intracellular vacuoles in vivo. *Nature*, 442(7101), 453–456. doi:10.1038/nature04923
- Kaully, T., Kaufman-Francis, K., Lesman, A., & Levenberg, S. (2009). Vascularization--the conduit to viable engineered tissues. *Tissue engineering Part B, Reviews*, 15(2), 159–169. doi:10.1089/ten.teb.2008.0193
- Kim, S., Bell, K., Mousa, S. A., & Varner, J. A. (2000). Regulation of angiogenesis in vivo by ligation of integrin alpha5beta1 with the central cell-binding domain of fibronectin. *AJPA*, 156(4), 1345–1362.

- Kniazeva, E., & Putnam, A. J. (2009). Endothelial cell traction and ECM density influence both capillary morphogenesis and maintenance in 3-D. *American Journal of Physiology. Cell physiology*, 297(1), C179–87. doi:10.1152/ajpcell.00018.2009
- Koffler, J., Kaufman-Francis, K., Shandalov, Y., Yulia, S., Egozi, D., Dana, E., Pavlov, D. A., et al. (2011). Improved vascular organization enhances functional integration of engineered skeletal muscle grafts. *Proceedings of the National Academy of Sciences of the United States of America*, 108(36), 14789–14794. doi:10.1073/pnas.1017825108
- Koh, C. J., & Atala, A. (2004). Tissue engineering, stem cells, and cloning: Opportunities for regenerative medicine. *Journal of the American Society of Nephrology*, 15(5), 1113–1125. doi:10.1097/01.ASN.0000119683.59068.F0
- Koh, W., Stratman, A. N., Sacharidou, A., & Davis, G. E. (2008). In vitro three dimensional collagen matrix models of endothelial lumen formation during vasculogenesis and angiogenesis. *Methods in enzymology*, 443, 83–101. doi:10.1016/S0076-6879(08)02005-3
- Koike, N., Fukumura, D., Gralla, O., Au, P., Schechner, J., & Jain, R. (2004). Creation of long-lasting blood vessels. *Nature*, 428(6979), 138–139. doi:10.1038/428138a
- Kornberg, L., Earp, H. S., Parsons, J. T., Schaller, M., & Juliano, R. L. (1992). Cell adhesion or integrin clustering increases phosphorylation of a focal adhesion-associated tyrosine kinase. *The Journal of biological chemistry*, 267(33), 23439–23442.
- Koyama, H., Raines, E. W., Bornfeldt, K. E., Roberts, J. M., & Ross, R. (1996). Fibrillar

- collagen inhibits arterial smooth muscle proliferation through regulation of Cdk2 inhibitors. *Cell*, 87(6), 1069–1078.
- Laham, R. J., Sellke, F. W., Edelman, E. R., Pearlman, J. D., Ware, J. A., Brown, D. L., Gold, J. P., et al. (1999). Local perivascular delivery of basic fibroblast growth factor in patients undergoing coronary bypass surgery: results of a phase I randomized, double-blind, placebo-controlled trial. *Circulation*, 100(18), 1865–1871.
- Laliberte, K., Arneson, C., Jeffs, R., Hunt, T., & Wade, M. (2004). Pharmacokinetics and steady-state bioequivalence of treprostinil sodium (Remodulin) administered by the intravenous and subcutaneous route to normal volunteers. *Journal of cardiovascular pharmacology*, 44(2), 209–214.
- Langer, R., & Vacanti, J. P. (1993). Tissue engineering. *Science (New York, N.Y.)*, 260(5110), 920–926.
- LaRue, A. C., Mironov, V. A., Argraves, W. S., Czirik, A. S., Fleming, P. A., & Drake, C. J. (2003). Patterning of embryonic blood vessels. *Developmental Dynamics*, 228(1), 21–29. doi:10.1002/dvdy.10339
- Laschke, M. W., Mussawy, H., Schuler, S., Eglin, D., Alini, M., & Menger, M. D. (2010). Promoting external inosculation of prevascularised tissue constructs by pre-cultivation in an angiogenic extracellular matrix. *European cells & materials*, 20, 356–366.
- Laufs, U., Marra, D., Node, K., & Liao, J. K. (1999). 3-Hydroxy-3-methylglutaryl-CoA reductase inhibitors attenuate vascular smooth muscle proliferation by preventing rho GTPase-induced down-regulation of p27(Kip1). *The Journal of biological chemistry*,

274(31), 21926–21931.

- Lederman, R. J., Mendelsohn, F. O., Anderson, R. D., Saucedo, J. F., Tenaglia, A. N., Hermiller, J. B., Hillegass, W. B., et al. (2002). Therapeutic angiogenesis with recombinant fibroblast growth factor-2 for intermittent claudication (the TRAFFIC study): a randomised trial. *Lancet*, 359(9323), 2053–2058.
- Leslie-Barbick, J. E., Moon, J. J., & West, J. L. (2009). Covalently-immobilized vascular endothelial growth factor promotes endothelial cell tubulogenesis in poly(ethylene glycol) diacrylate hydrogels. *Journal of biomaterials science Polymer edition*, 20(12), 1763–1779. doi:10.1163/156856208X386381
- Lesman, A., Koffler, J., Atlas, R., Blinder, Y. J., Kam, Z., & Levenberg, S. (2011). Engineering vessel-like networks within multicellular fibrin-based constructs. *Biomaterials*, 1–14. doi:10.1016/j.biomaterials.2011.07.003
- Levenberg, S., Rouwkema, J., Macdonald, M., Garfein, E., Kohane, D., Darland, D., Marini, R., et al. (2005). Engineering vascularized skeletal muscle tissue. *Nature Biotechnology*, 23(7), 879–884. doi:10.1038/nbt1109
- Lewis, J. M., & Schwartz, M. A. (1995). Mapping in vivo associations of cytoplasmic proteins with integrin beta 1 cytoplasmic domain mutants. *Molecular biology of the cell*, 6(2), 151–160.
- Li, C., & Xu, Q. (2000). Mechanical stress-initiated signal transductions in vascular smooth muscle cells. *Cellular signalling*, 12(7), 435–445.
- Lin, C.-C., & Anseth, K. S. (2008). PEG Hydrogels for the Controlled Release of Biomolecules in Regenerative Medicine. *Pharmaceutical research*, 26(3), 631–643.

doi:10.1007/s11095-008-9801-2

- Lindner, V., & Reidy, M. A. (1991). Proliferation of smooth muscle cells after vascular injury is inhibited by an antibody against basic fibroblast growth factor. *Proceedings of the National Academy of Sciences of the United States of America*, 88(9), 3739–3743.
- Liu, W. F., Nelson, C. M., Tan, J. L., & Chen, C. S. (2007). Cadherins, RhoA, and Rac1 are differentially required for stretch-mediated proliferation in endothelial versus smooth muscle cells. *Circulation research; Circulation research*, 101(5), e44–52. doi:10.1161/CIRCRESAHA.107.158329
- Liu, X., Holzwarth, J. M., & Ma, P. X. (2012). Functionalized synthetic biodegradable polymer scaffolds for tissue engineering. *Macromolecular bioscience*, 12(7), 911–919. doi:10.1002/mabi.201100466
- Lloyd-Jones, D., Adams, R. J., Brown, T. M., Carnethon, M., Dai, S., De Simone, G., Ferguson, T. B., et al. (2010). Heart disease and stroke statistics--2010 update: a report from the American Heart Association. *Circulation*, 121(7), e46–e215. doi:10.1161/CIRCULATIONAHA.109.192667
- Lourenço, A. P., Fontoura, D., Henriques-Coelho, T., & Leite-Moreira, A. F. (2011). Current pathophysiological concepts and management of pulmonary hypertension. *International Journal of Cardiology*, 1–12. doi:10.1016/j.ijcard.2011.05.066
- Lovett, M., Lee, K., Edwards, A., & Kaplan, D. L. (2009). Vascularization strategies for tissue engineering. *Tissue engineering Part B, Reviews*, 15(3), 353–370. doi:10.1089/ten.TEB.2009.0085

- Lusis, A. J. (2000). Atherosclerosis. *Nature*, *407*(6801), 233–241. doi:10.1038/35025203
- Lutolf, M. P., & Hubbell, J. A. (2003). Synthesis and physicochemical characterization of end-linked poly(ethylene glycol)-co-peptide hydrogels formed by Michael-type addition. *Biomacromolecules*, *4*(3), 713–722. doi:10.1021/bm025744e
- Lutolf, M. P., & Hubbell, J. A. (2005). Synthetic biomaterials as instructive extracellular microenvironments for morphogenesis in tissue engineering. *Nature Biotechnology*, *23*(1), 47–55. doi:10.1038/nbt1055
- Macchiarini, P., Jungebluth, P., Go, T., Asnaghi, M. A., Rees, L. E., Cogan, T. A., Dodson, A., et al. (2008). Clinical transplantation of a tissue-engineered airway. *The Lancet*, *372*(9655), 2023–2030. doi:10.1016/S0140-6736(08)61598-6
- Mancuso, P., Martin-Padura, I., Calleri, A., Marighetti, P., Quarna, J., Rabascio, C., Braidotti, P., et al. (2011). Circulating perivascular progenitors: a target of PDGFR inhibition. *International journal of cancer. Journal international du cancer*, *129*(6), 1344–1350. doi:10.1002/ijc.25816
- Marcos, E., Fadel, E., Sanchez, O., Humbert, M., Dartevelle, P., Simonneau, G., Hamon, M., et al. (2004). Serotonin-induced smooth muscle hyperplasia in various forms of human pulmonary hypertension. *Circulation research; Circulation research*, *94*(9), 1263–1270. doi:10.1161/01.RES.0000126847.27660.69
- Masson, S., Latini, R., & Anand, I. S. (2010). An update on cardiac troponins as circulating biomarkers in heart failure. *Current heart failure reports*, *7*(1), 15–21. doi:10.1007/s11897-010-0001-0
- Matsumura, G., Hibino, N., Ikada, Y., Kurosawa, H., & Shin'oka, T. (2003). Successful

- application of tissue engineered vascular autografts: clinical experience. *Biomaterials*, 24(13), 2303–2308.
- McDonnell, P. J., Toyne, P. A., & Hutchins, G. M. (1983). Primary pulmonary hypertension and cirrhosis: are they related? *The American review of respiratory disease*, 127(4), 437–441.
- McLaughlin, V. V., Benza, R. L., Rubin, L. J., Channick, R. N., Voswinckel, R., Tapson, V. F., Robbins, I. M., et al. (2010). Addition of inhaled treprostinil to oral therapy for pulmonary arterial hypertension: a randomized controlled clinical trial. *Journal of the American College of Cardiology*, 55(18), 1915–1922. doi:10.1016/j.jacc.2010.01.027
- Melani, M., & Weinstein, B. M. (2010). Common Factors Regulating Patterning of the Nervous and Vascular Systems. *Annual review of cell and developmental biology*. doi:10.1146/annurev.cellbio.093008.093324
- Melero-Martin, J. M., de Obaldia, M. E., Kang, S.-Y., Khan, Z. A., Yuan, L., Oettgen, P., & Bischoff, J. (2008). Engineering robust and functional vascular networks in vivo with human adult and cord blood-derived progenitor cells. *Circulation research; Circulation research*, 103(2), 194–202. doi:10.1161/CIRCRESAHA.108.178590
- Miller, J. S., Shen, C. J., Legant, W. R., Baranski, J. D., Blakely, B. L., & Chen, C. S. (2010). Bioactive hydrogels made from step-growth derived PEG-peptide macromers. *Biomaterials*, 31(13), 3736–3743. doi:10.1016/j.biomaterials.2010.01.058
- Miller, J. S., Stevens, K. R., Yang, M. T., Baker, B. M., Nguyen, D.-H. T., Cohen, D. M., Toro, E., et al. (2012). Rapid casting of patterned vascular networks for perfusable

engineered three-dimensional tissues. *Nature Publishing Group*.

doi:10.1038/nmat3357

- Monahan, T. S., Andersen, N. D., Panossian, H., Kalish, J. A., Daniel, S., Shrikhande, G. V., Ferran, C., et al. (2007). A novel function for cadherin 11/osteoblast-cadherin in vascular smooth muscle cells: modulation of cell migration and proliferation. *Journal of vascular surgery : official publication, the Society for Vascular Surgery [and] International Society for Cardiovascular Surgery, North American Chapter*, 45(3), 581–589. doi:10.1016/j.jvs.2006.12.016
- Moon, J. J., Lee, S.-H., & West, J. L. (2007). Synthetic biomimetic hydrogels incorporated with ephrin-A1 for therapeutic angiogenesis. *Biomacromolecules*, 8(1), 42–49. doi:10.1021/bm060452p
- Moon, J. J., Saik, J. E., Poche, R. A., Leslie-Barbick, J. E., Lee, S.-H., Smith, A. A., Dickinson, M. E., et al. (2011). Biomimetic hydrogels with pro-angiogenic properties. *Biomaterials*, 31(14), 3840–3847. doi:10.1016/j.biomaterials.2010.01.104
- Murakami, M., Nguyen, L. T., Zhuang, Z. W., Zhang, Z. W., Moodie, K. L., Carmeliet, P., Stan, R. V., et al. (2008). The FGF system has a key role in regulating vascular integrity. *Journal of Clinical Investigation*, 118(10), 3355–3366. doi:10.1172/JCI35298
- Nabel, E. G., Yang, Z., Liptay, S., San, H., Gordon, D., Haudenschild, C. C., & Nabel, G. J. (1993). Recombinant platelet-derived growth factor B gene expression in porcine arteries induce intimal hyperplasia in vivo. *Journal of Clinical Investigation*, 91(4), 1822–1829. doi:10.1172/JCI116394

- Network, O. P. A. T. N., & Recipients, S. R. O. T. (2011). *OPTN/SRTR 2010 Annual Data Report* (pp. 1–142). Department of Health and Human Services, Health Resources and Services Administration, Healthcare Systems Bureau, Division of Transplantation.
- Newby, A. C., & Zaltsman, A. B. (2000). Molecular mechanisms in intimal hyperplasia. *The Journal of pathology*, *190*(3), 300–309. doi:10.1002/(SICI)1096-9896(200002)190:3<300::AID-PATH596>3.0.CO;2-I
- Nguyen, L. L., & D'Amore, P. A. (2001). Cellular interactions in vascular growth and differentiation. *International review of cytology*, *204*, 1–48.
- Niwa, K., Sakai, J., Watanabe, T., Ohyama, T., & Karino, T. (2007). Improved arterial wall model by coculturing vascular endothelial and smooth muscle cells. *In vitro cellular & developmental biology. Animal*, *43*(1), 17–20. doi:10.1007/s11626-006-9003-3
- Ogawa, A., Nakamura, K., Matsubara, H., Fujio, H., Ikeda, T., Kobayashi, K., Miyazaki, I., et al. (2005). Prednisolone inhibits proliferation of cultured pulmonary artery smooth muscle cells of patients with idiopathic pulmonary arterial hypertension. *Circulation*, *112*(12), 1806–1812. doi:10.1161/CIRCULATIONAHA.105.536169
- Oh, H. H., Lu, H., Kawazoe, N., & Chen, G. (2011). Spatially Guided Angiogenesis by Three-Dimensional Collagen Scaffolds Micropatterned with Vascular Endothelial Growth Factor. *Journal of biomaterials science Polymer edition*. doi:10.1163/092050611X611693
- Orlando, G., Baptista, P., Birchall, M., De Coppi, P., Farney, A., Guimaraes-Souza, N.

- K., Opara, E., et al. (2011a). Regenerative medicine as applied to solid organ transplantation: current status and future challenges. *Transplant international : official journal of the European Society for Organ Transplantation*, 24(3), 223–232. doi:10.1111/j.1432-2277.2010.01182.x
- Orlando, G., Wood, K. J., Stratta, R. J., Yoo, J. J., Atala, A., & Soker, S. (2011b). Regenerative medicine and organ transplantation: past, present, and future. *Transplantation*, 91(12), 1310–1317. doi:10.1097/TP.0b013e318219ebb5
- Pandya, N. M., Dhalla, N. S., & Santani, D. D. (2006). Angiogenesis—a new target for future therapy. *Vascular Pharmacology*, 44(5), 265–274. doi:10.1016/j.vph.2006.01.005
- Paquet, C., Larouche, D., Bisson, F., Proulx, S., Simard-Bisson, C., Gaudreault, M., Robitaille, H., et al. (2010). Tissue engineering of skin and cornea: Development of new models for in vitro studies. *Annals of the New York Academy of Sciences*, 1197, 166–177. doi:10.1111/j.1749-6632.2009.05373.x
- Passaniti, A., Taylor, R. M., Pili, R., Guo, Y., Long, P. V., Haney, J. A., Pauly, R. R., et al. (1992). A simple, quantitative method for assessing angiogenesis and antiangiogenic agents using reconstituted basement membrane, heparin, and fibroblast growth factor. *Laboratory investigation; a journal of technical methods and pathology*, 67(4), 519–528.
- Peters, M. C., Polverini, P. J., & Mooney, D. J. (2002). Engineering vascular networks in porous polymer matrices. *Journal of Biomedical Materials Research*, 60(4), 668–678.

- Phelps, E. A., & García, A. J. (2010). Engineering more than a cell: vascularization strategies in tissue engineering. *Current opinion in biotechnology*, 21(5), 704–709. doi:10.1016/j.copbio.2010.06.005
- Phng, L.-K., & Gerhardt, H. (2009). Angiogenesis: a team effort coordinated by notch. *Developmental Cell*, 16(2), 196–208. doi:10.1016/j.devcel.2009.01.015
- Pietra, G. G., Edwards, W. D., Kay, J. M., Rich, S., Kernis, J., Schloo, B., Ayres, S. M., et al. (1989). Histopathology of primary pulmonary hypertension. A qualitative and quantitative study of pulmonary blood vessels from 58 patients in the National Heart, Lung, and Blood Institute, Primary Pulmonary Hypertension Registry. *Circulation*, 80(5), 1198–1206.
- Pirone, D. M., Liu, W. F., Ruiz, S. A., Gao, L., Raghavan, S., Lemmon, C. A., Romer, L. H., et al. (2006). An inhibitory role for FAK in regulating proliferation: a link between limited adhesion and RhoA-ROCK signaling. *The Journal of Cell Biology*, 174(2), 277–288. doi:10.1083/jcb.200510062
- Porter, K. E., Naik, J., Turner, N. A., Dickinson, T., Thompson, M. M., & London, N. J. M. (2002). Simvastatin inhibits human saphenous vein neointima formation via inhibition of smooth muscle cell proliferation and migration. *Journal of vascular surgery : official publication, the Society for Vascular Surgery [and] International Society for Cardiovascular Surgery, North American Chapter*, 36(1), 150–157.
- Qiao, H., Bell, J., Juliao, S., Li, L., & May, J. M. (2009). Ascorbic acid uptake and regulation of type I collagen synthesis in cultured vascular smooth muscle cells. *Journal of vascular research*, 46(1), 15–24. doi:10.1159/000135661

- Quaegebeur, A., Segura, I., & Carmeliet, P. (2010). Pericytes: blood-brain barrier safeguards against neurodegeneration? *Neuron*, *68*(3), 321–323.
doi:10.1016/j.neuron.2010.10.024
- Radice, G. L., Rayburn, H., Matsunami, H., Knudsen, K. A., Takeichi, M., & Hynes, R. O. (1997). Developmental defects in mouse embryos lacking N-cadherin. *Developmental biology*, *181*(1), 64–78. doi:10.1006/dbio.1996.8443
- Rafii, S., & Lyden, D. (2003). Therapeutic stem and progenitor cell transplantation for organ vascularization and regeneration. *Nature Medicine*, *9*(6), 702–712.
doi:10.1038/nm0603-702
- Raghavan, S., Nelson, C. M., Baranski, J. D., Lim, E., & Chen, C. S. (2010a). Geometrically controlled endothelial tubulogenesis in micropatterned gels. *Tissue Engineering Part A*, *16*(7), 2255–2263. doi:10.1089/ten.TEA.2009.0584
- Raghavan, S., Shen, C. J., Desai, R. A., Sniadecki, N. J., Nelson, C. M., & Chen, C. S. (2010b). Decoupling diffusional from dimensional control of signaling in 3D culture reveals a role for myosin in tubulogenesis. *Journal of cell science*, *123*(17), 2877–2883. doi:10.1242/jcs.055079
- Raines, E. W. (2000). The extracellular matrix can regulate vascular cell migration, proliferation, and survival: relationships to vascular disease. *INTERNATIONAL JOURNAL OF EXPERIMENTAL PATHOLOGY*, *81*(3), 173–182.
- Rattazzi, M., Bertacco, E., Puato, M., Faggini, E., & Pauletto, P. (2012). Hypertension and vascular calcification. *Journal of Hypertension*, *1*.
doi:10.1097/HJH.0b013e328356c257

- Reaume, A. G., de Sousa, P. A., Kulkarni, S., Langille, B. L., Zhu, D., Davies, T. C., Juneja, S. C., et al. (1995). Cardiac malformation in neonatal mice lacking connexin43. *Science (New York, N.Y.)*, *267*(5205), 1831–1834.
- Reid, L. M., Fiorino, A. S., Sigal, S. H., Brill, S., & Holst, P. A. (1992). Extracellular matrix gradients in the space of Disse: relevance to liver biology. *Hepatology (Baltimore, Md.)*, *15*(6), 1198–1203.
- Ren, X. D., & Schwartz, M. A. (2000). Determination of GTP loading on Rho. *Methods in enzymology*, *325*, 264–272.
- Richardson, A., Malik, R. K., Hildebrand, J. D., & Parsons, J. T. (1997). Inhibition of cell spreading by expression of the C-terminal domain of focal adhesion kinase (FAK) is rescued by coexpression of Src or catalytically inactive FAK: a role for paxillin tyrosine phosphorylation. *Molecular and cellular biology*, *17*(12), 6906–6914.
- Risau, W., & Flamme, I. (1995). Vasculogenesis. *Annual review of cell and developmental biology*, *11*, 73–91. doi:10.1146/annurev.cb.11.110195.000445
- Rivron, N. C., Vrij, E. J., Rouwkema, J., Le Gac, S., van den Berg, A., Truckenmüller, R. K., & van Blitterswijk, C. A. (2012). Tissue deformation spatially modulates VEGF signaling and angiogenesis. *Proceedings of the National Academy of Sciences of the United States of America*. doi:10.1073/pnas.1201626109
- Roovers, K., & Assoian, R. K. (2003). Effects of rho kinase and actin stress fibers on sustained extracellular signal-regulated kinase activity and activation of G(1) phase cyclin-dependent kinases. *Molecular and cellular biology*, *23*(12), 4283–4294.
- Rosengart, T. K., Lee, L. Y., Patel, S. R., Kligfield, P. D., Okin, P. M., Hackett, N. R.,

- Isom, O. W., et al. (1999). Six-month assessment of a phase I trial of angiogenic gene therapy for the treatment of coronary artery disease using direct intramyocardial administration of an adenovirus vector expressing the VEGF121 cDNA. *Annals of surgery*, 230(4), 466–70– discussion 470–2.
- Rouwkema, J., Rivron, N. C., & van Blitterswijk, C. A. (2008). Vascularization in tissue engineering. *Trends in biotechnology*, 26(8), 434–441.
doi:10.1016/j.tibtech.2008.04.009
- Rubens, C., Ewert, R., Halank, M., Wensel, R., Orzechowski, H. D., Schultheiss, H. P., & Hoeffken, G. (2001). Big endothelin-1 and endothelin-1 plasma levels are correlated with the severity of primary pulmonary hypertension. *Chest*, 120(5), 1562–1569.
- Rubin, L. J. (1997). Primary pulmonary hypertension. *The New England journal of medicine*, 336(2), 111–117. doi:10.1056/NEJM199701093360207
- Rubin, L. J., Badesch, D. B., Barst, R. J., Galie, N., Black, C. M., Keogh, A., Pulido, T., et al. (2002). Bosentan therapy for pulmonary arterial hypertension. *The New England journal of medicine*, 346(12), 896–903. doi:10.1056/NEJMoa012212
- Rubin, L. J., Groves, B. M., Reeves, J. T., Frosolono, M., Handel, F., & Cato, A. E. (1982). Prostacyclin-induced acute pulmonary vasodilation in primary pulmonary hypertension. *Circulation*, 66(2), 334–338.
- Ruhrberg, C., Gerhardt, H., Golding, M., Watson, R., Ioannidou, S., Fujisawa, H., Betsholtz, C., et al. (2002). Spatially restricted patterning cues provided by heparin-binding VEGF-A control blood vessel branching morphogenesis. *Genes & Development*, 16(20), 2684–2698. doi:10.1101/gad.242002

- Rustad, K. C., Sorkin, M., Levi, B., Longaker, M. T., & Gurtner, G. C. (2010). Strategies for organ level tissue engineering. *Organogenesis*, 6(3), 151–157.
- Saharinen, P., Eklund, L., Miettinen, J., Wirkkala, R., Anisimov, A., Winderlich, M., Nottebaum, A., et al. (2008). Angiopoietins assemble distinct Tie2 signalling complexes in endothelial cell-cell and cell-matrix contacts. *Nature Cell Biology*, 10(5), 527–537. doi:10.1038/ncb1715
- Schermuly, R. T., Dony, E., Ghofrani, H. A., Pullamsetti, S., Savai, R., Roth, M., Sydykov, A., et al. (2005). Reversal of experimental pulmonary hypertension by PDGF inhibition. *Journal of Clinical Investigation*, 115(10), 2811–2821. doi:10.1172/JCI24838
- Schumacher, B., Pecher, P., Specht, von, B. U., & Stegmann, T. (1998). Induction of neoangiogenesis in ischemic myocardium by human growth factors: first clinical results of a new treatment of coronary heart disease. *Circulation*, 97(7), 645–650.
- Schwartz, S. M., & Benditt, E. P. (1977). Aortic endothelial cell replication. I. Effects of age and hypertension in the rat. *Circulation research; Circulation research*, 41(2), 248–255.
- Schwartz, S., Campbell, G., & Campbell, J. (1986). Replication of smooth muscle cells in vascular disease. *Circulation research; Circulation research*, 58(4), 427–444.
- Seger, R., & Krebs, E. G. (1995). The MAPK signaling cascade. *The FASEB journal : official publication of the Federation of American Societies for Experimental Biology*, 9(9), 726–735.
- Seglen, P. O. (1976). Preparation of isolated rat liver cells. *Methods in cell biology*, 13,

29–83.

- Senger, D. R., Claffey, K. P., Benes, J. E., Perruzzi, C. A., Sergiou, A. P., & Detmar, M. (1997). Angiogenesis promoted by vascular endothelial growth factor: regulation through $\alpha 1\beta 1$ and $\alpha 2\beta 1$ integrins. *Proceedings of the National Academy of Sciences of the United States of America*, *94*(25), 13612–13617.
- Shalaby, F., Rossant, J., Yamaguchi, T. P., Gertsenstein, M., Wu, X. F., Breitman, M. L., & Schuh, A. C. (1995). Failure of blood-island formation and vasculogenesis in Flk-1-deficient mice. *Nature*, *376*(6535), 62–66. doi:10.1038/376062a0
- Shaw, A., & Xu, Q. (2003). Biomechanical stress-induced signaling in smooth muscle cells: an update. *Current vascular pharmacology*, *1*(1), 41–58.
- Shyu, K.-G., Chao, Y.-M., Wang, B.-W., & Kuan, P. (2005). Regulation of discoidin domain receptor 2 by cyclic mechanical stretch in cultured rat vascular smooth muscle cells. *Hypertension*, *46*(3), 614–621. doi:10.1161/01.HYP.0000175811.79863.e2
- Silva, R., D'Amico, G., Hoidalva-Dilke, K. M., & Reynolds, L. E. (2008). Integrins: the keys to unlocking angiogenesis. *Arteriosclerosis, Thrombosis, and Vascular Biology*, *28*(10), 1703–1713. doi:10.1161/ATVBAHA.108.172015
- Simon, A. M., & McWhorter, A. R. (2002). Vascular abnormalities in mice lacking the endothelial gap junction proteins connexin37 and connexin40. *Developmental biology*, *251*(2), 206–220.
- Simon-Assmann, P., Orend, G., Mammadova-Bach, E., Spenlé, C., & Lefebvre, O. (2011). Role of laminins in physiological and pathological angiogenesis. *The*

International journal of developmental biology, 55(4-5), 455–465.

doi:10.1387/ijdb.103223ps

Simons, M. (2005). Angiogenesis: where do we stand now? *Circulation*, 111(12), 1556–1566. doi:10.1161/01.CIR.0000159345.00591.8F

Sklepkiwicz, P., Schermuly, R. T., Tian, X., Ghofrani, H. A., Weissmann, N., Sedding, D., Kashour, T., et al. (2011). Glycogen synthase kinase 3beta contributes to proliferation of arterial smooth muscle cells in pulmonary hypertension. (P.

Sklepkiwicz, R. T. Schermuly, X. Tian, H. A. Ghofrani, N. Weissmann, D. Sedding, T. Kashour, et al., Eds.) *PLoS ONE*, 6(4), e18883.

doi:10.1371/journal.pone.0018883.g008

Soejima, K., Negishi, N., Nozaki, M., & Sasaki, K. (1998). Effect of cultured endothelial cells on angiogenesis in vivo. *Plastic and reconstructive surgery*, 101(6), 1552–1560.

Söhl, G., & Willecke, K. (2004). Gap junctions and the connexin protein family.

Cardiovascular research, 62(2), 228–232. doi:10.1016/j.cardiores.2003.11.013

Stenmark, K. R., Meyrick, B., Galie, N., Mooi, W. J., & McMurtry, I. F. (2009). Animal models of pulmonary arterial hypertension: the hope for etiological discovery and pharmacological cure. *American journal of physiology Lung cellular and molecular physiology*, 297(6), L1013–32. doi:10.1152/ajplung.00217.2009

Stewart, D. J., Kutryk, M. J. B., Fitchett, D., Freeman, M., Camack, N., Su, Y., Siega, Della, A., et al. (2009). VEGF gene therapy fails to improve perfusion of ischemic myocardium in patients with advanced coronary disease: results of the NORTHERN trial. *Molecular therapy : the journal of the American Society of Gene Therapy*,

17(6), 1109–1115. doi:10.1038/mt.2009.70

Stouffer, G. A., Hu, Z., Sajid, M., Li, H., Jin, G., Nakada, M. T., Hanson, S. R., et al.

(1998). Beta3 integrins are upregulated after vascular injury and modulate thrombospondin- and thrombin-induced proliferation of cultured smooth muscle cells. *Circulation*, 97(9), 907–915.

Stratman, A. N., Malotte, K. M., Mahan, R. D., Davis, M. J., & Davis, G. E. (2009).

Pericyte recruitment during vasculogenic tube assembly stimulates endothelial basement membrane matrix formation. *Blood*, 114(24), 5091–5101.

doi:10.1182/blood-2009-05-222364

Strilic, B., Kucera, T., Eglinger, J., Hughes, M. R., Mcnagny, K. M., Tsukita, S., Dejana, E., et al. (2009).

The molecular basis of vascular lumen formation in the developing mouse aorta. *Developmental Cell*, 17(4), 505–515. doi:10.1016/j.devcel.2009.08.011

Su, J.-L., Yang, P.-C., Shih, J.-Y., Yang, C.-Y., Wei, L.-H., Hsieh, C.-Y., Chou, C.-H., et al. (2006).

The VEGF-C/Flt-4 axis promotes invasion and metastasis of cancer cells. *Cancer cell*, 9(3), 209–223. doi:10.1016/j.ccr.2006.02.018

Taipale, J., Makinen, T., Arighi, E., Kukk, E., Karkkainen, M., & Alitalo, K. (1999).

Vascular endothelial growth factor receptor-3. *Current topics in microbiology and immunology*, 237, 85–96.

Tan, J. L., Tien, J., Pirone, D. M., Gray, D. S., Bhadriraju, K., & Chen, C. S. (2003).

Cells lying on a bed of microneedles: an approach to isolate mechanical force.

Proceedings of the National Academy of Sciences of the United States of America, 100(4), 1484–1489. doi:10.1073/pnas.0235407100

- Tateishi-Yuyama, E., Matsubara, H., Murohara, T., Ikeda, U., Shintani, S., Masaki, H., Amano, K., et al. (2002). Therapeutic angiogenesis for patients with limb ischaemia by autologous transplantation of bone-marrow cells: a pilot study and a randomised controlled trial. *Lancet*, *360*(9331), 427–435. doi:10.1016/S0140-6736(02)09670-8
- Tengood, J. E., Kovach, K. M., Vescovi, P. E., Russell, A. J., & Little, S. R. (2010). Sequential delivery of vascular endothelial growth factor and sphingosine 1-phosphate for angiogenesis. *Biomaterials*, *31*(30), 7805–7812. doi:10.1016/j.biomaterials.2010.07.010
- Tengood, J. E., Ridenour, R., Brodsky, R., Russell, A. J., & Little, S. R. (2011). Sequential Delivery of Basic Fibroblast Growth Factor and Platelet-Derived Growth Factor for Angiogenesis. *Tissue Engineering Part A*, *17*(9-10), 1181–1189. doi:10.1089/ten.tea.2010.0551
- Thurston, G., Rudge, J. S., Ioffe, E., Zhou, H., Ross, L., Croll, S. D., Glazer, N., et al. (2000). Angiopoietin-1 protects the adult vasculature against plasma leakage. *Nature Medicine*, *6*(4), 460–463. doi:10.1038/74725
- Thurston, G., Suri, C., Smith, K., McClain, J., Sato, T., Yancopoulos, G., & McDonald, D. (1999). Leakage-resistant blood vessels in mice transgenically overexpressing angiopoietin-1. *Science (New York, N.Y.)*, *286*(5449), 2511.
- Thwaites, J. W., Reebye, V., Mintz, P., Levicar, N., & Habib, N. (2012). Cellular replacement and regenerative medicine therapies in ischemic stroke. *Regenerative medicine*, *7*(3), 387–395. doi:10.2217/rme.12.2
- Thyberg, J., Hedin, U., Sjölund, M., Palmberg, L., & Bottger, B. A. (1990). Regulation of

- differentiated properties and proliferation of arterial smooth muscle cells.
Arteriosclerosis (Dallas, Tex), 10(6), 966–990.
- Tian, L., & George, S. C. (2011). Biomaterials to Prevascularize Engineered Tissues.
Journal of Cardiovascular Translational Research. doi:10.1007/s12265-011-9301-3
- Tomita, S., Li, R. K., Weisel, R. D., Mickle, D. A., Kim, E. J., Sakai, T., & Jia, Z. Q.
(1999). Autologous transplantation of bone marrow cells improves damaged heart
function. *Circulation*, 100(19 Suppl), II247–56.
- Torres-Vázquez, J., Gitler, A. D., Fraser, S. D., Berk, J. D., van N Pham, Fishman, M. C.,
Childs, S., et al. (2004). Semaphorin-plexin signaling guides patterning of the
developing vasculature. *Developmental Cell*, 7(1), 117–123.
doi:10.1016/j.devcel.2004.06.008
- Traktuev, D. O., Prater, D. N., Merfeld-Clauss, S., Sanjeevaiah, A. R., Saadatzadeh, M.
R., Murphy, M., Johnstone, B. H., et al. (2009). Robust functional vascular network
formation in vivo by cooperation of adipose progenitor and endothelial cells.
Circulation research; Circulation research, 104(12), 1410–1420.
doi:10.1161/CIRCRESAHA.108.190926
- Tran, P.-K., Tran-Lundmark, K., Soininen, R., Tryggvason, K., Thyberg, J., & Hedin, U.
(2004). Increased intimal hyperplasia and smooth muscle cell proliferation in
transgenic mice with heparan sulfate-deficient perlecan. *Circulation research;*
Circulation research, 94(4), 550–558. doi:10.1161/01.RES.0000117772.86853.34
- Tsihlis, N. D., Oustwani, C. S., Vavra, A. K., Jiang, Q., Keefer, L. K., & Kibbe, M. R.
(2011). Nitric oxide inhibits vascular smooth muscle cell proliferation and neointimal

- hyperplasia by increasing the ubiquitination and degradation of UbcH10. *Cell biochemistry and biophysics*, 60(1-2), 89–97. doi:10.1007/s12013-011-9179-3
- Vacanti, J. P. (2012). Tissue engineering and the road to whole organs. *The British journal of surgery*, 99(4), 451–453. doi:10.1002/bjs.7819
- Vacanti, J. P., & Langer, R. (1999). Tissue engineering: the design and fabrication of living replacement devices for surgical reconstruction and transplantation. *The Lancet*, 354, S32–S34. doi:10.1016/S0140-6736(99)90247-7
- Vatter, H., Zimmermann, M., Jung, C., Weyrauch, E., Lang, J., & Seifert, V. (2002). Effect of the novel endothelin(A) receptor antagonist LU 208075 on contraction and relaxation of isolated rat basilar artery. *Clinical science (London, England : 1979)*, 103 Suppl 48, 408S–413S. doi:10.1042/CS103S408S
- Vernon, R. B., & Sage, E. H. (1996). Contraction of fibrillar type I collagen by endothelial cells: a study in vitro. *Journal of cellular biochemistry*, 60(2), 185–197. doi:10.1002/(SICI)1097-4644(19960201)60:2<185::AID-JCB3>3.0.CO;2-T
- Wallez, Y., & Huber, P. (2008). Endothelial adherens and tight junctions in vascular homeostasis, inflammation and angiogenesis. *Biochimica et Biophysica Acta (BBA) - Biomembranes*, 1778(3), 794–809. doi:10.1016/j.bbamem.2007.09.003
- Wang, A. Y., Leong, S., Liang, Y.-C., Huang, R. C. C., Chen, C. S., & Yu, S. M. (2008). Immobilization of growth factors on collagen scaffolds mediated by polyanionic collagen mimetic peptides and its effect on endothelial cell morphogenesis. *Biomacromolecules*, 9(10), 2929–2936. doi:10.1021/bm800727z
- Wang, Y., & Kovanen, P. T. (1999). Heparin proteoglycans released from rat serosal

- mast cells inhibit proliferation of rat aortic smooth muscle cells in culture.
Circulation research; Circulation research, 84(1), 74–83.
- Welsh, C. F., Roovers, K., Villanueva, J., Liu, Y., Schwartz, M. A., & Assoian, R. K. (2001). Timing of cyclin D1 expression within G1 phase is controlled by Rho.
Nature Cell Biology, 3(11), 950–957. doi:10.1038/ncb1101-950
- White, S., Hingorani, R., Arora, R., Hughes, C. C. W., George, S., & Choi, B. (2012). Longitudinal in vivo imaging to assess blood flow and oxygenation in implantable engineered tissues. *Tissue engineering. Part C, Methods*.
doi:10.1089/ten.TEC.2011.0744
- Williams, R. L., Courtneidge, S. A., & Wagner, E. F. (1988). Embryonic lethality and endothelial tumors in chimeric mice expressing polyoma virus middle T oncogene.
Cell, 52(1), 121–131.
- Wolf, S. C., Sauter, G., Risler, T., & Brehm, B. R. (2005). Effects of combined endothelin and angiotensin II antagonism on growth factor-induced proliferation of vascular smooth muscle cells isolated from uremic rats. *Renal failure*, 27(4), 465–474.
- Wolinsky, H. (1970). Response of the rat aortic media to hypertension. Morphological and chemical studies. *Circulation research; Circulation research*, 26(4), 507–522.
- Wu, M.-H. (2009). Simple poly(dimethylsiloxane) surface modification to control cell adhesion. *Surface and Interface Analysis*, 41(1), 11–16. doi:10.1002/sia.2964
- Xu, E. Z., Kantores, C., Ivanovska, J., Engelberts, D., Kavanagh, B. P., McNamara, P. J., & Jankov, R. P. (2010). Rescue Treatment with a Rho-Kinase Inhibitor Normalizes

- Right-Ventricular Function and Reverses Remodeling in Juvenile Rats with Chronic Pulmonary Hypertension. *American journal of physiology Heart and circulatory physiology*. doi:10.1152/ajpheart.00595.2010
- Xu, J., Rodriguez, D., Petitelerc, E., Kim, J. J., Hangai, M., Moon, Y. S., Davis, G. E., et al. (2001). Proteolytic exposure of a cryptic site within collagen type IV is required for angiogenesis and tumor growth in vivo. *The Journal of Cell Biology*, 154(5), 1069–1079. doi:10.1083/jcb.200103111
- Yanaga, H., Imai, K., Fujimoto, T., & Yanaga, K. (2009). Generating ears from cultured autologous auricular chondrocytes by using two-stage implantation in treatment of microtia. *Plastic and reconstructive surgery*, 124(3), 817–825. doi:10.1097/PRS.0b013e3181b17c0e
- Yoshida, T., Komaki, M., Hattori, H., Negishi, J., Kishida, A., Morita, I., & Abe, M. (2010). Therapeutic Angiogenesis by Implantation of a Capillary Structure Constituted of Human Adipose Tissue Microvascular Endothelial Cells. *Arteriosclerosis, Thrombosis, and Vascular Biology*. doi:10.1161/ATVBAHA.109.198994
- Yu, S. M., Hung, L. M., & Lin, C. C. (1997). cGMP-elevating agents suppress proliferation of vascular smooth muscle cells by inhibiting the activation of epidermal growth factor signaling pathway. *Circulation*, 95(5), 1269–1277.
- Zervantonakis, I. K., Hughes-Alford, S. K., Charest, J. L., Condeelis, J. S., Gertler, F. B., & Kamm, R. D. (2012). Three-dimensional microfluidic model for tumor cell intravasation and endothelial barrier function. *Proceedings of the National Academy*

of Sciences of the United States of America, 109(34), 13515–13520.

doi:10.1073/pnas.1210182109

Zhan, Y., Kim, S., Izumi, Y., Izumiya, Y., Nakao, T., Miyazaki, H., & Iwao, H. (2003).

Role of JNK, p38, and ERK in platelet-derived growth factor-induced vascular proliferation, migration, and gene expression. *Arteriosclerosis, Thrombosis, and Vascular Biology*, 23(5), 795–801. doi:10.1161/01.ATV.0000066132.32063.F2

Zhang, Z., Ramirez, N. E., Yankeelov, T. E., Li, Z., Ford, L. E., Qi, Y., Pozzi, A., et al.

(2008). alpha2beta1 integrin expression in the tumor microenvironment enhances tumor angiogenesis in a tumor cell-specific manner. *Blood*, 111(4), 1980–1988.

doi:10.1182/blood-2007-06-094680

Zhao, J. H., Reiske, H., & Guan, J. L. (1998). Regulation of the cell cycle by focal

adhesion kinase. *The Journal of Cell Biology*, 143(7), 1997–2008.

Zheng, Y., Chen, J., Craven, M., Choi, N. W., Totorica, S., Diaz-Santana, A., Kermani,

P., et al. (2012). In vitro microvessels for the study of angiogenesis and thrombosis.

Proceedings of the National Academy of Sciences of the United States of America.

doi:10.1073/pnas.1201240109

Zheng, Y., Henderson, P. W., Choi, N. W., Bonassar, L. J., Spector, J. A., & Stroock, A.

D. (2011). Microstructured templates for directed growth and vascularization of soft tissue in vivo. *Biomaterials*, 32(23), 5391–5401.

doi:10.1016/j.biomaterials.2011.04.001

Ziegler, T., Alexander, R. W., & Nerem, R. M. (1995). An endothelial cell-smooth

muscle cell co-culture model for use in the investigation of flow effects on vascular

biology. *Annals of biomedical engineering*, 23(3), 216–225.

Zisch, A. H., Lutolf, M. P., Ehrbar, M., Raeber, G. P., Rizzi, S. C., Davies, N., Schmökel, H., et al. (2003). Cell-demanded release of VEGF from synthetic, biointeractive cell ingrowth matrices for vascularized tissue growth. *The FASEB journal : official publication of the Federation of American Societies for Experimental Biology*, 17(15), 2260–2262. doi:10.1096/fj.02-1041fje